

5-2011

ATM Signaling to TSC2: Mechanisms and Implications for Cancer Therapy

Angela Alexander

Follow this and additional works at: https://digitalcommons.library.tmc.edu/utgsbs_dissertations



Part of the [Cancer Biology Commons](#), [Cell Biology Commons](#), and the [Neoplasms Commons](#)

Recommended Citation

Alexander, Angela, "ATM Signaling to TSC2: Mechanisms and Implications for Cancer Therapy" (2011).
*The University of Texas MD Anderson Cancer Center UTHealth Graduate School of Biomedical Sciences
Dissertations and Theses (Open Access)*. 140.
https://digitalcommons.library.tmc.edu/utgsbs_dissertations/140

This Dissertation (PhD) is brought to you for free and open access by the The University of Texas MD Anderson Cancer Center UTHealth Graduate School of Biomedical Sciences at DigitalCommons@TMC. It has been accepted for inclusion in The University of Texas MD Anderson Cancer Center UTHealth Graduate School of Biomedical Sciences Dissertations and Theses (Open Access) by an authorized administrator of DigitalCommons@TMC. For more information, please contact digitalcommons@library.tmc.edu.

ATM SIGNALING TO TSC2: MECHANISMS AND IMPLICATIONS FOR CANCER THERAPY

By

Angela Alexander, B.S.

APPROVED:

Cheryl L. Walker, Ph.D.
Supervisory Professor

David Johnson, Ph.D.

Karen Vasquez, Ph.D.

Robert Bast, M.D.

Eric Jonasch, M.D.

APPROVED:

Dean, The University of Texas
Graduate School of Biomedical Sciences at Houston

ATM SIGNALING TO TSC2: MECHANISMS AND IMPLICATIONS FOR CANCER THERAPY

A

DISSERTATION

Presented to the Faculty of
The University of Texas
Health Science Center at Houston
and
The University of Texas
M. D. Anderson Cancer Center
Graduate School of Biomedical Sciences
in Partial Fulfillment

of the Requirements

for the Degree of

DOCTOR OF PHILOSOPHY

By

Angela Alexander, B.S.
Houston, Texas

May, 2011

DEDICATION

I dedicate this dissertation to my parents who have always stood by my side from 1500 miles away, always encouraged me through the trials and tribulations of graduate school, taught me the importance of hard work and perseverance and congratulated me on my successes. You put up with my many late-night phone calls returning voicemails left earlier in the evening while I was still in the lab, and tolerating my often short yearly visits home. I could not have asked for more loving and supportive parents.

To my friends, who kept me grounded in reality, been great companions in the rare amount of free time I've had in the past 7 years. I hope to be repay your kindness soon.

ACKNOWLEDGEMENTS

This thesis would not have been possible without the generous time and support of many people. I owe my deepest gratitude to my mentor Cheryl Walker, who agreed to take me on as a naïve young PhD student without lab experience (coming from a finance undergraduate program) but passionate about doing translational research, and molded me over the past almost 7 years into a mature scientist capable of critically thinking about scientific problems.

I also would like to thank my committee members both current and previous members, Dr Karen Vasquez, Dr David Johnson, Dr Robert Bast, Dr Eric Jonasch, Dr Claudio Conti and Dr John DiGiovanni for all their helpful scientific comments and suggestions. A special thank you to Becky Brooks for all her help with negotiating the day-to-day challenges of graduate school rules and regulations and just “getting stuff done”.

My labmates both current and former members have been a great work family for me – I truly appreciate the technical assistance from Tia, Sean and Helena, and I’d like to especially acknowledge Amanda for taking care of all my mice, an often thankless but very important task that I would feel most uncomfortable doing myself. And lastly but certainly not least, my collaborator and bench-mate (until recently) on this project, Jinhee for all the practical advice, and help with getting our publications written up and published.

I have a small but close-knit group of friends, some of whom started out as scientific colleagues, but over time have become personal friends, to thank also. Thanks for all the great chats and encouragement online (Mary Canady and Sally Church), walks around the park during long experiments (Tiffany Bredfeldt), dinners/coffee break company while visiting Houston (Jeannine Garnett).

My work has been funded over the past two years by the generous support of the Sowell and Huggins families, through the generous support of a GSBS/MD Anderson fellowship in their name, for which I am incredibly thankful for, and will always cherish having met you and heard your story driving your commitment to cancer research. Your support and recognition means a lot to me, and kept me motivated through this challenge.

Publication Number: _____

Angela Alexander, B.S.

Supervisory Professor: Cheryl L. Walker, Ph.D.

Ataxia telangiectasia mutated (ATM) is a critical component of the cellular response to DNA damage, where it acts as a damage sensor, and signals to a large network of proteins which execute the important tasks involved in responding to the damage, namely inducing cell cycle checkpoints, inducing DNA repair, modulating transcriptional responses, and regulating cell death pathways if the damage cannot be repaired faithfully. We have now discovered that an additional novel component of this ATM-dependent damage response involves induction of autophagy in response to oxidative stress. In contrast to DNA damage-induced ATM activation however, oxidative stress induced ATM, occurs in the cytoplasm, and does not require nuclear-to-cytoplasmic shuttling of ATM. Using several cell culture systems including MCF7 breast carcinoma cells, SKOV3 ovarian cancer cells, and various lineages of mouse embryonic fibroblasts, we showed that once activated by reactive oxygen species (ROS), ATM signals to mTORC1 to induce autophagy via the LKB1-AMPK-TSC2 pathway. Targeting dysregulation of mTORC1 in *Atm*-deficient mice, which succumb to lymphomagenesis within 3-4 months of age with daily administration of rapamycin, could significantly extend survival and cause regression of tumors, suggesting that pharmacologically targeting this pathway has therapeutic implications in cancer.

We also identified a second contrasting pathway for DNA damage-induced mTORC1 repression which does not require AMPK activation, but does require ATM and TSC2. Several potential mechanisms including mTOR localization and p53-mediated pathways were ruled out

however we identified that TSC2 may be an additional cytoplasmic direct ATM substrate that is engaged in response to DNA damage specifically.

Lastly, a study was performed to examine whether autophagy induced by ovarian cancer therapeutics (focusing on cisplatin, since paclitaxel does not induce autophagy in the SKOV3 cell line model we used) plays a role in resistance to therapy since autophagy can play both pro-survival mechanisms or be a mechanism of cell death. Using a genetic approach to knock-down Atg5 expression with shRNA in SKOV3 ovarian carcinoma cells, we compared the cytotoxicity of cisplatin in vector or Atg5 knock-down cells, and demonstrated that autophagy does not play any significant role in the response to cisplatin in this cell line.

TABLE OF CONTENTS

Approval Page	i
Title Page	ii
Dedication	iii
Acknowledgements	iv
Abstract	v
Table of Contents	vii
List of Illustrations	xii
List of Tables	xvi
List of Abbreviations	xvii
 Chapter 1: Introduction	 1
1.1 DNA damage and DNA damage response	1
1.2 ROS	3
1.3 ATM	6
1.3.1 ATM subcellular localization	11
1.3.2 ATM cellular trafficking	13
1.4 TSC2 regulation of mTOR	13
1.4.1 mTOR	14
1.4.2 Regulation of TSC2	16
1.5 Autophagy	20
1.5.1 Autophagy, physiology and disease	22
1.5.2 Regulation of autophagy	24
 Chapter 2: Materials and Methods	 27
2.1 Antibodies, equipment and reagents	27
2.2 Cell culture	27

2.3	Plasmids	30
2.4	Measurement of ROS by 5-6-chloromethyl-2'-7'-dichlorohydrofluorescein (CM-H ₂ -DCFDA)	30
2.5	Western Blots	30
2.6	siRNA transfection	31
2.7	Immunoprecipitations	32
2.8	TSC2 functional assay	32
2.9	Subcellular fractionations	32
2.10	GFP-LC3 localization	33
2.11	Electron microscopy	33
2.12	Animal studies	34
2.13	Immunofluorescence	34
2.14	Peroxisome protease assay	34
2.15	Cell growth assay	35
Chapter 3: Identification of ROS induced activation of cytoplasmic ATM signaling pathway to activate LKB1, AMPK and TSC2 to repress mTOR and induce autophagy		36
3.1	Introduction	36
3.2	Results	37
3.2.1	Confirmation of elevated ROS levels in ATM and TSC2-deficient cells	37
3.2.2	ROS induced mTORC1 suppression.....	44
3.2.3	Role of ATM in ROS-induced mTORC1 repression	48
3.2.4	Role of LKB1 in ATM signaling to mTORC1	56
3.2.5	AMPK activation by ROS leads to TSC2 activation	60
3.2.6	Localization of activated ATM signaling to LKB1 and AMPK	65
3.2.7	mTORC1 dependent autophagy regulation by ROS	70

3.3	Discussion	80
Chapter 4: In vivo study of mTOR signaling in Atm-deficient mice		82
4.1	Background into Atm knockout mouse model	84
4.2	Rationale for study	84
4.3	Results	84
4.3.1	Analysis of mTORC1 signaling and AMPK activation in Atm mouse model	84
4.3.2	Response of lymphomas to rapamycin	85
4.4	Discussion	91
Chapter 5: Peroxisomal localization of ATM-TSC2 signaling node to regulate pexophagy		94
5.1	Introduction.....	94
5.2	Peroxisome biology	94
5.3	Results	97
5.3.1	Predicted peroxisome localization sequences in TSC2, TSC1, mTOR and ATM	97
5.3.2	Experimental evidence for peroxisomal localization of TSC2, TSC1, mTOR and ATM	97
5.3.3	Loss of peroxisomal targeting sequences perturbs mTORC1 signaling	104
5.3.4	Cells from Zellweger patients possess basal elevated oxidative stress and altered mTORC1 regulation	107
5.3.5	ROS-induction of autophagy induces peroxisome turnover	111
5.4	Discussion.....	111

Chapter 6: Identification of ATM and TSC2-dependent, but AMPK-independent115

DNA damage signaling pathway to regulate mTOR

6.1	Introduction	115
6.2	Results	116
6.2.1	Characterization of mTORC1 regulation by DNA damage.....	116
6.2.2	Determination of the mechanism of ATM signaling to mTORC1	122
	in response to DNA damage	
6.3	Discussion	125

Chapter 7: Is mTOR suppression and autophagy induction relevant134

with regard to response to therapy in ovarian cancer?

7.1	Introduction	134
7.1.1	Ovarian cancer and therapeutics	134
7.1.2	Role of autophagy in ovarian cancer	136
7.2	Results	138
7.3	Discussion	146

Chapter 8: Summary and future directions148

8.1	Summary	148
8.2	Future directions	149
8.2.1	Mechanism of ROS-induced ATM activation	149
8.2.2	The role and regulation of pexophagy	150
8.2.3	Determination of p53-independent DNA damage-induced	151
	mTORC1 suppression mechanisms	
8.2.4	ATM as a therapeutic target in cancer	151

References152

Vita175

List of Illustrations

CHAPTER 1

Figure 1: Types of DNA damage, sources and cellular responses to damage	2
Figure 2: Hierarchy in signaling pathways in response to DNA damage	7
Figure 3: Structure of ATM protein	8
Figure 4: mTOR complex schematic	15
Figure 5: TSC2 sites based on human nomenclature	18
Figure 6: Model depicting TSC2 localization and function	19
Figure 7: Schematic of the autophagy process	21

CHAPTER 2 (no illustrations)

CHAPTER 3

Figure 8: Confirmation of elevated ROS in ATM-deficient cells	38
Figure 9: Confirmation of elevated ROS in Tsc2-deficient cells	39
Figure 10: ATM and TSC2 are epistatic in oxidative stress response	40
Figure 11: Rapamycin rescues elevated ROS levels in Tsc2-deficient MEFs	41
Figure 12: Rapamycin rescues elevated ROS levels in ATM-deficient lymphoblasts	42
Figure 13: Feedback model for the role of ATM and TSC2 in coordinately regulating mTOR and ROS levels	43
Figure 14: Dose-response showing mTORC1 suppression by H ₂ O ₂	45
Figure 15: mTORC1 is repressed by endogenous ROS	46
Figure 16: Time-dependent repression of mTORC1 by H ₂ O ₂	47
Figure 17: Antioxidant treatment rescues mTORC1 suppression by ROS	49
Figure 18: Activation of ATM by ROS	50
Figure 19: Role of ATM in mediating signaling to mTORC1	51

Figure 20: mTORC1 suppression in primary mouse embryonic fibroblasts	52
Figure 21: siRNA validation of ATM participation in signaling to mTORC1	53
Figure 22: ATR is not required for mTORC1 suppression by ROS	54
Figure 23: siRNA validation that ATR is not required for mTORC1 suppression	55
Figure 24 LKB1 reconstitution of HeLa S3 cells and responsiveness to ROS	57
Figure 25: LKB1 phosphorylation in response to ROS	58
Figure 26: siRNA validation of LKB1 participation in signaling to mTORC1	59
Figure 27: AMPK activation by ROS	61
Figure 28: Activation of AMPK prior to mTORC1 repression	62
Figure 29: AMPK inhibition blocks mTORC1 suppression by ROS	63
Figure 30: AMPK phosphorylation of TSC2 mediates mTORC1 suppression by ROS	64
Figure 31: Tsc2 involvement in signaling to mTORC1 in MEF cells	66
Figure 32: Role of TSC2 in signaling to mTORC1 in human cells	67
Figure 33: p53 is not required for mTORC1 suppression by ROS	68
Figure 34: Fractionation showing localization of ATM-LKB1-AMPK signaling node	69
Figure 35: Leptomycin B does not block ATM signaling to mTORC1 in response to ROS	71
Figure 36: Equivalent ATM activation and mTORC1 suppression in	72
cytoplasmic fraction of leptomycin B treated MCF7 cells	
Figure 37: GFP-LC3 localization in response to ROS	74
Figure 38: Increased LC3 lipidation in response to ROS	75
Figure 39: LC3 II accumulation in the presence of chloroquine indicates increase	77
in autophagic flux	
Figure 40: Degradation of p62 in response to ROS	78
Figure 41: Electron microscopy images showing autophagosome increase	79
after ROS exposure	

CHAPTER 4

Figure 42: mTORC1 activity is elevated in lymphomas from <i>Atm</i> ^{-/-} mice	86
Figure 43: Quantitation of mTORC1 elevation in lymphomas from <i>Atm</i> ^{-/-} mice	87
Figure 44: AMPK is not activated in <i>Atm</i> ^{-/-} mice	88
Figure 45: Quantitation of AMPK activation in <i>Atm</i> ^{-/-} mice	89
Figure 46: Histological characterization of response to rapamycin in short-term treated mice	90
Figure 47: Kaplan-Meier survival curve for long-term study of rapamycin as a therapeutic for lymphoma	92

CHAPTER 5

Figure 48: Immunofluorescence showing TSC2 and TSC1 colocalization..... with peroxisomal marker PMP70	100
Figure 49: Fractionation showing PTS1-disrupted mutants fail to localize correctly	101
to membrane and peroxisome fractions.	
Figure 50: Fractionation showing endogenous TSC2 localization to the	102
peroxisome and membrane fractions	
Figure 51: Fractionation showing ROS-signaling node localized to the peroxisome	103
Figure 52: Protease protection assay showing that TSC2, TSC1 and ATM	105
are localized on the outer surface of the peroxisome	
Figure 53: Functional assay for TSC2 activity towards mTORC1	106
Figure 54: Reintroducing TSC2 to the peroxisome restores functionality	108
towards mTORC1	
Figure 55: Elevated ROS in Zellweger cells and partial rescue by rapamycin	109
Figure 56: Dysregulated ROS signaling to mTORC1 in Zellweger cells	110
Figure 57: Degradation of peroxisome proteins in response to ROS	112

CHAPTER 6

Figure 58: mTORC1 signaling in response to etoposide in MCF7 cells	117
Figure 59: Etoposide does not induce autophagy in MCF7 cells	118
Figure 60: mTORC1 signaling in response to ionizing radiation in MCF7 cells	119
Figure 61: mTORC1 signaling in response to neocarzinostatin in MCF7 cells	120
Figure 62: Neocarzinostatin does not induce autophagy in MCF7 cells	121
Figure 63: mTORC1 response to etoposide in MEFs	124
Figure 64: mTORC1 response to neocarzinostatin in MEFs	126
Figure 65: siRNA validation of role of TSC2 and ATM in mTORC1 suppression by IR	127
Figure 66: siRNA showing a role for TSC2 in ATM activation	128
Figure 67: mTOR localization does not change in response to DNA damaging agents	129
Figure 68: Schematic of TSC2 showing putative ATM phosphorylation sites in	132
relation to selected other known features	
Figure 69: Model for dual mechanisms for signaling from ATM to TSC2	133

CHAPTER 7

Figure 70: Cisplatin induces mTORC1 suppression without AMPK activation	139
in SKOV3 cells	
Figure 71: ROS is not generated by cisplatin in SKOV3 cells.....	140
Figure 72: Autophagy induction by cisplatin in SKOV3 cells	141
Figure 73: Comparison of autophagy induction in isogenic cisplatin sensitive	143
and resistant cells	
Figure 74: ATG5 expression in isolated clones	144
Figure 75: Cell death in response to cisplatin does not depend on	145
ATG5 expression in SKOV3 cells	

List of Tables

Table 1: Summary of different types of ROS and their chemical formulas	4
Table 2: List of antibodies used	28
Table 3: Peroxisome targeting sequences summary	96
Table 4: Peroxisome targeting sequences found in proteins of interest	98
Table 5: Summary of cell-type difference in response to DNA damage	123

List of Abbreviations

°C	degrees celsius
μL	microliter
μM	micromolar
μg	microgram
4E-BP1	eukaryotic initiation factor 4E binding protein
53BP1	p53-binding protein 1
ACC	acetyl co-A carboxylase
ALS	Amyotrophic lateral sclerosis disease
AMPK	5' adenosine monophosphate-activated protein kinase
ATM	ataxia telangiectasia mutated
ATP	adenosine triphosphate
ATR	ataxia telangiectasia and Rad3 related protein
C-terminus	carboxyl terminus
CAG	trinucleotide repeat consisting of cytosine, adenine and guanine
Chk2	checkpoint protein kinase 2
CKIP-1	casein kinase-2 interacting protein-1
DAPK	death-associated protein kinase
DCFDA	dichlorohydrofluorescein
DMSO	dimethylsulfoxide
DNA	deoxyribonucleic acid
DRAM	damage-regulated autophagy modulator
DSB	double strand breaks (in DNA)
dsRNA	double-stranded RNA (ribonucleic acid)
ERK	extracellular signal-regulated kinase
FAT	FRAP-ATM-TRRAP domain
FATC	FAT-carboxyl-terminal domain

FBS	fetal bovine serum
GAP	GTPase activating protein
GAPDH	glyceraldehydes 3-phosphate dehydrogenase
GCN2	general control nonrepressed 2
GDP	guanosine diphosphate
GFP	green fluorescent protein
GSK	glycogen synthase kinase
GTP	guanosine triphosphate
Gy	gray (unit of radiation exposure)
H ₂ O ₂	hydrogen peroxide
H4K16	histone H4 acetylated at lysine 16
HCl	hydrochloric acid
HDAC	histone deacetylase
HEK 293	human embryonic kidney 293 cells
HER2	human epidermal growth factor receptor 2
hMOF	human ortholog of MOF
HNSCC	head and neck squamous cell carcinoma
IKK	I κ B-kinase
IP	immunoprecipitation
IR	ionizing radiation
ISG20L1	interferon-stimulated 20kDa exonuclease-like
JNK	c-Jun N-terminal kinase
LDH	lactate dehydrogenase
LKB1	Liver kinase B1
M	molar (or membrane fraction if in figure)
MAPK	mitogen activated protein kinase

MEF	mouse embryonic fibroblasts
mM	millimolar
mPTS	membrane peroxisomal targeting sequence
mRNA	messenger RNA (ribonucleic acid)
MT	mutant
mTOR	mammalian-target-of-rapamycin
mTORC1	mammalian-target-of-rapamycin complex 1
mTOR	mammalian-target-of-rapamycin complex 2
NAC	N-acetyl cysteine
NCS	neocarzinostatin
ND	not determined
NEMO	nuclear factor kappaB essential modulator protein
NF κ B	nuclear factor kappaB
NP-40	Tergitol-type NP-40 detergent (nonyl phenoxypolyethoxylethanol)
NSCLC	non-small cell lung cancer
NT	no treatment
p4E-BP1	phosphorylated 4E-BP1
pACC	phosphorylated ACC
pAMPK	phosphorylated AMPK
pATM	phosphorylated ATM
pChk2	phosphorylated Chk2
PEITC	phenylethylisothiocyanate
pp53	phosphorylated p53
pS6K	phosphorylated S6K
pS6	phosphorylated S6 ribosomal protein
PBS	phosphate buffered saline
PERK	protein kinase RNA-like endoplasmic reticulum kinase

PI3K	phosphoinositide 3-kinase
PKR	protein kinase R
PMP70	70kDa peroxisomal membrane protein
PP2A	protein phosphatase 2A
PTEN	phosphatase and tensin homolog
PTS1	peroxisomal targeting sequence type 1
PTS2	peroxisomal targeting sequence type 2
ROS	reactive oxygen species
rpm	revolutions per minute
S1981	serine at position 1981 in protein
S1987	serine at position 1987 in protein
S6K	ribosomal S6-kinase
SDS-PAGE	sodium dodecyl sulfate-polyacrylamide gel electrophoresis
Ser	serine
shRNA	short-hairpin ribonucleic acid
siRNA	short-interfering ribonucleic acid
smc1	Stability of MiniChromosomes
SQ	serine followed by glutamine
T366A	threonine at position 366 substituted with alanine
Thr	threonine
TSC	Tuberous sclerosis complex
TSC1	Tuberous sclerosis complex 1/hamartin
TSC2	Tuberous sclerosis complex 2/tuberin
TQ	threonine followed by glutamine
TUNEL	terminal deoxynucleotidyl transferase dUTP nick end labeling
ULK1	unc-51-like kinase 1

UVA	ultraviolet radiation A, long wave
WT	wild-type

Introduction

1.1 DNA damage and DNA damage response

Cellular DNA is constantly under attack by a variety of exogenous sources of damage and endogenous processes, causing 10,000-100,000 DNA lesions every day per cell (1). As a result, cells have evolved intricate mechanisms to detect and repair such damage to survive such insults. Failure to do so faithfully results in mutations, genomic instability, or even cell death, and has been implicated in many diseases including cancer (2). This process has been termed the DNA damage response (3).

Damage to DNA can occur due to spontaneous base chemical modifications (including oxidation by reactive oxygen species, methylation or hydrolysis via deamination reactions) or replication errors. These endogenous sources of damage are mostly unavoidable since they occur as a consequence of normal metabolic processes. The other major source of DNA damage is exogenous mutagens such as many chemotherapeutic drugs (e.g. etoposide, doxorubicin, cisplatin), ultraviolet and ionizing radiation, and man-made chemicals such as polyaromatic hydrocarbons. A variety of different lesions are generated depending on the type of damage, including base modifications, DNA adducts, inter- and intra-strand crosslinks, single- or double-strand breaks, which are the most lethal forms of damage. These lesions and downstream consequences are described in more depth in figure 1.

Responses to DNA damage involves a cascade of proteins, beginning with a series of damage sensors, which transmit signals via transducer proteins (mostly kinases which amplify this signal) to effector proteins which execute the various processes in the cell. These well-described processes include cell cycle checkpoints, recruitment of DNA repair factors to the sites of damage, transcription around the damage and if the damage is too severe to be repaired, induction of apoptosis. In this thesis, I describe a previously unappreciated aspect of cellular responses to damage, namely mTORC1 repression and induction of autophagy in response to ROS.

Figure 1:

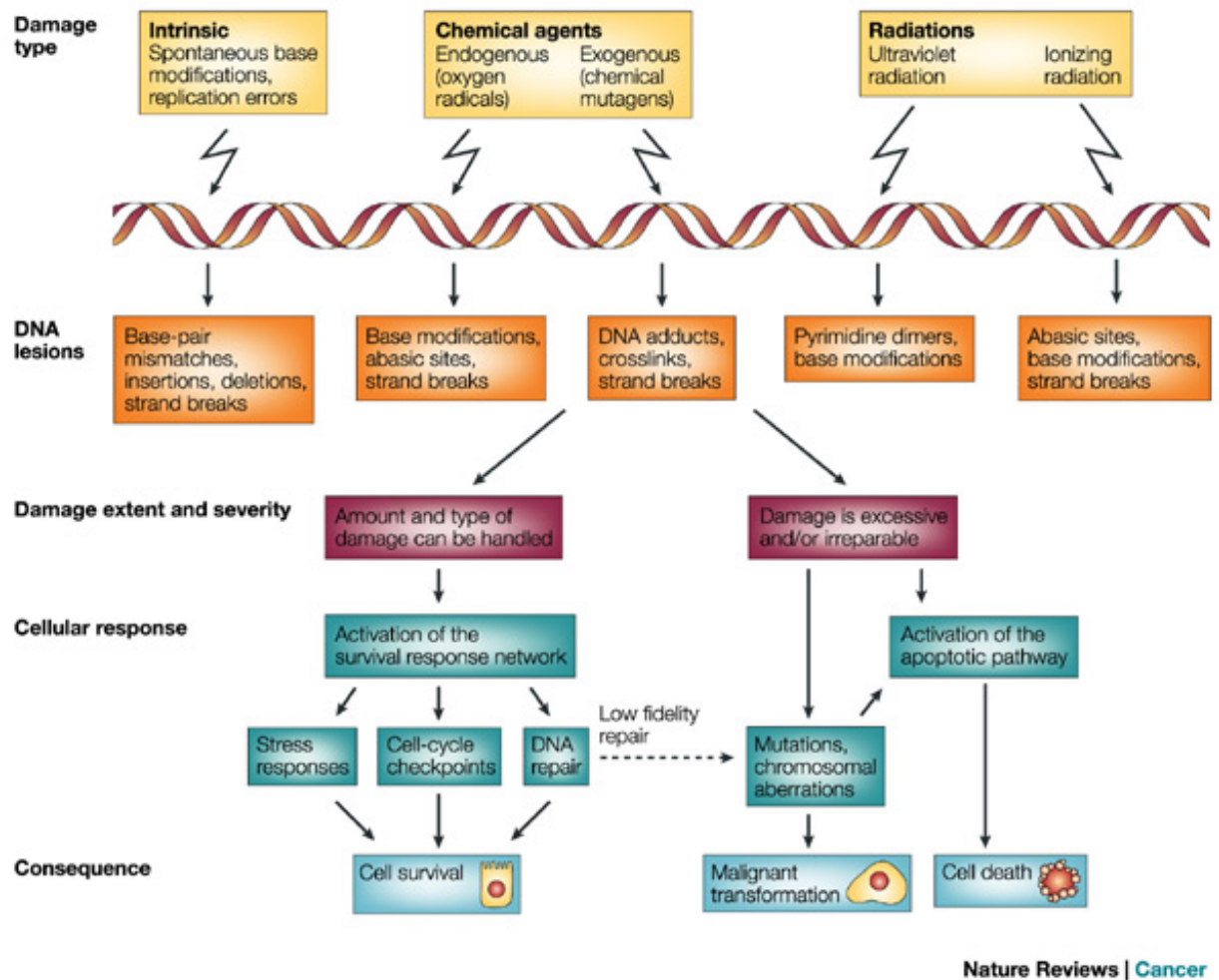


Figure 1: **Types of DNA damage, sources and cellular responses to damage.** Illustration showing both endogenous and exogenous sources of DNA damage, types of lesions generated, and downstream cellular consequences. Reprinted by permission from Macmillan Publishers Ltd: Nature Reviews Cancer (4) Copyright 2003

If the damage cannot be repaired in an error-free manner, one of the potential consequences is the development of cancer. The evidence for this relationship came from a number of studies from cell culture, animal models and human tumors, showing that the DNA damage response (ie markers of double strand breaks and downstream ATM-dependent pathways) could be detected in precursor lesions, leading to cell senescence or apoptosis, thereby acting as an anti-cancer barrier (5). In addition, oncogenes such as Myc have also been shown to directly induce DNA damage (6, 7) and activate the DNA damage response to induce apoptosis, whereas cells that have lost tumor suppressor gene function, such as p53-deficient cells, possess a constitutively active DNA damage response, as measured by Chk2 phosphorylation and 53BP1 localization at DSB (8). Taken together these results provide insights into the mechanisms of DNA damage response pathways, which is likely to lead to better ways of eliminating damaged cells that may eventually lead to tumors.

1.2 Reactive oxygen species (ROS)

ROS are highly reactive oxygen-containing molecules that can damage cells via reversible or irreversible reactions with proteins, lipids and DNA. These ROS molecules can either contain one or more unpaired electrons (known as “free radicals”) or be a non-radical species, which although do not contain any unpaired electrons, are still chemically reactive and may be converted to radical species. The most commonly encountered forms of ROS in biological systems are listed in table 1. When levels of ROS are increased beyond a threshold where the cell can manage, the cell encounters a state known as oxidative stress.

Table 1:

Free radical species		Non-radical species	
Superoxide	O_2^-	Hydrogen peroxide	H_2O_2
Nitric oxide	NO	Peroxynitrite	$ONOO^-$
Hydroxyl radicals	OH^\cdot	Hydroxide	OH
		Ozone	O_3

Table 1: **Summary of major forms of ROS in biological systems and their chemical formulas.**

In spite of their ability to cause cellular damage, ROS play important physiological functions in regulating signaling pathways including cell growth/cell death pathways and differentiation (9, 10). At a biochemical level, ROS such as hydrogen peroxide can directly oxidize protein phosphatases and kinases, growth factor receptors and transcription factors. At the organismal level, they can also initiate inflammatory responses via upregulation of cytokines, and can influence the immune response. Mitochondria are the main physiological sources of ROS, which is generated when electrons leak from the respiratory chain and react with molecular oxygen (O_2) to form superoxide which can then be readily converted to other forms of ROS. In addition to the mitochondria, the peroxisome is a major source of ROS generated as a byproduct of β -oxidation of fatty acids, and detoxification reactions by cytochrome P450 enzymes.

There is now an extensive body of literature describing the significant roles that oxidative stress plays in the pathogenesis of a variety of metabolic, cardiovascular, neurodegenerative diseases, as well as in the induction and promotion stages of cancer (11-14). The metabolic syndrome, a collection of risk factors for cardiovascular disease, including increased body mass index, hypertension, elevated blood glucose and triglycerides has been attributed to a systemic increase in oxidative stress, which may also partially explain the link between metabolic syndrome and cancer (15, 16). In cancer, there is a delicate balance of ROS, since although there is increased generation of ROS due to higher metabolic rates, dysfunctional mitochondria as a result of deregulated oncogene activity, cancer cells also express higher levels of antioxidant enzymes (6, 17-20). However, the net effect is still a higher than baseline level of ROS which plays critical roles in cell function (21).

In cancer, ROS can directly induce mutations in both nuclear and mitochondrial DNA, and function as signaling molecules to regulate cell growth and differentiation, glucose metabolism, and inflammation (14). Some important examples of pathways regulated by ROS include the MAPK/ERK pathway (for example via Ras oxidation leading to activation) and the PI3K/AKT pathway (via PTEN inactivation) (22-26). The other important pathway that is

activated by oxidative stress is the IKK-NF- κ B pathway. To deal with the constant barrage of stress, cells must possess intricate defense mechanisms for continued survival. These fall into 2 broad classes, one involving upregulation of antioxidant enzymes such as superoxide dismutase and catalase (27) and the other being induction of DNA repair pathways for example, via Gadd45 (28).

1.3 ATM

The locus involved in the the disease ataxia telangiectasia was mapped to chromosome 11q22-23 in 1988 and it took 7 more years for the gene to be cloned by the Shiloh laboratory (29, 30). AT is a systemic disease affecting many organ systems. The two most prominent pathological features of this disease are a significant propensity to spontaneously develop hematopoietic malignancies (leukemias and lymphomas), and a progressive neurodegeneration involving loss of cerebellar neuronal function, that leads to the ataxia phenotype. As a result, most patients do not live beyond their second or third decade of life. However beyond these major symptoms, patients have other abnormalities including metabolic defects, immunodeficiency and are hypersensitive to ionizing radiation. It was this last phenotype that first lead to the discovery of ATM's cellular function, although this wide spectrum of defects suggestions that ATM may play pleiotropic functions.

The best characterized function played by ATM in the cell is as a DNA damage sensor. As a "first responder" to DNA double-strand breaks, the ATM protein, which has kinase enzymatic activity, serves as an initiator of many pathways including DNA repair, induction of cell cycle checkpoints, and if necessary induction of cell death (apoptosis) if the damage is too severe to be repaired (31, 32). These pathways are triggered via ATM phosphorylation of transducer proteins which signal to effector proteins, as shown in the schematic in figure 2.

The mechanism of ATM activation by DNA damage has now been fairly well described. Upon double-strand break occurrence, ATM dimers are rapidly recruited to the broken DNA

Figure 2:

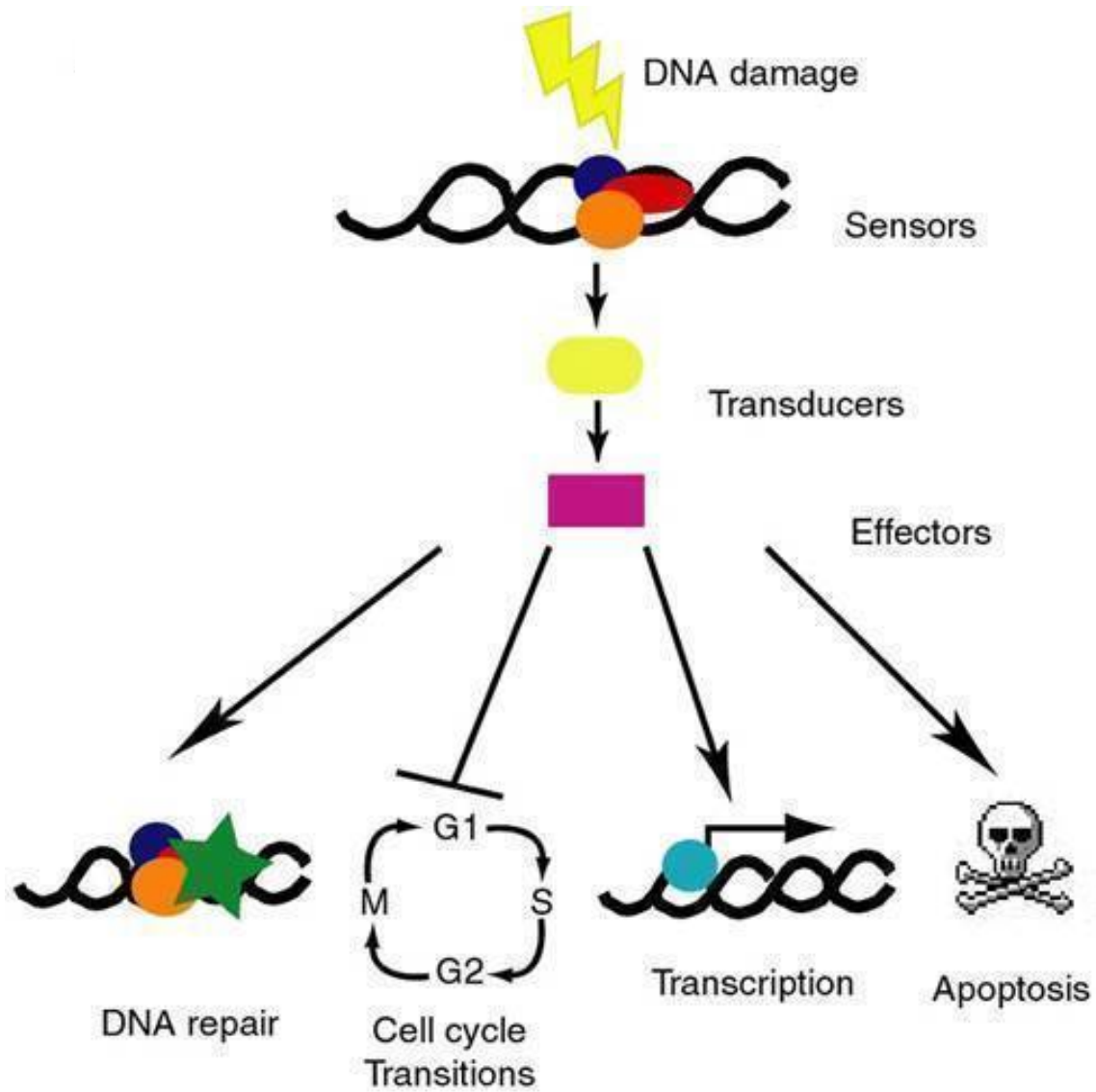
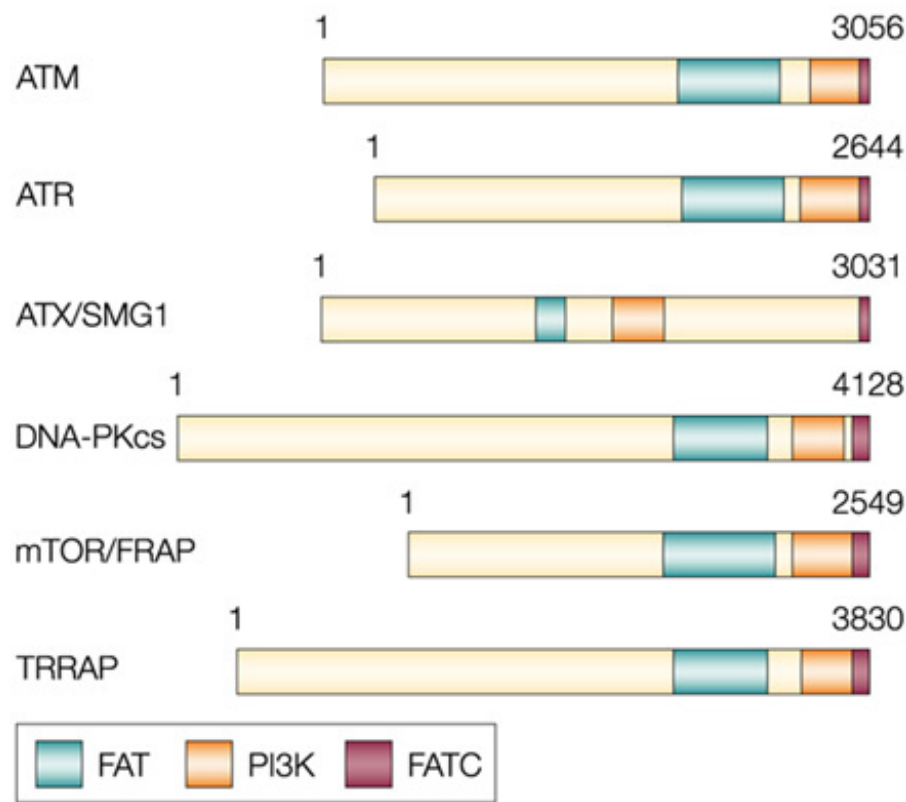


Figure 2: **Hierarchy in signaling pathways in response to DNA damage.** Illustration shows that ATM acts as a proximal sensor of DNA damage (double strand breaks) initiating signaling via a cascade of proteins that are transducers to effector proteins. [From (33) under creative commons license (URL: <http://atlasgeneticsoncology.org/Deep/DoubleStrandBreaksID20008.html>)]

Figure 3:



Nature Reviews | Cancer

Figure 3: **Structure of ATM protein.** Schematic showing the domains found in ATM and other family members. Reprinted by permission from Macmillan Publishers Ltd: Nature Reviews Cancer (4) Copyright 2003

ends. In a dimer structure, ATM is inactive because the kinase domain of one molecule of ATM is blocked by the FAT domain of the other molecule (4). Figure 3 illustrates the different domains in the ATM family of proteins. In order to convert these dimers to an active form via transphosphorylation of a serine residue (S1981 in human/S1987 in mouse) which releases active monomers which can now signal to downstream substrates containing consensus phosphorylation sites of SQ/TQ.

The requirement for phosphorylation at S1981/S1987 has recently been called into question from studies utilizing a mutant protein lacking this phosphorylation site. If phosphorylation of S1981/7 was required for ATM activation, then this mutant would be expected to be unable to reconstitute ATM function in ATM-deficient cells and even function as a dominant negative. Surprisingly, MEFs generated from a knock-in mouse where Ser 1987 is mutated to alanine had a perfectly functional ATM-dependent DNA damage response (ie phosphorylation of Smc1 and chk2, and recruitment to double strand breaks), and the mouse developed normally (34). These results suggest that S1987 autophosphorylation is not a mechanism of ATM activation, but rather is a consequence of ATM activation.

Other posttranslational modifications involved in ATM activation have also been identified, including four more autophosphorylation sites and acetylation. In response to DNA damage therefore a total of five autophosphorylation sites are increased - S367, T1885, S1893, S1981 and S2996 are increased in an ATM and Mre11-dependent manner (35, 36). These sites are all individually important in full ATM function in classical DNA damage responses such as cell cycle checkpoint induction and DNA repair, since single alanine mutants fail to correct the defect in ATM-deficient cells. Several years ago, DNA damage-inducible acetylation of a C-terminus lysine was identified (37, 38). This rapid modification by the Tip60 acetyl transferase results in activation of ATM's kinase activity, promotes the conversion of the inactive dimers to active monomers, therefore allowing phosphorylation of ATM substrates such as p53 and Chk2. Another acetyltransferase called hMOF is also upstream of ATM and can directly interact with ATM (39). However a direct acetylation site has

not been identified. Rather hMOF's HAT activity towards H4K16 plays a role in regulating ATM activation, by a poorly characterized general mechanism involving altered chromatin structure.

In unstressed conditions, ATM autophosphorylation is inhibited by the presence of phosphatases, including protein phosphatase 2A (PP2A), which interacts physically with ATM via its scaffolding subunit (40). Upon damage by ionizing radiation, PP2A dissociates from ATM, allowing the previously described activation mechanisms to proceed. In contrast to this mechanism, another serine-threonine protein phosphatase, PP5 interacts with ATM in a DNA damage-inducible manner, and is important for ATM activation by removing other inhibitory phosphorylation groups (41).

ATM is known to be phosphorylated in response to a number of types of stresses beyond DNA damage, including replication stress (secondary to ATR activation). Large scale chromatin structure alteration such as that which occurs after treatment with HDAC inhibitors, or chloroquine also has been shown to regulate ATM activation (42). Also of importance to this thesis as a whole is the observation the ATM is activated by oxidative stress.

Interestingly, the mechanism of ATM activation by oxidative stress has now been shown to occur by a separate mechanism from the DSB-mediated pathway, although ROS can cause DNA base damage that can be converted to DSBs in the process of being repaired. The first paper identifying a direct link between oxidative stress and ATM activation showed that free sulfhydryl (SH) groups on cysteines could be modified in response to 2 agents that generate ROS: N-methyl-N'-nitro-nitrosoguanidine (MNNG) and 15-deoxy- $\Delta^{12,14}$ prostaglandin J_2 , which is a more physiological compound produced during inflammation during prostaglandin D2 metabolism (43). ATM could be activated both *in vitro* and *in vivo* in an NBS1 and MSH6-deficient background, demonstrating that DNA damage is not the only mechanism of ATM activation. ROS is also produced as a byproduct of UVA radiation which can activate ATM to induce apoptosis (44). In polyglutamine diseases arising from long CAG repeat tracts, such as Huntington's disease, ATM is also activated as a result of the ROS generated by these protein

aggregates, which is thought to contribute to the neurodegenerative symptoms of the disease (45). More recently Tanya Paull's group showed that ROS can directly oxidize ATM at Cys 2991, which promotes formation of a disulfide-crosslinked ATM dimer that is active (in contrast to the DNA damage activated ATM which is a monomer) (46). In chapter 3 of this thesis I show that ROS can robustly activate both nuclear ATM (likely as a result of DNA damage) as well as cytoplasmic ATM, and that this specific pool of ATM can signal to LKB1, AMPK, TSC2 and mTORC1 to induce autophagy.

1.3.1 ATM subcellular localization

ATM's functions in sensing DNA damage and signaling to DNA repair and cell cycle checkpoints would strongly suggest that this protein is localized to the nucleus. Indeed, this is the case; however a substantial portion can be localized to organelles outside of the nucleus. Subcellular fractions from lymphoblastoid and fibroblasts were probed with antibodies to ATM, and ATM was detected in the nucleus. In addition about 20% of the total cellular pool of ATM was found in the microsomal fraction in vesicles of varying size (from 60-230nm) (47). This was confirmed by electron microscopy using immunogold-conjugated secondary antibodies. The punctate staining seen in these studies led to the discovery that a portion of these vesicles were peroxisomes, and that ATM could be delivered to peroxisomes via binding to the type 1 import receptor, peroxin 5. In chapter 4, I will elaborate further on the localization and function of ATM that is localized at the peroxisome.

Apart from the peroxisome, the other vesicular organelle that ATM has been found to reside in is the endosome (48). ATM was found to directly interact with β -adaptin using a yeast 2-hybrid screen. β -adaptin is a component of the clathrin-mediated receptor endocytosis pathway. This interaction was confirmed *in vivo* and a neuronal-specific β -adaptin homolog β -NAP (which was identified as an autoimmune antigen in a patient with cerebellar degeneration) was also determined to be an ATM binding partner suggesting that ATM may have physiological functions in the endocytic pathway.

ATM has also been reported to be recruited to the plasma membrane by the casein kinase-2 interacting protein-1 (CKIP-1), and is phosphorylated at S1981 when membrane-localized (49). CKIP-1 plays a number of seemingly distinct roles in processes ranging from muscle differentiation, to regulation of the actin cytoskeleton and recruiting casein kinase 2 to the plasma membrane. While the *in vivo* relevance of ATM localized to the plasma membrane is not completely clear, it appears that ATM plays a role in CKIP-1 mediated phosphorylation and stabilization of p53. Interestingly, ATM deficient cells have been reported to have cytoskeletal defects and structural abnormalities in the plasma membrane (50). The interaction with CKIP-1, and subsequent regulation of actin therefore may partially explain these structural defects in AT-cells.

Genomic instability is one of the hallmarks of ATM-deficient cells, attributed both to the DNA repair and cell cycle checkpoint functions that are regulated by ATM, as well as an extra-nuclear role at the centrosome. There are now several pieces of evidence regarding ATM playing an important role in the spindle. At the gross level, ATM-deficient cells have both numerical and structural chromosomal instability, and in an *Atm*-deficient background p21 could suppress aneuploidy (51). The ATM-p53-p21 damage response pathway has been shown to be activated early on during tumorigenesis (5), and centrosome amplification is also an early event during tumorigenesis, leading to the hypothesis that ATM could play a role in maintaining appropriate centrosome number as an additional mechanism of controlling genomic stability. Several years ago, Shen and co-authors reported that ATM could be detected in purified centrosomes (51), and this study also provided direct evidence that ATM deficiency induced centrosome amplification. The mechanism for ATM regulation of centrosome number appears to require p53 and p21, since *Atm*, p21 double knockout MEFs or *Atm*, p53 double knockout MEFs did not display a more severe centrosome amplification phenotype, suggesting these proteins are epistatic. ATM is activated with relatively slow kinetics (8-24 hours) by mitotic stresses like nocodazole or taxol, further implicating a role in the mitotic stress response. One additional potential mechanism for ATM activity at the

centrosome is via regulating polo-like-kinase 1 in response to mitotic stress, which is prematurely elevated in ATM-deficient cells (52).

1.3.2 ATM cellular trafficking

The studies described above regarding different subcellular localizations of ATM raises an interesting question regarding whether ATM shuttles between these compartments or whether there are distinct pools of ATM that reside in these locations, perhaps with different functions. Recent studies have shown that indeed ATM can shuttle out of the nucleus in a mechanism first described by Wu et al (53). As a result of DNA double-strand breaks and ATM activation, ATM phosphorylates NEMO, which is a regulatory subunit of the I- κ B kinase, at Ser 85, which serves as a signal for mono-ubiquitination of NEMO. This modification allows NEMO and ATM to translocate out of the nucleus where NEMO serves as an adaptor protein to bring together the IKK complex and ELKS (another regulatory subunit), activating this signaling cascade, which allows activated NF- κ B to re-enter the nucleus to transcriptionally regulate anti-apoptotic genes. However, my work that will be described in chapter 3 suggests that in addition to shuttling, there are distinct cytoplasmic pools of ATM, suggesting that differential localization of ATM can dictate what functions it plays.

1.4 TSC2 regulation of mTOR

Tuberous sclerosis complex (TSC) is a highly penetrant autosomal dominant disease caused by mutations in either the TSC2 (tuberin) or TSC1 (hamartin) tumor suppressor genes. Patients with TSC develop benign hamartomas in a wide range of tissues early in life. The brain is the most common organ affected by 3 main types of lesions: giant cell astrocytomas, cortical tumors and subependymal nodules (54). These tumors cause the bulk of the morbidity associated with TSC, due to causing seizures that may affect learning, memory and behavior, depending upon their size and location. In addition to the brain, tumors often arise in the kidneys (angiomyolipomas, or rarely renal cell carcinomas), lungs (similar to

lymphangioliomyomas, but thought to be metastases from angiomyolipomas), heart (cardiac rhabdomyosarcomas) as well as facial angiofibromas (54). Currently there is no cure for tuberous sclerosis complex, however recent studies with mTOR inhibitors have had promising results in reducing tumor size.

These GTP-ase activating proteins (GAP) function as a heterodimer in the cell, to negatively regulate cell growth via inhibiting the Rheb GTPase. Rheb functions as an activator of mTORC1, so the net result of TSC2 activation is mTORC1 repression (55). In the following section I will describe mTOR function more thoroughly.

1.4.1 mTOR

The mammalian target of rapamycin (mTOR) is an important serine-threonine kinase that belongs to the phosphoinositide-3-kinase (PI3K)-related family of kinases (PIKKs) that includes ATM, ATR, DNA-PK and hSMG1. TOR is conserved across eukaryotes from yeast to mammals, and is required for development in mouse, worms (*C. elegans*) and drosophila due to an early block in cell growth when this gene is deleted (56-59).

mTOR exists in two distinct large protein complexes know as mTORC1 and mTORC2, which have a number of differences (and similarities) (60). One major difference is the composition of these complexes: mTORC1 complex contains mTOR, raptor, mLST8, PRAS40 and Deptor, whereas mTORC2 contains mTOR, rictor, mLST8, Deptor, mSIN1, and Proctor-1. These complexes and example substrates are depicted in figure 4. Importantly, rapamycin can only bind and inhibit the mTORC1 complex through binding to FKBP12, which is why mTORC1 became known as the “rapamycin-sensitive” complex, whereas at least upon acute treatment with rapamycin, mTORC2 (thought to be “rapamycin-insensitive”) substrates are unaffected. However it is known that prolonged exposure to rapamycin can affect mTORC2 activity via destabilizing this complex in certain cell lines, therefore inhibiting AKT, one of the best characterized substrates of mTORC2 (61).

Figure 4:

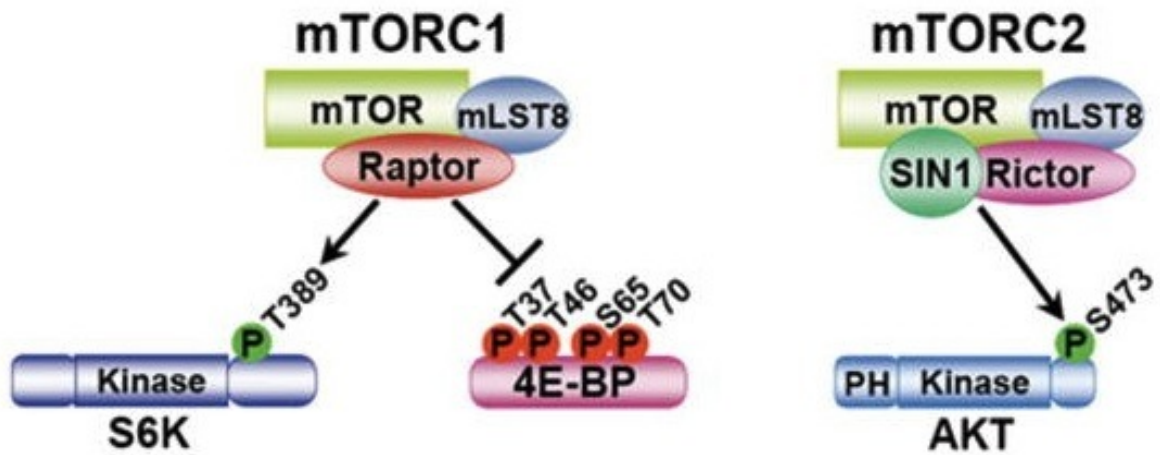


Figure 4: **mTOR complex schematic** mTOR is a component of two distinct protein complexes known as mTORC1 and mTORC2 that have different downstream substrates. S6K and 4E-BP1 are the most frequently used mTORC1-specific substrates, while AKT is the most frequently used mTORC2-specific substrate.

mTOR regulates many substrates important in translation, cell size and autophagy. One of the earliest identified substrates of mTORC1 was S6K, which was found to be upstream of ribosomal protein S6 (known as S6), involved in protein synthesis. Another important mTOR substrate is 4E-BP1, which binds to eukaryotic initiation factor 4E (eIF-4E) inhibiting its function. When 4E-BP1 is phosphorylated (and inactivated) by mTORC1, eIF-4E is released from this complex, forming a complex with eIF4G, eIF4A and eIF3 ribosomes, which enhances translation of 5' capped mRNAs (63, 64). The substrates that are important in regulating autophagy are less well characterized, and will be described further in the section on autophagy.

mTOR plays a very important role in cellular and organismal homeostasis due to its central role in regulating metabolic processes both anabolic and catabolic in response to diverse stimuli such as nutrients, energy, growth factor signaling, oxygen and stresses such as DNA damage (65). In addition I have shown that oxidative stress can serve as a regulator of mTOR activity via signaling from ATM, as described in chapter 3.

1.4.2 Regulation of TSC2

TSC2 serves as a nexus in the cell, since it is regulated by multiple upstream mitogenic and energy sensing pathways, and its cellular localization also plays a role in its activity. Under conditions of nutrient deprivation, TSC2 activity is increased via phosphorylation by AMPK at Thr 1227 (Thr 1271 in human) and Ser 1345 (Ser 1387 in human), however other sites including Ser 1337 and Ser 1341 are impacted as a result of mutation of Ser 1345. AMPK activation of TSC2 plays a major role in turning off mTORC1 (ie phosphorylation of S6K) in response to glucose deprivation (ATP depletion), which acts as a survival mechanism to low-energy (66). AMPK phosphorylation of TSC2 at Ser 1345 also functions as a priming event for further activation of TSC2 activity via the Wnt-GSK pathway which is independent of β -catenin activity (67). Wnt signaling therefore acts as a TSC2 activation mechanism via inhibiting GSK3-mediated phosphorylation which is normally an inhibitory event.

When cellular levels of AMP rise due to energy deprivation (therefore increasing the AMP:ATP ratio), AMP binds to the γ -subunit of AMPK (which is a heterotrimer consisting of a catalytic subunit, AMPK α and 2 regulatory subunits called AMPK β and AMPK γ). This binding has been proposed to induce a conformational change in the AMPK complex which improves the ability of AMPK α to serve as a substrate for upstream kinases such as LKB1.

In contrast to AMPK-mediated activation of TSC2, when cells are stimulated with mitogens or growth factors, the PI3K-AKT pathway is activated. As a result, AKT phosphorylates and inactivates TSC2 (68-70) which promotes binding to 14-3-3 in the cytoplasm (71). Five independent AKT phosphorylation sites have been identified, which are shown in figure 5.

. Our lab has previously shown that TSC2 functions in a cellular endomembrane compartment when active, and that as a result of inactivation by AKT, leaves this compartment and binds to 14-3-3 (72). This model for localization-dependent activity of TSC2 is depicted in figure 6.

In addition to activating the PI3K-AKT pathway, mitogens activate the MAPK/ERK pathway which has also been shown to inactivate TSC2 via phosphorylation. Two direct ERK phosphorylation sites, Ser 540 and Ser 664 have been shown to be involved in inhibition of TSC2 function via dissociating the TSC2:TSC1 complex (73). In addition, in response to phorbol esters or activated Ras, RSK can phosphorylate TSC2 in an AKT-independent manner on Ser 1798 and Ser 664 which are inhibitory signals as well (74). Figure 5 summarizes all the known phosphorylation sites on TSC2 that have been described in this section.

Figure 5:

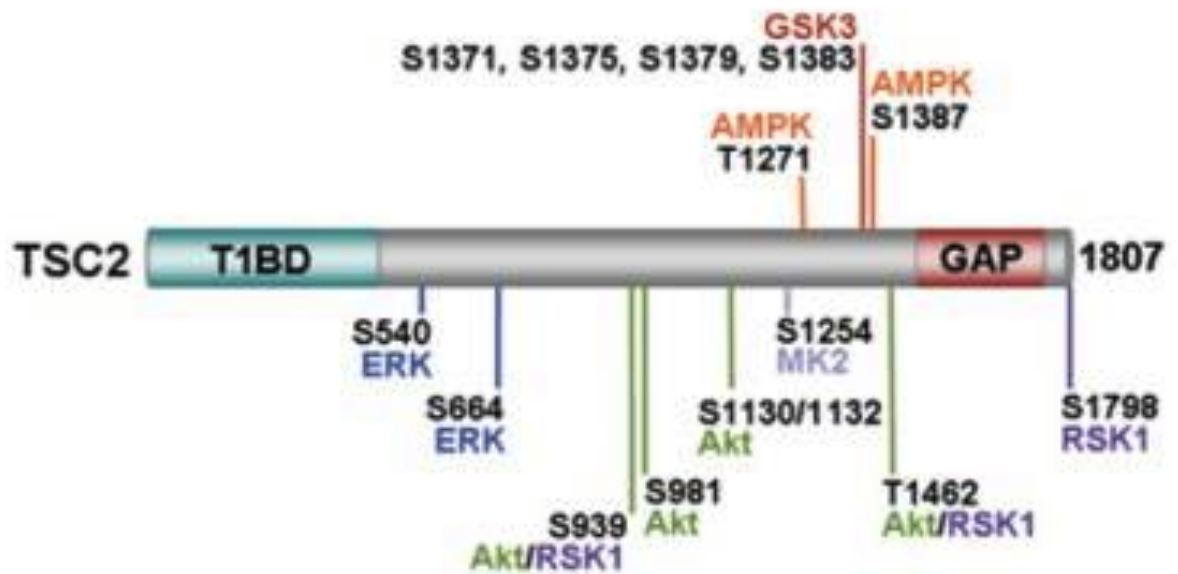


Figure 5: **TSC2 phosphorylation sites based on human nomenclature** A schematic showing the major phosphorylation sites in human TSC2 protein and their upstream kinases

Figure 6:

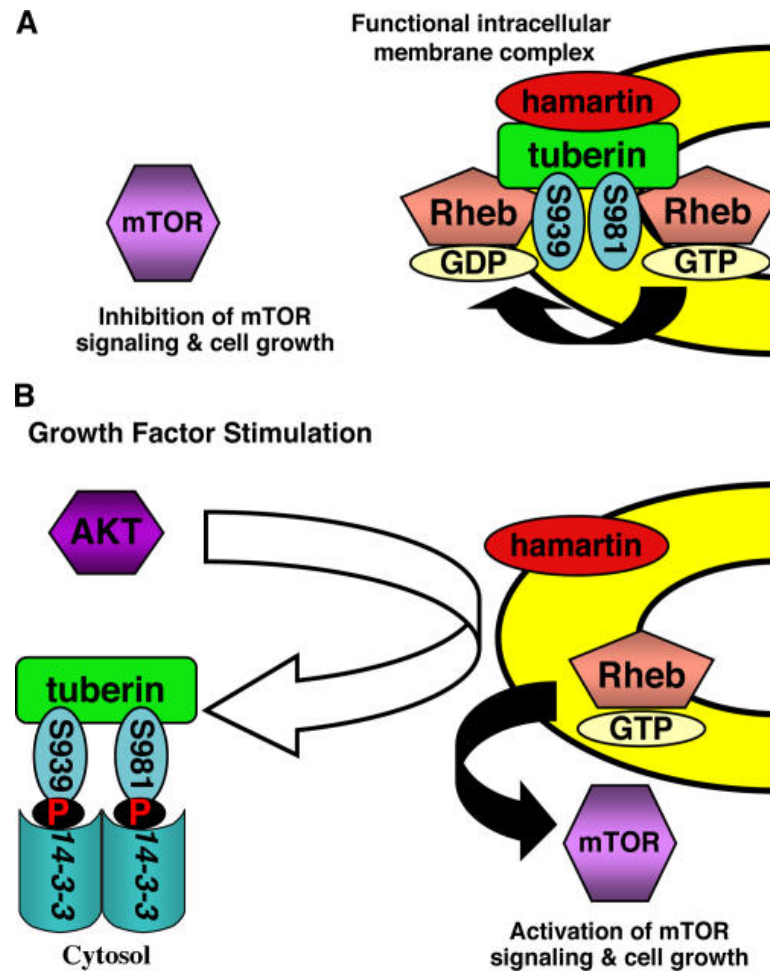


Figure 6: **Model depicting TSC2 localization and function** Active TSC2:TSC1 heterodimers are found in an endomembrane compartment where they can associate with Rheb maintaining it in an inactive GDP-bound form. Upon growth factor stimulation, AKT phosphorylates TSC2 and causes it to leave the membrane and bind to 14-3-3, and as a result Rheb become bound to GTP which allows activation of mTOR (mTORC1 complex). [Reprinted from (72) under Creative Commons License]

1.5 Autophagy

Autophagy is a catabolic process utilized by cells to recycle cellular constituents, via lysosomal degradation (75). There are 3 fundamental forms of autophagy: macroautophagy, microautophagy and chaperone-mediated autophagy (CMA) which more similar to microautophagy (76, 77). Macroautophagy involves *de novo* formation of an isolation membrane which surrounds the cargo to be degraded, in contrast to microautophagy which engulfs material directly into the lysosome. The source of this autophagosome membrane is still a controversial area of research, however there is strong evidence that both the plasma membrane and the mitochondria can provide these lipids in mammals (78-80) and in yeast the golgi has been identified as an additional potential membrane source (81, 82). Chaperone-mediated autophagy involves translocation of unfolded proteins across the lysosome membrane with the assistance of the chaperone protein Hsc70 which is both in the cytoplasm and in the lumen of the lysosome.

A variety of cellular components are targeted for degradation by autophagy including individual proteins, protein aggregates, ubiquitinated substrates and entire organelles can be engulfed. Many organelles are degraded by specific forms of autophagy such as mitophagy (for mitochondria), pexophagy (for peroxisomes), ERphagy (for endoplasmic reticulum) and ribophagy (for ribosomes). Once this membrane completely surrounds the cytoplasmic material, the vesicle becomes known as the autophagosome, which fuses to the lysosome which contains the proteases and other enzymes which degrade the contents. Figure 7 shows a schematic of the autophagy process. As a result, basic molecular building blocks (such as free amino acids and fatty acids) are released back into cells, which avoids the expenditure of energy to unnecessarily make these components. However, autophagy can also be a major component of type II non-apoptotic programmed cell death if taken too far.

The physiological role for autophagy appears to be primarily a stress response, as many types of stresses (including nutrient deprivation, oxidative stress and DNA damage)

Figure 7:

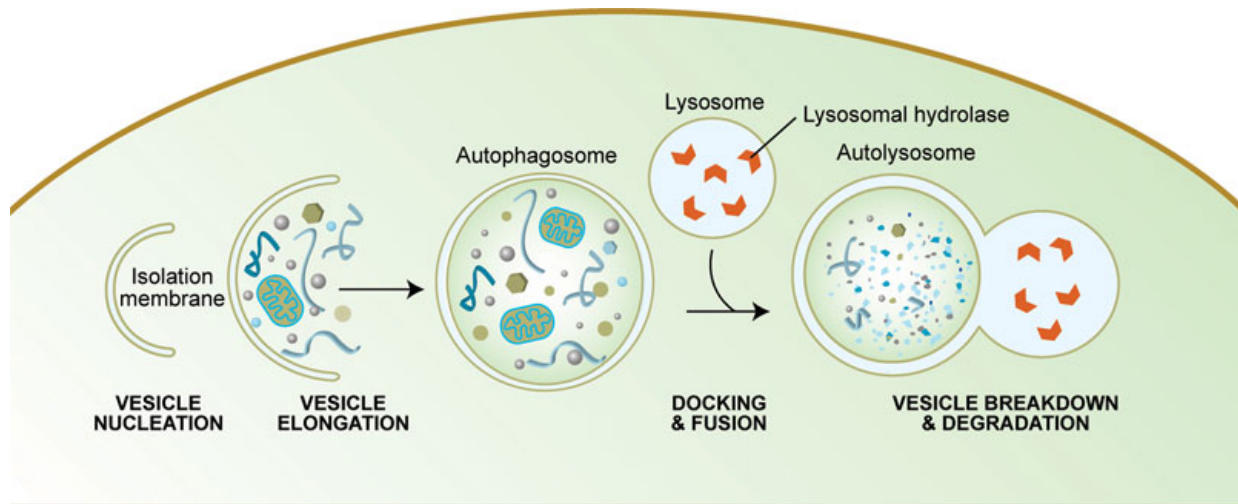


Figure 7: **Schematic of the autophagy process from engulfment of cargo to degradation.**

Autophagy begins by nucleation of an membrane which surrounds the cytoplasmic cargo to be degraded, forming an autophagosome, which then docks and fuses with a lysosome carrying enzymes such as hydrolases which catalyze the breakdown process in the autolysosomes.

[Reprinted from (83), under Creative Commons License]

induce autophagy, however even unstressed cells have a low basal rate of autophagy for turning over long-lived proteins (84). In addition, damaged organelles are often removed by autophagy, suggesting that autophagy also plays a quality control mechanism within cells to maintain optimal function. Not all of these pathways are fully characterized, but are being actively pursued by many laboratories including our own. It is known that autophagy is executed via a ubiquitin-like conjugation system involving a large number of core autophagy related genes, which are known as Atg genes (eg Atg5, Atg7 and Atg12). More than 30 Atg genes have been identified primarily from studies in yeast, but many have mammalian homologs (85).

1.5.1 Autophagy, physiology and disease

Inappropriate regulation of autophagy resulting from gains or losses of autophagy-regulating genes (or lysosomal genes) or dysregulation of signaling pathways that regulate autophagy have been linked to the pathophysiology of many diseases, including cancer, neurodegenerative disorders, and cardiovascular diseases (86, 87). A brief description of some of the roles of autophagy in physiology and disease will be discussed in the following section, but by no means will this be a comprehensive discussion of this broad topic which could fill many theses.

Autophagy is now thought to be a tumor suppressing mechanism early on in the development of tumors, but later on can be subverted by tumors to maintain proliferation capacity in spite of metabolic stress, hypoxia or other types of stresses including many types of therapy (88). In normal cells, autophagy plays an important housekeeping/quality control role in removing defective proteins and organelles, as well as maintaining genomic stability by limiting DNA damage and oxidative stress. One important protein involved in autophagy induction called beclin 1, which is a Bcl-2 interacting protein, has been shown to be a *bona fide* tumor suppressor gene from observations that this gene is monoallelically deleted in 40-75% of human breast, ovarian and prostate cancers. When beclin 1 is re-introduced into

cancer cells with loss of heterozygosity for beclin 1 (such as MCF7 cells), there is a significant decrease in proliferation, clonogenicity and *in vivo* tumorigenic potential (89). Studies in beclin 1 heterozygous mice have also supported the notion that beclin 1 is a tumor suppressor, since these mice develop more spontaneous tumors from a variety of tissues (including breast and lung carcinomas, hepatocellular carcinomas and lymphomas) (90).

Once tumors have developed, it is now generally believed that the role of autophagy switches to a pro-survival function since the cell can recycle constituents that are no longer needed, which serves as a backup energy source to maintain viability. Metabolic stress robustly activates autophagy which prolongs survival in apoptosis-deficient cells (a common feature in cancer cells). Recently Eileen White's and Alec Kimmelman's laboratory have discovered there are some tumor types that are addicted to autophagy to maintain oxidative metabolism, including pancreatic cancers and other Ras-driven tumors, which provides rationale for targeting these tumors with autophagy inhibitors such as chloroquine (91, 92).

There is significant crosstalk between autophagy and apoptosis, such as that seen in the DNA damage response, where induction of autophagy can delay apoptosis, and result in delayed caspase-independent cell death in noninvasive tumors. Unfortunately once the tumors have progressed and developed resistance to the genotoxic damage stimuli, this autophagic survival pathway is no longer relevant (93).

Autophagy can play a defense role against infection by a large variety of pathogens, in addition to more classical endocytic-phagocytic mechanisms of removing bacteria via delivery to the lysosome (94). Viruses are another class of pathogens that can be eliminated via autophagy. In contrast to bacterial-induced autophagy which is triggered by bacterial wall proteins, virus-induced autophagy is thought to be triggered as a consequence of the host cell secreting cytokines such as interferons. Some of these downstream pathways overlap with ER stress pathways that utilize the eIF2 α family of kinases that positively regulate autophagy, for example the dsRNA-dependent protein kinase PKR, PERK and GCN2. For a more detailed description of these pathways see (95, 96).

In the brain, autophagy is thought to be particularly important in neuroprotection, in its quality control role (97, 98). Since most mature neurons don't divide, individual cells must rely on basal autophagy to remove damaged organelles, unlike other somatic cycling cells which can gradually dilute out damaged organelles during cell division, even if there are minor decreases in autophagic flux over time. A large number of adult-onset neurodegenerative disorders have been linked to defective autophagy involving both decreased autophagosome formation as well as later stages of fusion and lysosomal degradation. Some particularly notable examples of diseases with strong evidence for defective autophagy are Alzheimers disease, ALS and Parkinson's disease. The ubiquitin ligase, Parkin and upstream kinase PINK1 are proteins that are frequently mutated in Parkinson's disease, and these proteins both are important in mitophagy of mitochondria with low membrane potential (99). In Parkinson's disease, the accumulation of damaged mitochondria is thought to be important in the pathophysiology of the disease. However autophagy not only is important for organelle homeostasis but also in the removal of aggregation-prone proteins, which are often caused by the disease-linked genetic mutations and are major sources of toxicity, such as tau in Alzheimers disease. Research into mechanisms of pharmacologically upregulating autophagy in a tissue-specific manner in these disease settings is now a major area of interest for pharmaceutical companies.

1.5.2 Regulation of autophagy

Over the past 10 years, a large number of signaling pathways have been identified as autophagy regulatory mechanisms, most of which promote autophagy induction. mTORC1 was the first pathway identified however that negatively regulates autophagy. While the precise mechanism remained elusive for many years, recently ULK1 has emerged as an mTORC1 substrate involved in regulating an early step in autophagosome formation (100-102). ULK1 is a part of a large protein complex in cells that also contains FIP200 and ATG13, which are both required for the localization of this complex to the isolation membrane and for

regulating the kinase activity of ULK1. A dual model has now emerged involving multiple phosphorylation events by AMPK or mTORC1 depending upon energy status. When cells are starved, AMPK is activated, and promotes autophagy via phosphorylating ULK1 at Ser 317 and Ser 777. However when nutrients are not limiting, mTORC1 activity is elevated, and as a result a different ULK1 phosphorylation site (Ser 757) is increased, which disrupts the interaction between AMPK and the ULK1 complex (103).

Another pathway for regulation of autophagy that has particular relevance to our studies is p53, one of the most frequently mutated genes in cancer (104, 105). p53 is a transcription factor that is stabilized in response to many types of stresses, and as a result transcriptionally regulates many genes important in damage responses, including DNA repair, cell cycle checkpoints and senescence. However in addition to these roles it also regulates autophagy by two separate mechanisms that are dependent upon its cellular localization. Nuclear p53 has been shown to positively regulate autophagy by transcriptionally upregulating genes such as sestrin 2, DRAM and ISG20L1 (106-108). However cytoplasmic p53 can also inhibit autophagy via inhibiting AMPK (109), and it is this function of p53 which is usually dominant in cells.

All three major MAPK kinase pathways have been shown to regulate autophagy. ERK1/2 have been shown to promote autophagy in human colorectal carcinoma cells via phosphorylating G α -interacting protein (110). This process was later shown to be antagonized by amino acid induced inhibition of Raf1, which is upstream of ERK activation (111). In addition to general macroautophagy induction, ERK2 has been shown to positively regulate mitophagy, a specific form of autophagy that degrades mitochondria (112). In general, it has been shown that ERK-regulated autophagy leads to type II-programmed cell death in response to a variety of toxicants or secondary to neuronal disease (113-117). The JNK arm of the MAPK pathway also promotes autophagy, however the functional outcome is much more variable. ER-stress induced JNK activation leads to enhanced survival (118), whereas JNK that is activated by etoposide, staurosporine, or with ceramide (which is a cellular second

messenger in stress and radiation responses), autophagic cell death occurs (119, 120). A non-canonical form of autophagy that is dependent on ERK and JNK activation, but is beclin 1 independent has been reported to be induced in response to ROS in cancer cells, and this autophagic response results in cell death by both autophagy and apoptosis (121). In this report, Atg 7 was identified as a downstream target of JNK activity. In contrast to ERK and JNK, the p38 α MAPK has been shown to inhibit both basal and starvation-induced autophagy via interfering with Atg9 translocation from the transgolgi network to the autophagosome membrane by competing for binding to a newly identified p38-interacting protein called p38IP (122). p38 α is known to be activated by osmotic stress and also after ionizing radiation. The functional consequence of autophagy inhibition by p38 is not completely clear, although one study showed that treatment of colorectal cancer cells with a p38 inhibitor resulted in autophagic cell death, suggesting that activation of p38 is a survival mechanism (123, 124).

Transforming growth factor β (TGF β), a multifunctional cytokine that regulates growth and differentiation of many cell types also promotes autophagy in hepatocellular carcinoma and mammary carcinoma cells (125). This mechanism of autophagy regulation requires both type I and type II receptors, and involves both activation of Smads, as well as signaling via JNK, which as previously described induces autophagy. Many of the classic molecules that are important in autophagy are upregulated by TGF β exposure, including beclin 1, ATG5, ATG7 and DAPK.

A final potentially relevant pathway of regulating autophagy in response to damage is the RB-E2F pathway. The first study implicating this pathway found that E2F1 could directly transcriptionally regulate a number of autophagy regulating genes including LC3, ATG1, ATG5 and DRAM (126). Later studies showed however that E2F1 can also inhibit autophagic flux via blocking fusion of the autophagosome with the lysosome (127, 128). DNA damage can activate E2F1 via ATM/ATR phosphorylation of Ser 31 which promotes stabilization of the protein (129).

Materials and Methods

2.1 Antibodies, equipment and reagents

A complete list of antibodies used may be found in table 2, and were from the following companies: Cell Signaling Technologies (Danvers, MA), Sigma-Aldrich (St. Louis, MO), Santa Cruz Biotechnology (Santa Cruz, CA), Epitomics (Burlingame, CA), R&D Systems (Minneapolis, MN), BD Biosciences (San Diego, CA), Zymed/Invitrogen (Carlsbad, CA) Abcam (Cambridge, MA) and GeneTex (Irvine, CA).

Most of the reagents we utilized were purchased from Sigma-Aldrich (St. Louis, MO) including hydrogen peroxide (H_2O_2 , which was purchased fresh approximately monthly), N-acetyl cysteine (which was dissolved in water immediately prior to treatment), DMSO, etoposide (which was dissolved in DMSO), doxorubicin (which was dissolved in water), neocarzinostatin, bovine catalase (which was dissolved in 50mM potassium phosphate buffer), and chloroquine (which was dissolved in water immediately prior to treatment). Compound C was from EMD/Calbiochem (San Diego, CA). Rapamycin, leptomycin B and cisplatin were purchased from LC Laboratories (Woburn, MA).

Cells were irradiated in closed plates with a Rad Source 2000 (Suwanee, GA) irradiator and returned to a 37°C incubator until harvesting. All cell media was purchased from Invitrogen (Carlsbad, CA) as pre-made solutions except for F12K which was purchased from American Type Culture Collection (ATCC). Fetal bovine serum was purchased from Hyclone/Fisher Scientific (Logan, UT) or more recently, Sigma-Aldrich (St. Louis, MO). Geneticin (G418) and puromycin were purchased from Sigma-Aldrich (St. Louis, MO).

2.2 Cell culture

All cells were grown in antibiotic-free conditions, except as described below, in a humidified 37°C incubator with 5 or 10% CO_2 . MCF7 breast carcinoma cells (from ATCC) were

Table 2

Protein	Source	Catalog #
4E-BP1	Cell Signaling Technologies	9452
Phospho-4E-BP1 (T37/46)	Cell Signaling Technologies	9459
ACC	Cell Signaling Technologies	3662
Phospho-ACC (S79)	Cell Signaling Technologies	3661
AMPK	Cell Signaling Technologies	2532
Phospho-AMPK (T172)	Cell Signaling Technologies	2531
ATM (2C1 mAb)	GeneTex	GTX70103
Phospho-ATM (S1981)	R & D Systems *	AF1655
Phospho-ATM (S1981)	Epitomics **	2152-1
B-integrin	BD Biosciences	610467
Catalase	Abcam	ab1877
Flag (M2)	Sigma-Aldrich	F3165
Gamma tubulin (GTU-88 clone)	Sigma-Aldrich	T6557
GAPDH	Santa Cruz Biotechnology	sc-25778
Lamin A/C	Cell Signaling Technologies	2032
LC3	Cell Signaling Technologies	2775
LDH	Chemicon	AB1222
LKB1	Cell Signaling Technologies	3050
Phospho-LKB1(T366)	(Dario Alessi Laboratory)	(N/A)
mTOR	Cell Signaling Technologies	2972
Myc	Santa Cruz Biotechnology	sc-40
p53	Cell Signaling Technologies	2524
p62	Santa Cruz Biotechnology	sc-28359
Phospho-p53 (S15)	Cell Signaling Technologies	9284
PMP70	Zymed (Invitrogen)	71-8300
Rheb	Cell Signaling Technologies	4935
S6	Cell Signaling Technologies	2217
Phospho-S6 (S235/6)	Cell Signaling Technologies	2211
S6K	Cell Signaling Technologies	9202
Phospho-S6K (T389)	Cell Signaling Technologies	9205
TSC1(5C8A12 mAb)	Zymed (Invitrogen)	37-0400
TSC2	Epitomics	1613-1
* Used for most of work		
** Used for human cells only		

Table 2: List of antibodies used and source

maintained in Improved Modified Eagle's Medium (IMEM) supplemented with 10% FBS. MCF7 cells stably expressing GFP-LC3 (kindly provided by Dr Gordon Mills, UT MD Anderson Cancer Center, Houston, TX) were maintained in RPMI 1640 supplemented with 10% FBS. *Tsc2*^{+/+}/*p53*^{-/-} and *Tsc2*^{-/-}/*p53*^{-/-} MEFs (kindly provided by Dr David Kwiatkowski, Harvard Medical School, Boston, MA) were maintained in Dulbecco's MEM (DMEM) supplemented with 10% FBS. ATM-deficient human lymphoblasts (GM01526) and control ATM-proficient human lymphoblasts (GM02184) (both purchased from Coriell Cell Repositories) were maintained in RPMI 1640 supplemented with 15% FBS. HeLa S3 (from ATCC) were maintained in F12K supplemented with 10% FBS. ATR-proficient fibroblasts (GM15871) and ATR-deficient fibroblasts (GM18366) were purchased from Coriell Cell Repositories, and maintained in Dulbecco's MEM supplemented with 15% FBS. The HeLa S3 derived clones expressing wild-type or mutant LKB1 were selected in and maintained in F12K supplemented with 800µg/mL G418 and 10% FBS. HEK 293 cells (kindly provided by Dr Yinling Hu, UT MD Anderson Cancer Center, Smithville, TX) were maintained in DMEM supplemented with 10% FBS. Primary MEFs were derived from genotype-confirmed *Atm*^{+/+}, *Atm*^{+/-} and *Atm*^{-/-} embryos at about E13 and maintained in DMEM supplemented with 10% (15% for the *Atm*^{-/-} lines) FBS and 1X pen-strep. Hela cells (kindly provided by Dr Mark Bedford UT MD Anderson Cancer Center, Smithville, TX) were maintained in Eagle's MEM supplemented with 10% FBS. SKOV3 ovarian carcinoma cells (kindly provided by Dr Gordon Mills, UT MD Anderson Cancer Center, Houston, TX) were maintained in RPMI 1640 supplemented with 10% FBS. Vector and ATG5-shRNA transfected SKOV3 clones were generated by a standard protocol allowing clonal selection and expansion in McCoy's 5A media supplemented with 10% FBS, 0.5µg/mL puromycin and 2mM L-Glutamine (Invitrogen, Carlsbad, CA), which was kept constant during experiments.

2.3 Plasmids

All of the plasmids I used apart from wild-type and mutant LKB1 were previously available in the laboratory. Full length TSC2 and TSC1 cDNAs were subcloned into pCMV-Tag2 as reported in (72). Mutants of TSC2 were generated by site-directed mutagenesis using the Stratagene (Austin, TX) Quikchange II Kit. The AMPK2A mutant contains alanine substitutions at Thr 1271 and Ser 1387. Human Rheb was subcloned by PCR from GST-Rheb into pCMV-Tag3B to generate a Myc-tagged construct. Hemagglutinin (HA)-tagged S6K was kindly provided by Dr John Blenis (Harvard Medical School, Boston, MA). Histidine-tagged LKB1 was kindly provided by Dr Ming-Hui Zou (University of Oklahoma Health Science Center, Oklahoma City, OK). All of the constructs were sequenced for validation prior to using for experiments.

2.4 Measurement of ROS by 5-6-chloromethyl-2',7'-dichlorohydrofluorescein (CM-H₂-DCFDA)

Cells were trypsinized from plates and counted. Equal numbers of cells (usually 250,000 cells per well) were placed into wells (n=3-6) of a black-bottomed 96-well plate and centrifuged at 1000 rpm for 10 minutes. The cells were then resuspended in the cell-permeable dye, CM-H₂-DCFDA [(Invitrogen, (Carlsbad, CA)] at a concentration of 10 μ M (dissolved in DMSO and then 1X PBS). The plate was incubated at 37°C for 30 minutes in the dark, since DCFDA is light-sensitive. The resulting fluorescence which is proportional to the amount of ROS in the cells (130) was measured with a Synergy HT Multidetector Microplate Reader (BioTek Instruments Inc, Winooski, VT) at an excitation wavelength of 485/10nm and an emission wavelength of 528/20nm.

2.5 Western Blots

Cell lysates were prepared for SDS-PAGE by scraping into lysis buffer [20mM Tris HCl (pH7.5), 150mM NaCl, 1mM Na₂EDTA, 1mM EGTA, 1% Triton X-100, 2.5mM Na₂P₂O₇ and

1mM β -glycerophosphate]. The following inhibitors were added to individual aliquots of buffer immediately prior to being added to cells and the unused portion was discarded: 1mM phenylmethylsulfonyl fluoride, 1mM Na_3VO_4 , 1mM NaF and 1X protease inhibitor cocktail (Roche, Indianapolis, IN).

Protein concentration was determined using the Pierce BCA assay (Thermo Fisher Scientific, Rockford, IL) and typically 30 μ g of total protein was loaded per lane. The BioRad (Hercules, CA) Criterion precast gel system was utilized for western blots performed by standard methods. For experiments requiring quantitation, films were scanned manually and densitrometry performed using ImageQuant software. For signaling studies requiring normalization, the phosphorylated protein density was divided by the total protein density, and the control was set to 1.

2.6 siRNA transfection

Chemically synthesized siRNA SMARTpools were obtained from Dharmacon (Thermo Fisher Scientific, Rockford, IL). The catalog numbers of the each siRNA pool ordered are:

- Human TSC2: M-003029-02
- Human ATM: L-003201-00-05
- Human ATR: L-003202-00
- Human LKB1: L-005035-00
- Human p53: M-003329-01
- Negative control/RISC-free: D-001220-01 (contains at least four mismatches to all known human, mouse and rat genes)

The oligonucleotides were resuspended in 1X buffer (Dharmacon) to a stock concentration of 20 μ M.

MCF7 cells were plated in 35mm plates approximately 36 hours prior to transfection. The stock concentrations of siRNA were diluted 1:100 in 1X buffer (making a final concentration of 10nM), and DharmaFECT1 transfection reagent was diluted 1:50 in OptiMEM

medium (Invitrogen, Carlsbad, CA). The diluted siRNA and diluted DharmaFECT were then incubated for 30 minutes at room temperature in a 1:2 ratio in a total volume of 600 μ L. The cells were washed with OptiMEM and regular IMEM medium was replaced to a total volume of 4mL plate (accounting for the 600 μ L of transfection master mix to be added). Knockdown efficiency was determined by western analysis at 48 hours after transfection; and hydrogen peroxide or DNA damaging agents were added as indicated in the figure legends.

2.7 Immunoprecipitation

HEK 293 cell lysates were prepared in lysis buffer as described in the previous section. Equal masses were aliquoted into tubes and made up to 300 μ L with PBS, precleared for 1 hour with protein A agarose beads (Santa Cruz Biotechnology, Santa Cruz, CA). After spinning down, the supernatant was incubated with LKB1 antibody at 1:100 dilution using a fresh aliquot of protein A beads overnight. After 3 washes with lysis buffer containing protease and phosphatase inhibitors as described previously, samples were boiled and loaded directly into gels.

2.8 TSC2 functional assay

HEK 293 cells were plated approximately 24 hours prior to transfection in 6-well plates to be 60-70% confluent at transfection. Mastermixes were made containing 3.3 μ g Flag-TSC2, 0.9 μ g Flag-TSC1, 0.4 μ g Myc-Rheb and 0.4 μ g HA-S6K DNA in OptiMEM and 10 μ L Lipofectamine 2000 (Invitrogen, Carlsbad, CA).

2.9 Subcellular fractionations

Cytoplasm and nuclear fractions were performed as described in (131). Briefly, cells were scraped into ice-cold hypotonic buffer [10mM HEPES (pH 7.2), 10mM KCl, 1.5mM MgCl₂, 0.1mM EGTA], dounced in a dounce homogenizer prior to centrifugation at 3,000rpm for 10 minutes in the cold room. The supernatant was collected as the cytoplasmic fraction, and the

pellet was re-dounced into hypotonic buffer to break up any remainins cells, and re-centrifuged. The pellet was the then washed three times in nuclear washing buffer [10mM Tris HCl (pH 7.4), 0.1% NP-40, 0.05% sodium deoxycholate, 1.5mM MgCl₂] and the nuclei extracted by incubation in ice-cold high-salt lysis buffer [20mM HEPES (pH 7.4), 0.5M NaCl, 0.5% NP-40, 1.5mM MgCl₂] for 2 hours in the cold room. The insoluble material was centrifuged out, and the supernatant removed into clean tube as nuclear fraction.

For the studies described in chapter 5, a modified protocol for isolating cytoplasmic, nuclear and membrane fractions was performed as described in (72).

Peroxisome fractionation was performed using the Peroxisome Isolation Kit from Sigma-Aldrich (St. Louis, MO) according to the manufacturer's instructions except that the volumes of the reagents were halved because our ultracentrifuge columns were too small to fix the entire volume as described in the manual.

2.10 GFP-LC3 localization

MCF7 cells stably transfected with GFP-LC3 were plated on Labtek II chamber slides and allowed to equilibrate for 24 hours. Cells were exposed to vehicle, rapamycin, or H₂O₂ for 1 hour and fixed for 10 minutes in 1:1 acetone/methanol. Coverslips were mounted using Prolong Gold antifade reagent (Invitrogen, Carlsbad, CA) and stored at -20°C until use. 20X images were captured using the panoramic setting on a Zeiss confocal microscope. Images were analyzed manually for presence of greater than 5 puncta per cell. Data is represented as puncta positive cells normalized to total number of GFP positive cells.

2.11 Electron microscopy studies

Cells were plated in 6-well plates and treated as indicated. After treatment, cells were rinsed with 0.1M sodium cacodylate buffer (pH 7.3) twice at room temperature, then fixed in fixation buffer containing 2% paraformaldehyde, 3% glutaraldehyde in 0.1M sodium cacodylate for 1 hour and stored at 4°C until setup for imaging by the electron microscopy core facility.

2.12 Animal studies

The care and handling of mice were in accordance with National Institute of Health guidelines and Association for the Accreditation of Laboratory Animal Care-accredited facilities, and all protocols involving the use of these animals were approved by the MD Anderson Animal Care and Use Committee. *Atm*^{+/+}, *Atm*^{+/-} and *Atm*^{-/-} mice on a pure 129 background were maintained on-site, on a 12-hour light/dark cycle as described in (132). For experiments involving starvation, the animals were kept overnight without food, but allowed water ad libitum throughout. Rapamycin treatment was performed by daily intraperitoneal injection of 200 μ L, equivalent to a dose of 15mg/kg, with TPE (Tween-80, polyethylene glycol and ethanol used as vehicle).

For histology sections, tissues were fixed for 24 hours in 10% neutral buffered formalin, prior to being stored in 70% ethanol before paraffin embedding, sectioning and staining by the UT MD Anderson Cancer Cancer Histology and Tissue Processing core facility on site. Sections were stained with hematoxylin and eosin to identify pathological features, and immunohistochemistry was performed using phospho-S6 (Cell Signaling Technology, Danvers, MA), p53 (Oncogene Science, Cambridge, MA), or Ki67 (Cell Signaling Technology, Danvers, MA) antibodies.

2.13 Immunofluorescence

Hela cells were plated onto chamber slides 18-24 hours before transfection with the indicated plasmids. At about 24 hours after transfection, the cells were fixed with 4% paraformaldehyde (in PBS) for 10 minutes, washed and stained by standard protocol as described in (131).

2.14 Peroxisomal protease assay

Protease protection was performed as described in (133). Briefly, crude peroxisome fraction was equally distributed to tubes containing freshly prepared proteinase K (Roche, Indianapolis, IN) at a final concentration of 100 μ g/mL. As a control, whole cell lysate in 1X lysis buffer was

used to monitor protease digestion over the incubation time. Samples were then split into two groups, one with 1% Triton X-100, and incubated on ice for 5, 10 or 30 minutes. Reactions were stopped by addition of PMSF and immediately processed for western analysis.

2.15 Cell growth assays

Cells were plated at 30,000 cells per well in 6-well plates approximately 24 hours prior to treatment. On the day of treatment, the media was aspirated and fresh media containing cisplatin or vehicle (0.9% NaCl) was added. After 48 hours of incubation the cells were counted using a coulter counter and cell number recorded.

Identification of ROS induced activation of cytoplasmic ATM signaling pathway to activate LKB1, AMPK and TSC2 to repress mTOR and induce autophagy

3.1 Introduction

ATM has been postulated to play a role in oxidative stress responses due to the finding that in ATM-deficient cells, high levels of ROS exist. Dysregulation of ROS in these cells has been linked to disease etiology both in lymphomagenesis as well as neurodegeneration. However, the underlying mechanism of how ATM acts as a ROS sensor and signals to other proteins as part of this oxidative damage response is not well characterized. Similarly, TSC2 deficient cells have been shown to possess elevated ROS, but the mechanism is unclear. These findings led us to ask whether ATM and TSC2-deficiency leads to elevated ROS via a similar pathway or not.

While our study did not set out to characterize an ATM-dependent stress response, we found a novel mechanism by which a specific cytoplasmic pool of ATM could signal to mTOR to induce autophagy. During our work however, additional mechanisms of ROS-induced autophagy have been identified as described in the introductory chapter.

The main focus of our lab over the recent years has been characterizing the functions of the TSC2 tumor suppressor. Our interest in the role of this protein in stress/damage responses was peaked by a report that activation of the p53 transcription factor, which occurs in response to many damaging agents, resulted in mTORC1 suppression and subsequent induction of autophagy (134). Since up until a few years ago, TSC2 was thought to be the primary cellular gatekeeper of mTORC1 activity, we hypothesized that TSC2 activation would mediate mTORC1 suppression by DNA damage, and possibly oxidative stress as well, since oxidative-induced damage of DNA could lead to p53 activation (105).

The pathway we found involves ATM phosphorylation of LKB1, which results in AMPK activation and TSC2 activation to repress mTORC1 and induce autophagy. Importantly, unlike the previously identified DNA damage pathway, this ROS-induced signaling pathway does not

require p53 activity. In chapter 6 I will elaborate further on DNA damage-induced signaling pathways resulting in mTORC1 suppression.

3.2 Results

3.21 Confirmation of elevated ROS levels in ATM and Tsc2-deficient cells

To optimize the protocol for measuring ROS levels using the fluorescent dye, 5,6-chloromethyl-2'7'-dichlorodihydrofluorescein diacetate (CM-H₂-DCFDA) in cultured cells, we obtained immortalized human lymphoblasts from AT-patients and control non-AT-patients to establish conditions where we could reproducibly detect differences between these cell lines. Figure 8 shows that ROS levels are increased by 2.6 fold in ATM-deficient cells versus ATM-expressing control cells ($p < 0.05$). Similarly, we confirmed the earlier finding that TSC2-deficiency results in elevated ROS (figure 9) using Tsc2-proficient and Tsc2-deficient MEFs, which were on a p53-deficient background since p53-inhibition is required to establish long-term proliferating cultures of these cells to override strong p53- and p21-dependent cellular senescence program (135).

To determine whether this common phenotype between ATM and Tsc2-deficient cells occurred as a result of a single downstream pathway, we utilized an siRNA approach where we reduced the expression of either ATM, TSC2 or both simultaneously, and measured the resulting ROS levels. Figure 10 shows that loss of both ATM and TSC2 does not further increase the ROS level beyond loss of either gene alone, showing that these genes are epistatic.

The next question we asked was whether elevated ROS in these cells was mTORC1-dependent, so we treated both sets of cell lines with 200nM rapamycin or vehicle control (DMSO), a selective mTORC1-inhibitor overnight, and measured the ROS levels in the cells. Figures 11 and 12 show that rapamycin could rescue the elevated ROS levels in both Tsc2-deficient and ATM-deficient cells. These results therefore place the ATM-TSC2 pathway at a critical point in a feedback loop between ROS levels and mTORC1 activity (figure 13).

Figure 8:

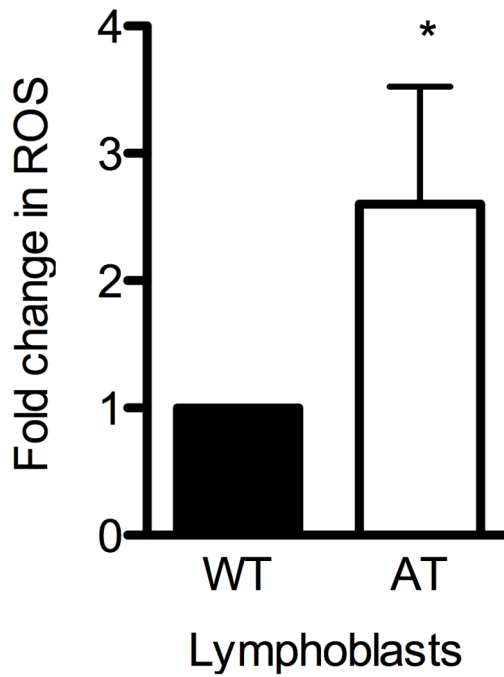


Figure 8: **Confirmation of elevated ROS in ATM-deficient cells** ATM proficient (GM02184) and ATM-deficient (GM01526) lymphoblasts were plated 24 hours prior to measurement of ROS by DCFDA method. Graph represents normalized values from 3 independent experiments, with 4 wells per cell line. The asterisk signifies statistical significance using one-sided students t-test ($p < 0.05$). [(Reprinted from (146))]

Figure 9:

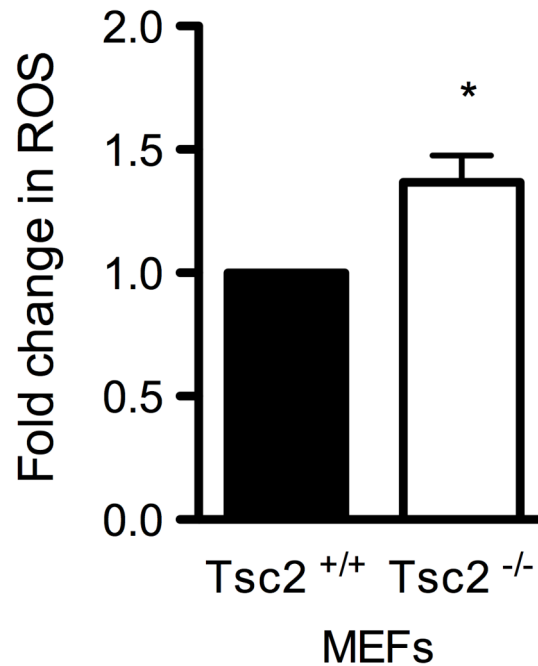


Figure 9: **Confirmation of elevated ROS in Tsc2-deficient cells** Tsc2 proficient (Tsc2^{+/+}, p53^{-/-}) and Tsc2-deficient MEFs (Tsc2^{-/-}, p53^{-/-}) were plated 24 hours prior to measurement of ROS by DCFDA method. Graph represents normalized values from 3 independent experiments, with 3 wells per cell line. The asterisk signifies statistical significance using one-sided students t-test (p<0.05). [(Reprinted from (146))]

Figure 10:

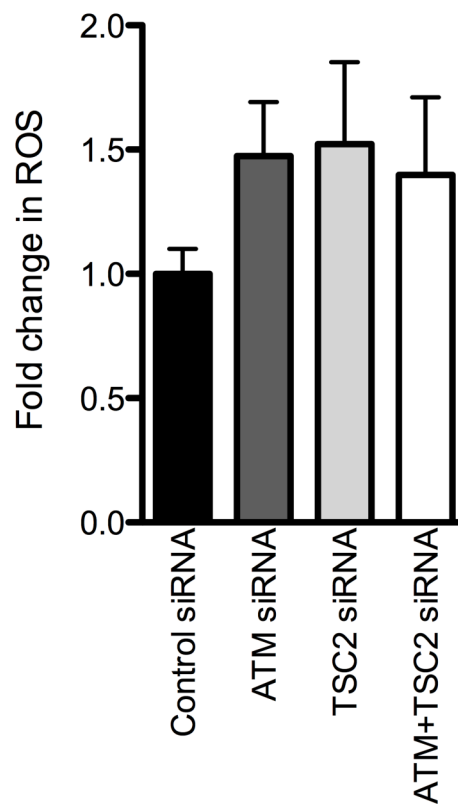


Figure 10: **ATM and TSC2 are epistatic in oxidative stress response** MCF7 cells were transfected with the indicated siRNAs 48 hours prior to measurement of ROS by DCFDA method. Graph represents normalized values from 4 wells per cell line.

Figure 11:

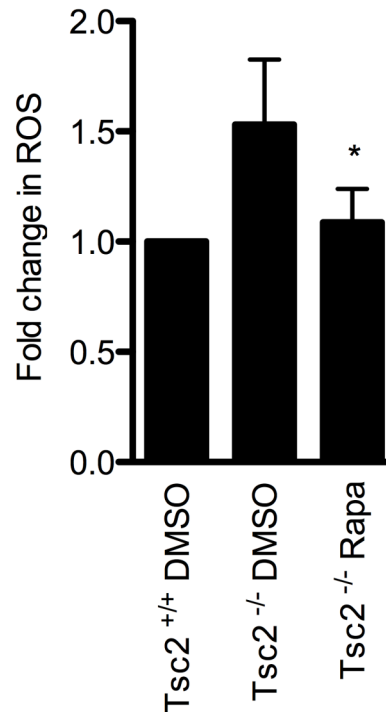


Figure 11: **Rapamycin rescues elevated ROS levels in Tsc2-deficient MEFs.** Tsc2 proficient (Tsc2^{+/+}, p53^{-/-}) and Tsc2-deficient MEFs (Tsc2^{-/-}, p53^{-/-}) were plated 24 hours prior to treatment with vehicle (DMSO) or 200nM rapamycin. ROS levels were measured by DCFDA method after 24 hours of treatment. Graph represents normalized values from 3 independent experiments, with 4 wells per cell line. The asterisk signifies statistical significance using one-sided students t-test (p<0.05). [(Reprinted from (146))]

Figure 12:

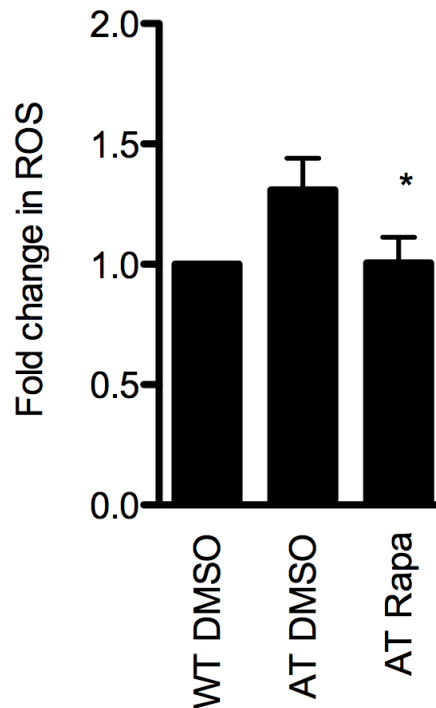


Figure 12: **Rapamycin rescues elevated ROS levels in ATM-deficient lymphoblasts** ATM proficient (GM02184) and ATM-deficient (GM01526) lymphoblasts were plated 24 hours prior to treatment with vehicle (DMSO) or 200nM rapamycin. ROS levels were measured by DCFDA method after 24 hours of treatment. Graph represents normalized values from 3 independent experiments, with 4 wells per cell line. The asterisk signifies statistical significance using one-sided students t-test ($p < 0.05$). [(Reprinted from (146)]

Figure 13:

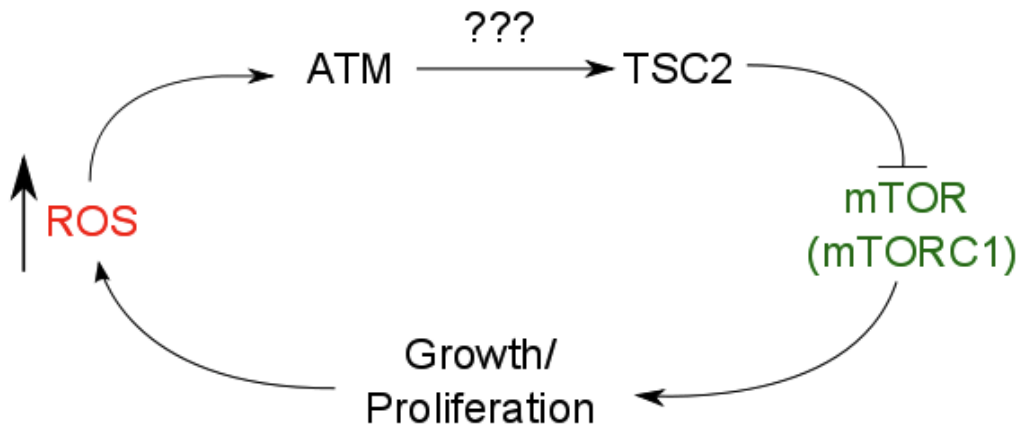


Figure 13: **Feedback model for the role of ATM and TSC2 in coordinately regulating mTOR and ROS levels**

3.2.2 ROS induced mTOR suppression

In the previous section, an ROS-mTORC1 feedback loop was established. To begin mechanistic studies into this phenomenon, we asked whether mTORC1 repression would occur in cells treated with ROS-generating agents. For most of these studies, we utilized hydrogen peroxide (H_2O_2) as a tool compound due to the fact that it is membrane permeable and readily diffusible into cells. While hydrogen peroxide does not contain unpaired electrons itself, it can be readily converted into more aggressive radical species such as the hydroxyl radical either via exposure to ultraviolet light, or more commonly *in vivo*, via the metal ion-catalyzed Fenton reaction (e.g. Fe^{2+}). A technical difficulty that we had to overcome during these experiments was that upon storage the efficacy of H_2O_2 decreased for reasons that we could not determine, after making sure the bottle was stored in the dark at 4 degrees. However, we found that purchasing this chemical freshly approximately once a month improved the consistency with which could successfully activate this pathway.

MCF7 cells were treated with increasing doses of H_2O_2 as shown in figure 14 for 1 hour, and mTOR signaling was analyzed by western blot. In a dose-dependent manner, both S6K and S6 phosphorylation are decreased. Similarly, in figure 16, we demonstrate that mTORC1 activity can be repressed within 30-60 minutes of treatment.

To determine whether mTORC1 suppression occurs in response to other agents that generate endogenous ROS, MCF7 cells were treated with the mitochondrial uncoupler, menadione as well as the phenylethylisothiocyanate (PEITC), which is a natural compound that depletes glutathione (which is an antioxidant enzyme). In addition, the chemotherapeutic drug, doxorubicin was used, since it not only generates DNA damage via intercalating into the DNA but also generates significant ROS which is thought to be the primary reason that it causes cardiac damage *in vivo* (136). Figure 15 shows that these other agents that generate endogenous ROS also potently and rapidly repress mTORC1 signaling in MCF7 cells.

To link mTORC1 suppression by hydrogen peroxide specifically to ROS, we utilized 2

Figure 14:

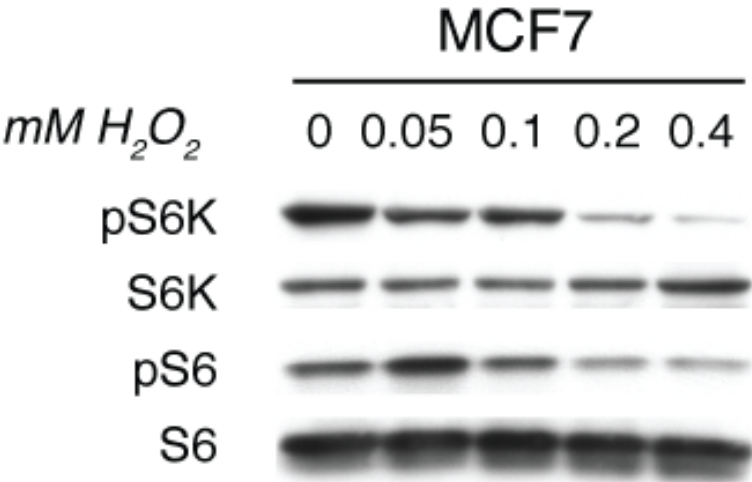


Figure 14: **Dose-response showing mTORC1 suppression by H₂O₂.** MCF7 cells were treated with the indicated doses of H₂O₂ for 1 hour. Lysates were subjected to western analysis with the antibodies indicated.

Figure 15:

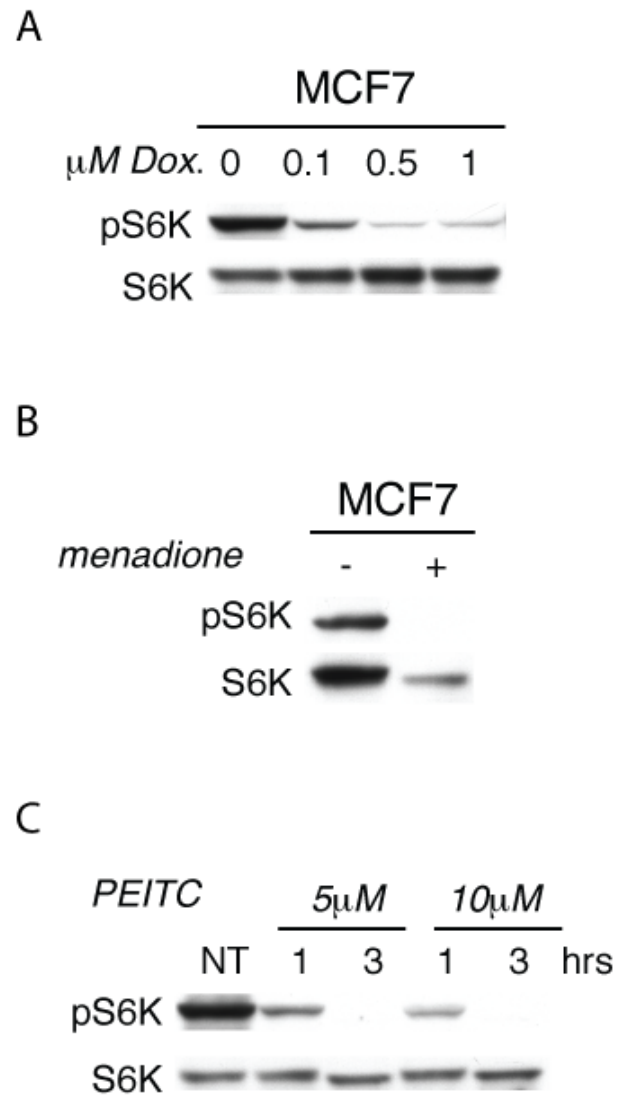


Figure 15: **mTORC1 is repressed by endogenous ROS** MCF7 cells were treated with: (A) doxorubicin for 24 hours, (B) 100 μM menadione for 1 hour or (C) PEITC as indicated. Lysates were subjected to western analysis with the antibodies indicated. [(Reprinted from (146))]

Figure 16:

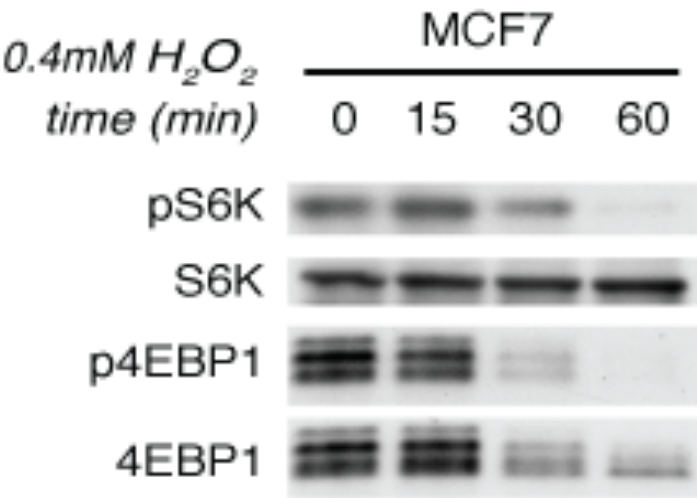


Figure 16: **Time-course showing mTORC1 suppression by H_2O_2 .** MCF7 cells were treated with the 0.4mM H_2O_2 for the time periods shown. Lysates were subjected to western analysis with the antibodies indicated.

ROS scavengers, N-acetyl cysteine (NAC) and catalase. MCF7 cells were pre-treated with 3mM NAC or 2950 units of bovine catalase for 1 hour, then challenged the cells with H₂O₂ for an additional 1 hour. Figure 17 shows that both these scavengers effectively block mTORC1 repression.

3.2.3 Role of ATM in ROS-induced mTOR repression

Since we hypothesized that ATM functions as an ROS sensor, we examined whether ROS induces ATM activation, as measured by phosphorylation of ATM at Ser 1981, and phosphorylation of Chk2 at Thr 68, a well-characterized ATM substrate. Figure 18 shows that ATM is activated in MCF7 cells in response to increasing doses of H₂O₂.

To determine whether ATM is required for mTORC1 suppression by ROS, we took 3 approaches. Firstly we compared the magnitude of mTORC1 suppression in ATM-proficient and ATM-deficient human lymphoblasts. Figure 19 shows a small, but reproducible difference in the ability to repress mTORC1 signaling under conditions of oxidative stress. When these cells were maintained in culture for several weeks however, even the ATM-proficient (WT-B) cells became non-responsive to ROS, for reasons we cannot explain. Importantly these cell lines were generated via Epstein-Barr virus-mediated transformation of primary B-lymphoblasts. To rule out *in vitro* immortalization as an inhibitory factor in our experiments, we isolated primary mouse-embryonic fibroblasts (MEFs) from *Atm*^{+/+}, *Atm*^{+/-} and *Atm*^{-/-} mice at approximately day 13 of development and performed similar studies on multiple clonal isolates from these cells. Figure 20 demonstrates that both *Atm* wild-type and heterozygous cell lines had equivalent responses to H₂O₂, however the cells lacking *Atm* had significantly attenuated responses (*p*<0.05). We confirmed these results in MCF7 cells using siRNA targeting ATM, and showed that when ATM is depleted, the ability to suppress S6K phosphorylation is decreased, as seen in figure 21. In contrast to ATM, we showed in figures 22 and 23 that ATR is not required for mTORC1 suppression by ROS, using ATR-deficient fibroblasts from a Seckel syndrome patient and siRNA targeting ATR.

Figure 17:

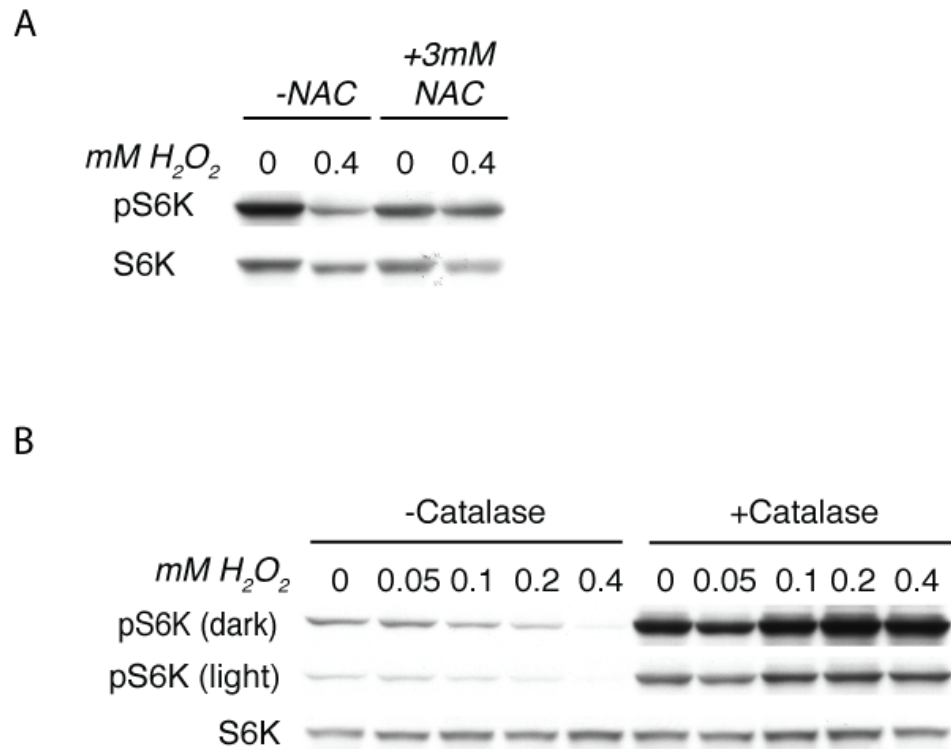


Figure 17: **Antioxidant treatment rescues mTORC1 suppression by ROS.** MCF7 cells were pre-treated with (A) 3mM NAC or (B) 2950 units of bovine catalase for 1 hour prior to treatment with H_2O_2 as shown. Lysates were subjected to western analysis with the antibodies indicated. [(Reprinted from (146)]

Figure 18:

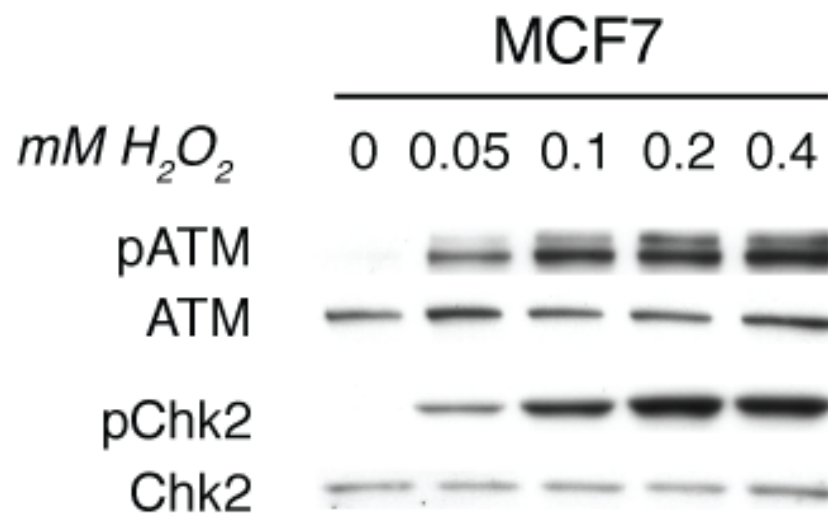


Figure 18: **Activation of ATM by ROS.** MCF7 cells were treated with increasing doses of H_2O_2 as shown. Lysates were subjected to western analysis with the antibodies indicated.

Figure 19:

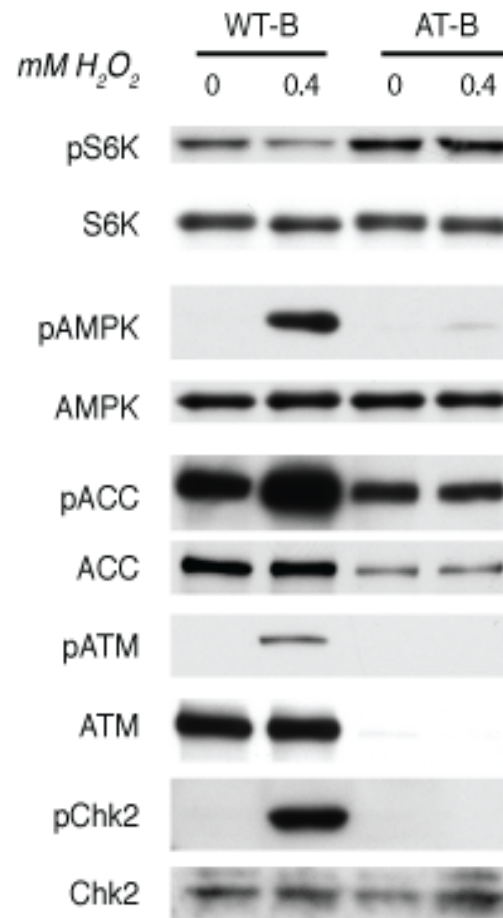


Figure 19: **Role of ATM in mediating signaling to mTORC1.** ATM proficient (“WT-B” - GM02184) and ATM-deficient (“AT-B” - GM01526) lymphoblasts were plated 24 hours prior to treatment with 0.4mM H_2O_2 for 1 hour, and lysates were analyzed by western blotting. [(Reprinted from (146))]

Figure 20:

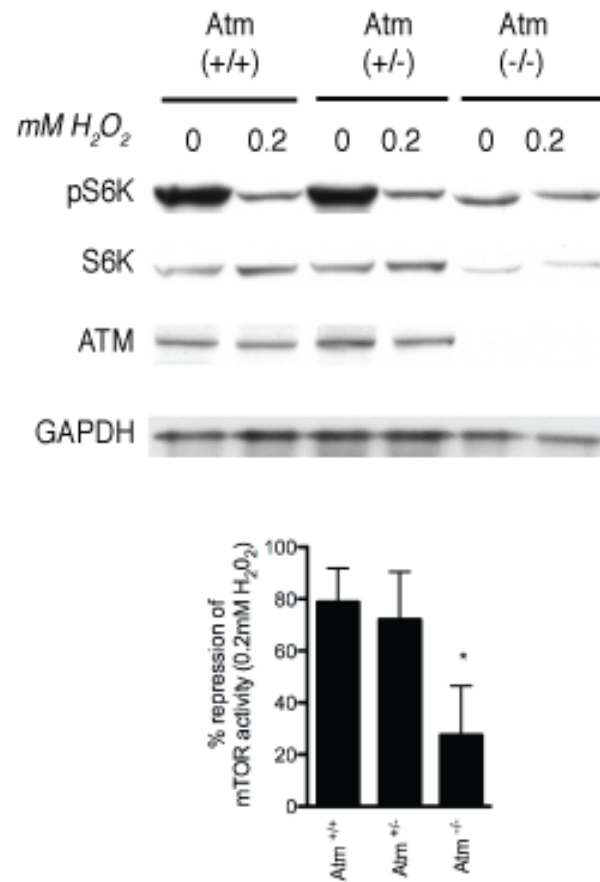


Figure 20: **mTORC1 suppression in primary mouse embryonic fibroblasts.** Mouse embryonic fibroblasts were generated from *Atm*^{+/+}, *Atm*^{+/-}, and *Atm*^{-/-} mice, and treated with 0.2mM H_2O_2 for 1 hour. The graph represents densitometric quantitation of the magnitude of suppression of S6K phosphorylation in multiple clonal isolates from each genotype (n=3 per group) and the asterisk signifies statistical significance by one-sided students t-test (p<0.05). [(Reprinted from (146)]

Figure 21:

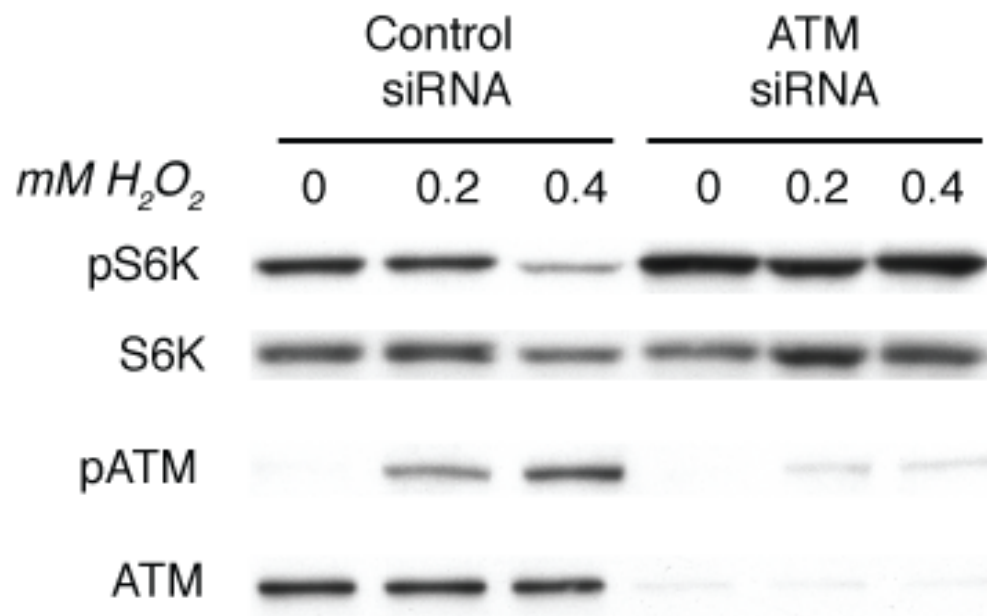


Figure 21: **siRNA validation of ATM participation in signaling to mTORC1.** MCF7 cells were transfected with siRNA targeting ATM 48 hours prior to treatment with H_2O_2 for 1 hour. Lysates were analyzed by western blot.

Figure 22:

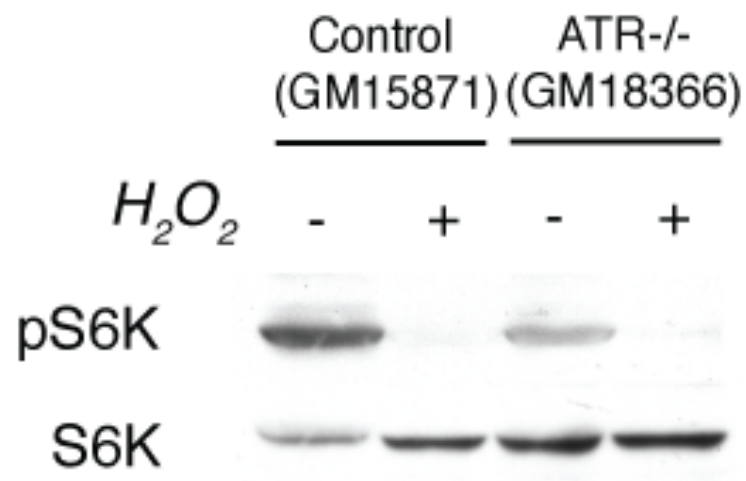


Figure 22: **ATR is not required for mTORC1 suppression by ROS** ATR-proficient (GM15871) and ATR-deficient (GM18366) fibroblasts were treated with 0.4mM H_2O_2 for 1 hour and lysates analyzed by western blot.

Figure 23:

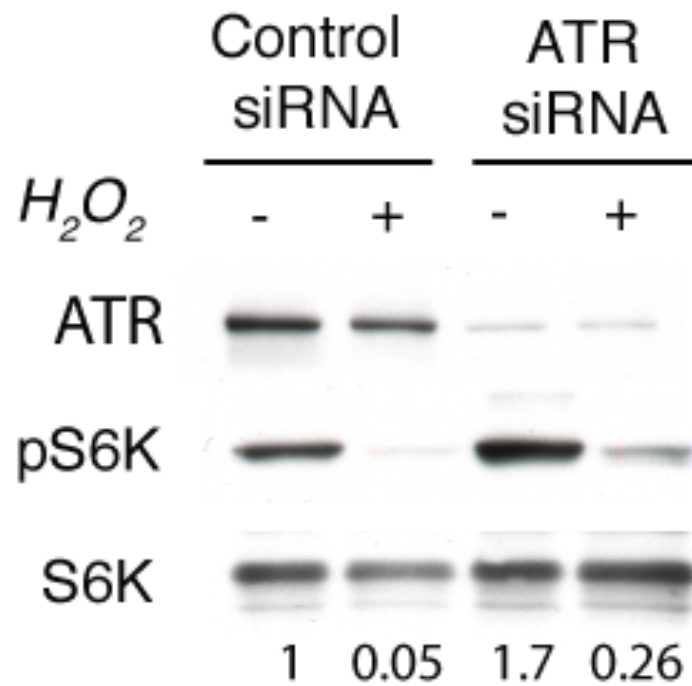


Figure 23: **siRNA validation that ATR is not required for mTORC1 suppression by ROS**
MCF7 cells were transfected with siRNA targeting ATR 48 hours prior to treatment with H_2O_2 for 1 hour. Lysates were analyzed by western blot. The numbers below S6K represent the normalized ratio for phosphorylated S6K/total S6K with the control siRNA untreated being set to 1.

3.2.4 Role of LKB1 in ATM signaling to mTORC1

To further investigate the mechanism by which ATM signals to mTORC1, we surveyed the literature for known potential ATM substrates that may lie upstream of mTORC1. One obvious potential protein we found during this search was LKB1, which is an upstream kinase for AMPK. LKB1 was previously shown by Dario Alessi's group to be phosphorylated by ATM in response to DNA damage (137). HeLa S3 cells, which are LKB1-null human cervical carcinoma cells, were utilized to establish a correlation between LKB1 expression and mTORC1 suppression, and as expected, these cells did not repress mTORC1 in response to ROS. However, stable reconstitution with wild-type LKB1 expression, restored these cells responsiveness to ROS. In contrast, cells reconstituted with an LKB1-construct lacking the ATM phosphorylation site did not respond to ROS, meaning that ATM phosphorylation at this site is required for signaling to mTORC1. Figure 24 shows the results of signaling analysis in representative clones from each construct, and the parental HeLa S3 as a control.

Direct evidence of LKB1 phosphorylation by ROS was obtained by performing immunoprecipitations of endogenous LKB1 and western blotting with a phospho-specific antibody generated by and kindly provided by Dario Alessi's group. Ionizing radiation was used as a positive control for activating this ATM-LKB1 pathway. As shown in figure 25, both H₂O₂ and ionizing radiation (IR) induce phosphorylation of LKB1 at Thr 366 in HEK 293 cells. siRNA knockdown of LKB1 was used as an additional method to show the requirement for LKB1 in signaling from ATM to mTORC1. Depletion of LKB1 results in a quantitative decrease in the responsiveness to ROS as seen in figure 25.

Figure 24:

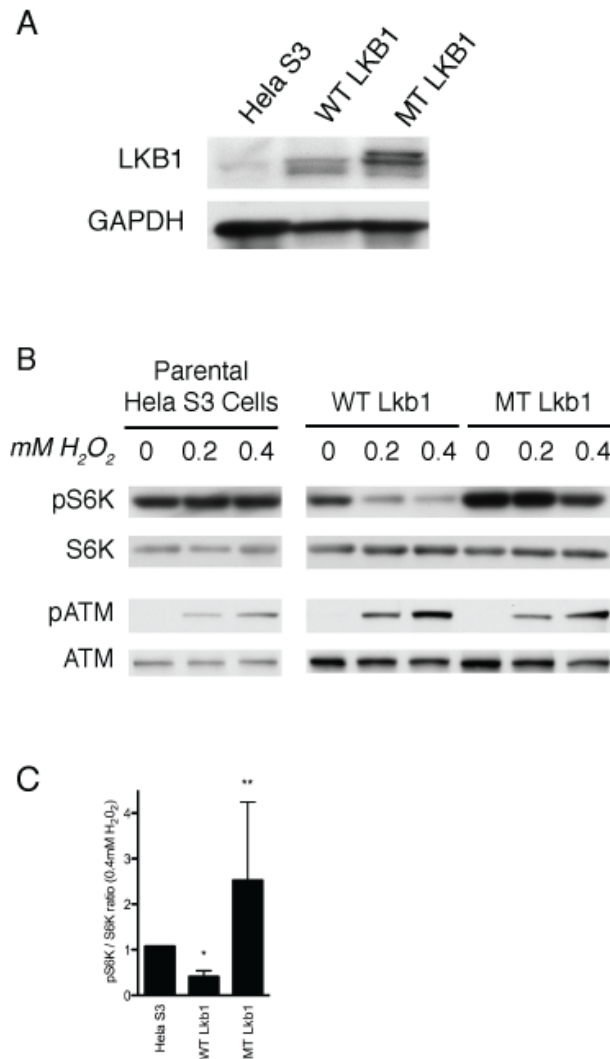


Figure 24: **LKB1 reconstitution of HeLa S3 cells and responsiveness to ROS.** (A)

Western blot showing LKB1 expression in stable clones shown in (B). (B) Western blot

analysis of mTORC1 repression in response to ROS. WT represents clone reconstituted with wild-type LKB1 and MT represents clone reconstituted with T366A mutant LKB1. (C) Graph

showing densitometric quantitation of mTORC1 repression in response to 0.4mM H₂O₂ in all clones analyzed (wild-type, n=4; T366A mutant, n=2). The single asterisk represent a

significant difference versus parental (p<0.03) and the double asterisks represent significance compared against wild-type(p<0.05), both using one-sided student's t-tests. [(Reprinted from

(146)]

Figure 25:

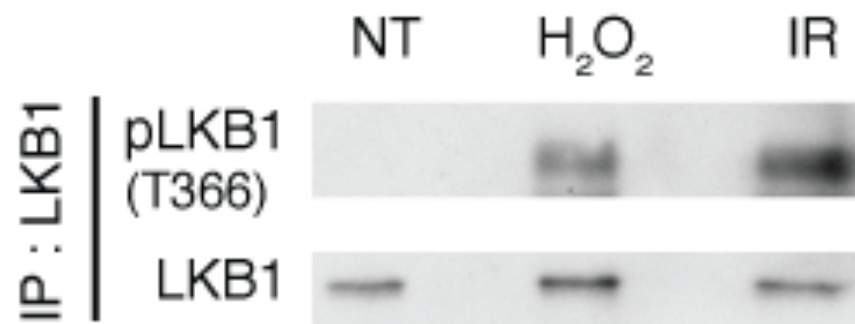


Figure 25: **LKB1 phosphorylation in response to ROS.** Immunoprecipitation and western analysis showing that endogenous LKB1 is phosphorylated in response to H₂O₂ in HEK 293 cells. [(Reprinted from (146)]

Figure 26:

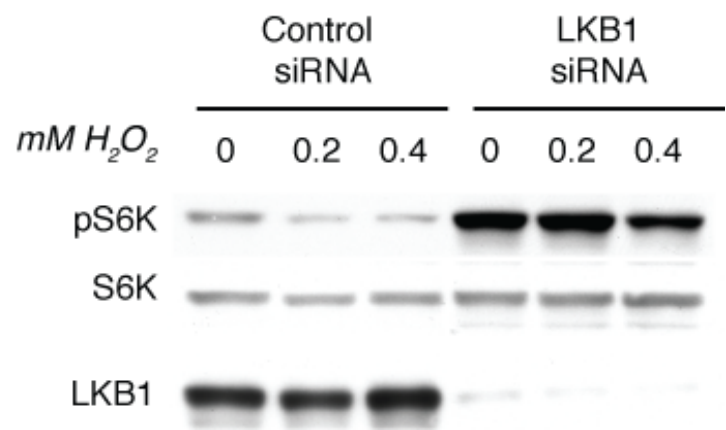


Figure 26: **siRNA validation of LKB1 participation in signaling to mTORC1.** MCF7 cells were transfected with siRNA targeting LKB1 48 hours prior to treatment with H₂O₂ for 1 hour. Lysates were analyzed by western blot. [(Reprinted from (146))]

3.2.5 AMPK activation by ROS leads to TSC2 activation

In the previous section we showed that LKB1 is activated in response to ROS. We next asked whether AMPK was subsequently activated. Using the MCF7 dose-response lysates generated for use in figure 14, AMPK activation was examined. We observed a dose-dependent activation of AMPK as shown in figure 27. As further evidence for AMPK activation resulting in mTORC1 suppression, we analyzed the kinetics of AMPK activation and mTORC1 in MCF7 cells. We observed an extremely rapid activation of AMPK (as measured by phosphorylation of acetyl co-A carboxylase, a downstream substrate of AMPK) within 5 minutes of treatment, whereas S6K phosphorylation took at least 30 minutes to decrease. (figure 28).

To determine whether AMPK activation is required for mTORC1 suppression by ROS, we utilized Compound C (6-[4-(2-Piperidin-1-yl-ethoxy)-phenyl]-3-pyridin-4-yl-pyrazolo[1,5-a]-pyrimidine), an ATP-competitive pharmacological inhibitor of AMPK discovered in a high-throughput chemical library screen (58). MCF7 cells were pre-treated with 20 μ M Compound C for 3-12 hours prior to treatment with 0.4mM H₂O₂ for 1 hour. Figure 29 shows that Compound C blocks the ability to suppress mTORC1 in response to ROS.

As the final potential step in the mechanism, we investigated whether AMPK phosphorylation of TSC2 is important in mediating mTORC1 repression by ROS. To answer this question, we developed a cellular functional assay in HEK 293 cells. Flag-tagged TSC2 and binding partner TSC1 constructs were cotransfected along with the GAP target Rheb which was Myc-tagged, and HA-tagged S6K as the mTORC1 substrate and readout. After transfection, cells were treated with H₂O₂ or left untreated, and phosphorylation of S6K analyzed by western blot. Since HEK 293 cells are very highly transfectable (>90% efficiency based on GFP expression), immunoprecipitation of over-expressed S6K was not necessary for accurate results. As figure 30 shows, when wild-type TSC2 is transfected, ROS can induce robust mTORC1 suppression, whereas if TSC2 lacking 2 of the major AMPK phosphorylation sites is transfected, mTORC1 suppression is significantly decreased.

Figure 27:

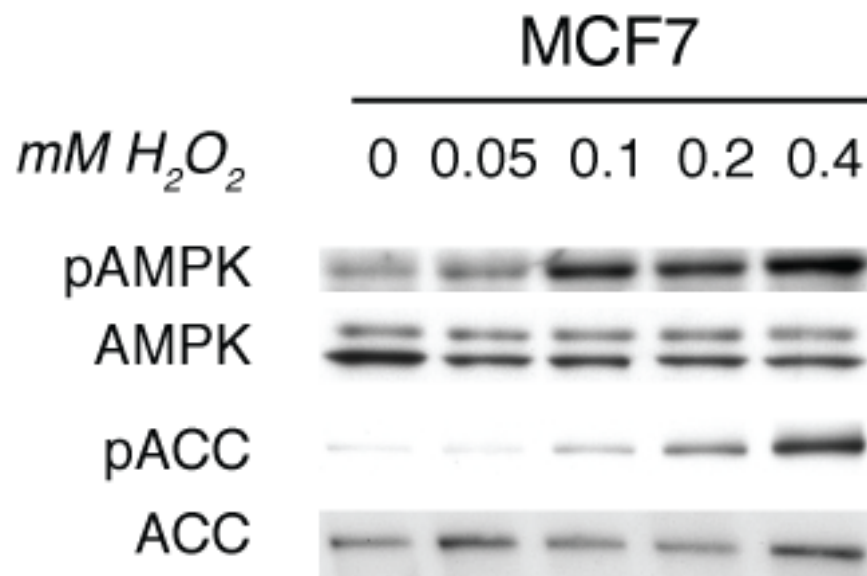


Figure 27: **AMPK activation by ROS.** MCF7 cells were treated with increasing doses of H_2O_2 as indicated and western blots performed as indicated. These lysates were from the same experiment as shown in figure 14.

Figure 28:

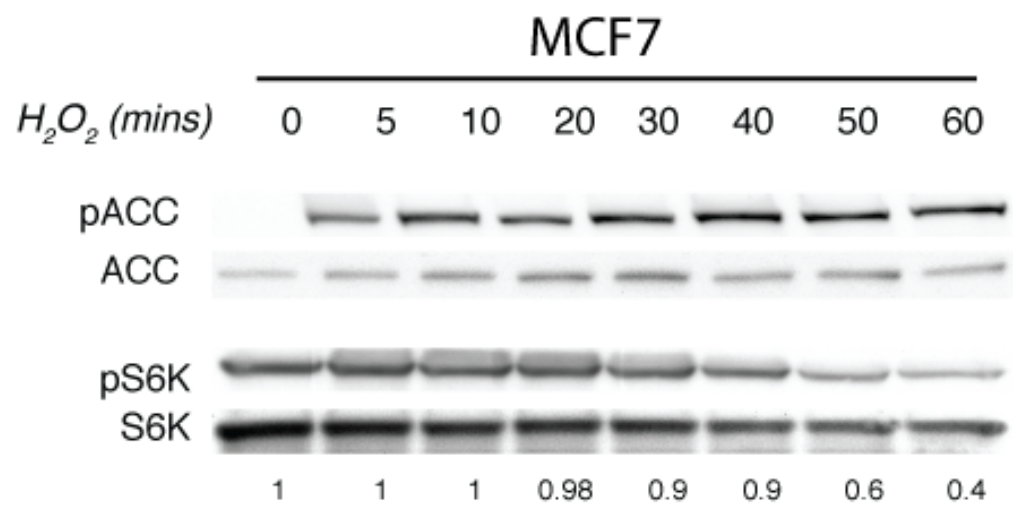


Figure 28: **Activation of AMPK prior to mTORC1 suppression.** MCF7 cells were treated with 0.4mM H₂O₂ for the indicated time points, prior to western blots as indicated. The numbers represent normalized densitometric ratios for phosphorylated S6K/total S6K, with the first lane being set to 1. [(Reprinted from (146)]

Figure 29:

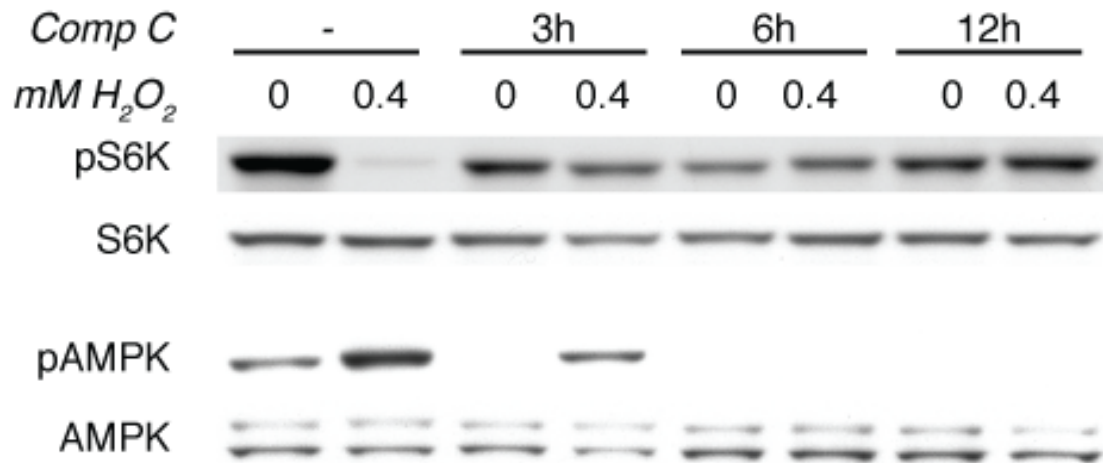


Figure 29: **AMPK inhibition blocks mTORC1 suppression by ROS.** MCF7 cells were pre-treated with 20 μ M Compound C for 3-12 hours as indicated, then challenged with 0.4mM H₂O₂. Western analysis shows that inhibition of AMPK with Compound C significantly blocks the ability to repress mTORC1. [(Reprinted from (146))]

Figure 30:

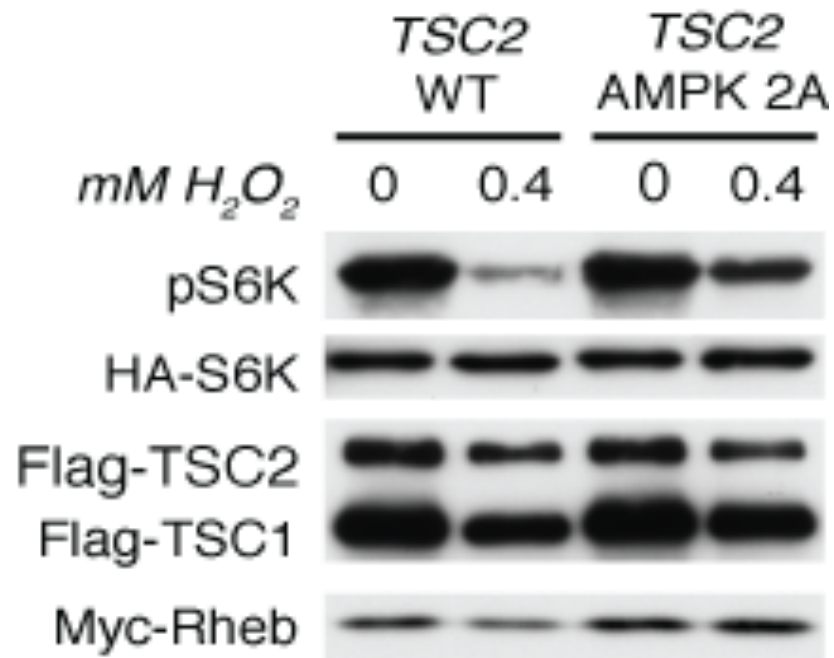


Figure 30: **AMPK phosphorylation of TSC2 mediates mTORC1 suppression by ROS.**

Western blots from TSC2 functional assay in HEK 293 cells showing that mutation of AMPK phosphorylation sites in TSC2 (TSC2 AMPK 2A) results in attenuated mTORC1 suppression by H₂O₂. [(Reprinted from (146)]

To more definitively determine whether TSC2 participates in this signaling pathway, we utilized Tsc2-deficient and Tsc2-proficient MEFs, and used siRNA targeted against TSC2 in MCF7 cells. At even the highest concentration of H₂O₂ tested (which has been our standard dose in many of the experiments previously described), MEFs lacking Tsc2 failed to repress mTORC1, while the Tsc2-expressing line did possess an intact signaling pathway from ATM to mTORC1 as shown in figure 31. Figure 32 shows that when TSC2 was quantitatively decreased using siRNA, we could also see a proportionally diminished response to ROS confirming the results in the MEFs previously demonstrated.

Since the Tsc2-proficient MEFs we utilized completely lacked p53 expression, and could repress mTORC1, we could also rule out a role for p53 in mediating an ATM-dependent pathway to mTORC1. siRNA targeting p53 in MCF7 cells was used to confirm that p53 is not required for mTORC1 repression by ROS, as shown in figure 33.

3.2.6 Localization of activated ATM signaling to LKB1 and AMPK

The mechanism described so far describing ATM as a ROS sensor, and signaling through LKB1 and AMPK to activate TSC2 and suppress mTORC1 present an interesting conundrum. While TSC2 has not been found to be localized to the nucleus outside of a few isolated reports that are not widely accepted in the field (138, 139). ATM has been found both in the nucleus and in various cytoplasmic organelles. Detailed studies of the activation status of extranuclear ATM have not been performed thoroughly. Identifying therefore the localization of ROS-activated ATM and the downstream components of this signaling pathway would further elaborate on the mechanism by which mTORC1 is regulated by ROS.

To begin to shed light on this question, untreated and H₂O₂-treated MCF7 cells were fractionated into cytoplasmic and nuclear fractions, and western blots were performed to look at the distribution of phosphorylated ATM and downstream proteins. Figure 34 shows that while ATM can be phosphorylated by in the cytoplasm and nuclear fractions, LKB1 is only expressed in the cytoplasm, and AMPK is also exclusively cytoplasmic.

Figure 31:

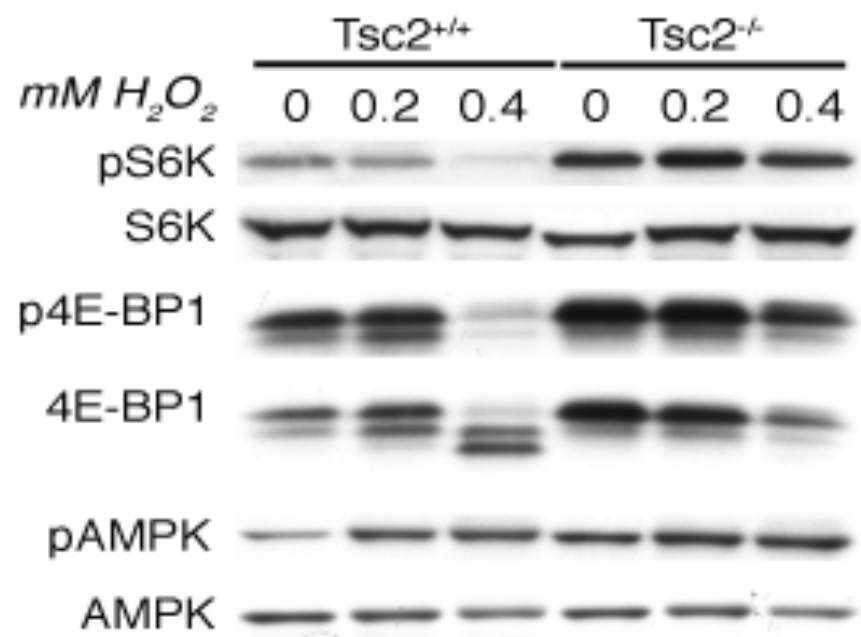


Figure 31: **Tsc2 involvement in signaling to mTORC1 in MEF cells.** Tsc2-proficient and Tsc2-deficient MEFs were treated with 0.2mM or 0.4mM H₂O₂ for 1 hour, and lysates were analyzed by western blot. [(Reprinted from (146)]

Figure 32:

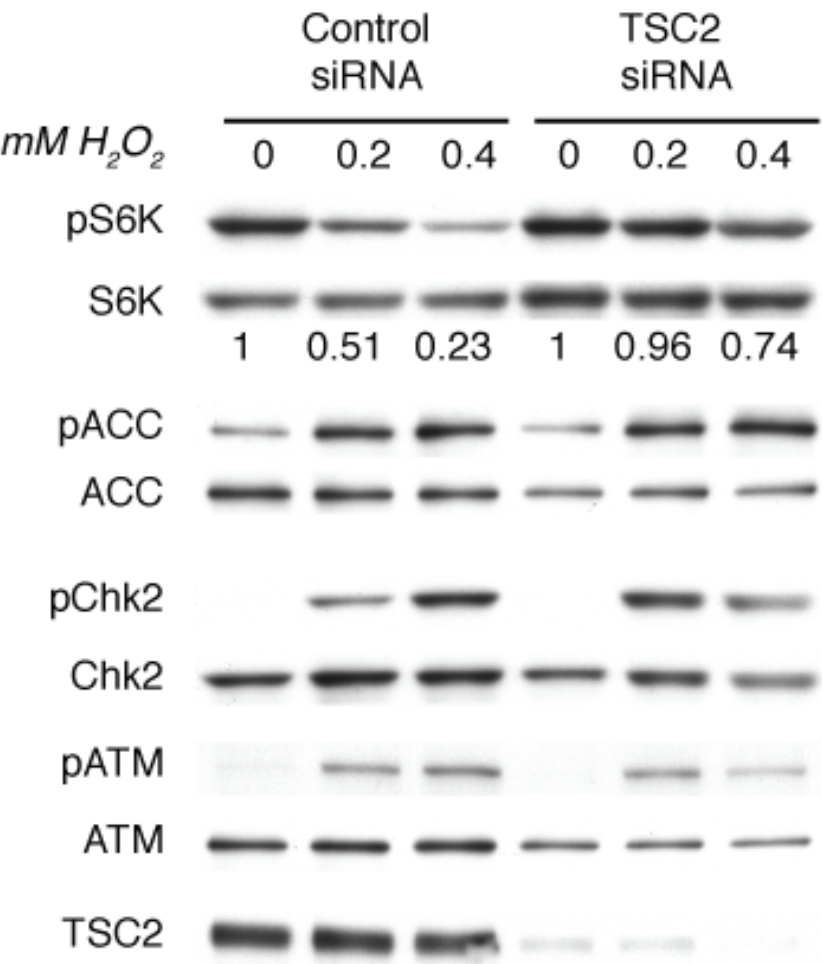


Figure 32: **Role of TSC2 in signaling to mTORC1 in human cells.** MCF7 cells were transfected with siRNA targeting TSC2 48 hours prior to treatment with H₂O₂ for 1 hour. Lysates were analyzed by western blot. [(Reprinted from (146))]

Figure 33:

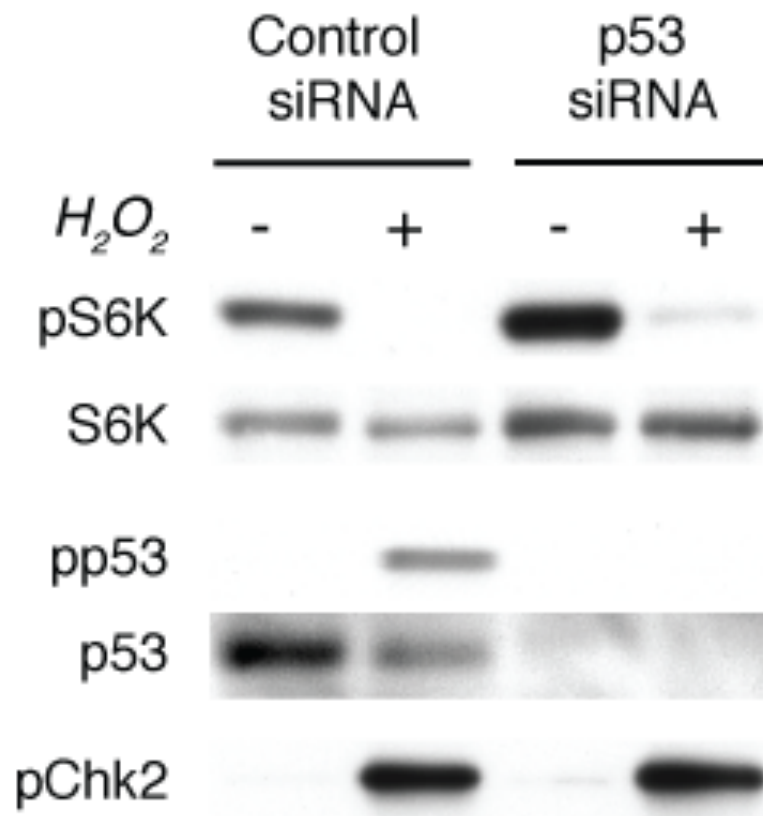


Figure 33: **p53 is not required for mTORC1 suppression by ROS.** MCF7 cells were transfected with siRNA targeting p53 48 hours prior to treatment with H₂O₂ for 1 hour. Lysates were analyzed by western blot. [(Reprinted from (146))]

Figure 34:

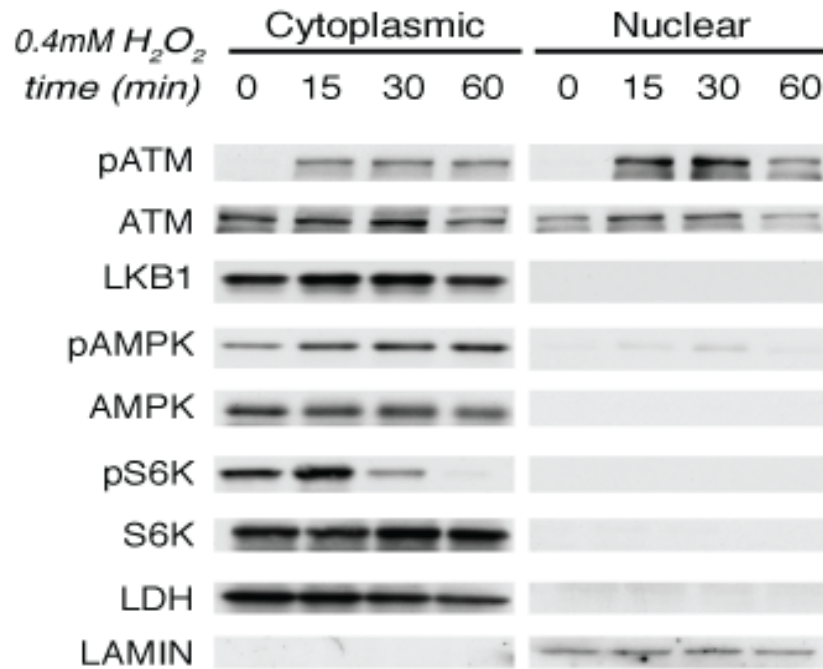


Figure 34: **Fractionation showing localization of ATM-LKB1-AMPK signaling node.**

Cytoplasmic and nuclear fractions from MCF7 cells treated with 0.4mM H_2O_2 for the indicated times were obtained, and western blots performed showing that although ATM is activated both in the cytoplasm and the nucleus, that LKB1 and AMPK are exclusively in the cytoplasm. LDH was used as a cytoplasmic marker, and LAMIN is a nuclear marker. [(Reprinted from (146)]

Activated ATM in the cytoplasm could be as a result of either activation of a cytoplasmic pool of ATM that is distinct from the nuclear pool, or translocation of activated ATM from the nucleus, similar to that seen after DNA damage to activate NF- κ B. To distinguish between these two possibilities, we utilized leptomycin B, a chemical inhibitor of nuclear export. Firstly we pre-treated MCF7 cells with 100ng/ml leptomycin B for 5 hours and asked whether ATM could be activated and mTORC1 inhibited by ROS. Figure 35 shows that leptomycin B had no effect on the ability for ROS to induce ATM activation and mTORC1 suppression. Next we performed a similar experiment but fractionated the cells into cytoplasmic and nuclear fractions, and as expected saw that the amount of ATM activated in the cytoplasm was equivalent in both treated and untreated cells (figure 36).

3.2.7 mTORC1-dependent autophagy regulation by ROS

The findings so far presented in this chapter have established that a cytoplasmic pool of ATM can be activated by ROS to repress mTORC1 signaling. mTORC1 itself can regulate multiple cellular processes, most notably protein synthesis and autophagy. During our signaling work, there was increased interest from the autophagy community regarding how ROS may be a physiological regulator of autophagy both under starvation conditions and some tissue-specific examples such as ischemia/reperfusion injury in the heart (140, 141). Therefore, we decided to look at whether ROS might regulate autophagy via the ATM-LKB1-AMPK-TSC2-mTOR pathway.

One of the best characterized experimental approaches for demonstrating the autophagy is induced is through use of the LC3 marker by western blot or cellular localization using a GFP-tagged construct. LC3 is the mammalian homolog of the yeast Atg8 protein, and is a necessary protein for autophagy induction in yeast (142). When autophagy is induced, LC3 becomes lipidated with the molecule phosphatidylethanolamine, which allows it to associate with the newly forming autophagosomal membrane. This lipidated form runs at a higher mobility, and therefore can be observed at an apparently smaller molecular weight

Figure 35:

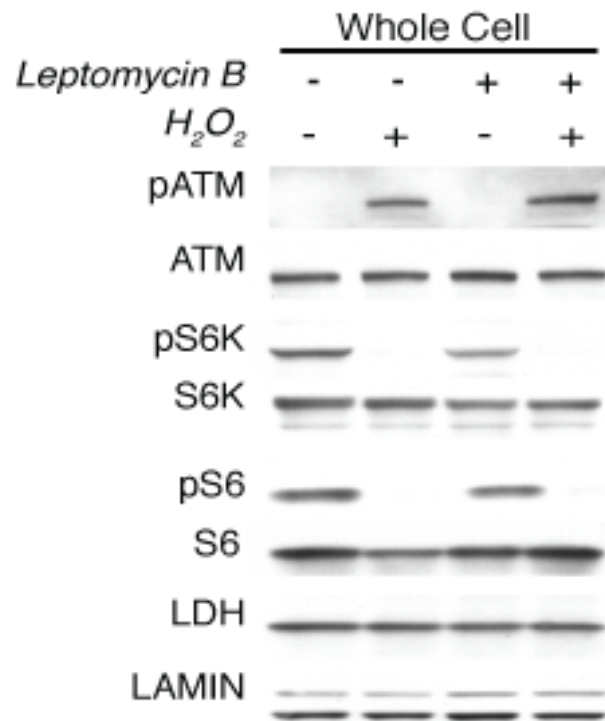


Figure 35: **Leptomycin B does not block ATM signaling to mTORC1 in response to ROS.**

MCF7 cells were treated with 100ng/mL leptomycin B or vehicle for 5 hours prior to treatment with 0.4mM H_2O_2 or vehicle for 1 hour. Whole cell lysates were taken for western analysis as shown in this figure. [(Reprinted from (146)]

Figure 36:

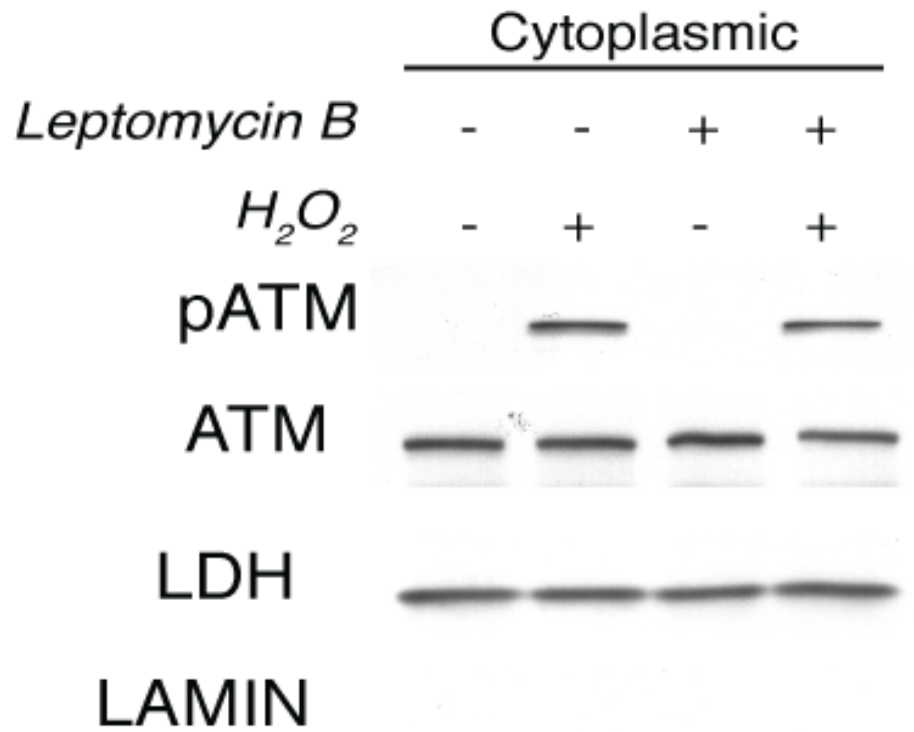


Figure 36: **Equivalent ATM activation in cytoplasmic fraction of leptomycin treated MCF7 cells.** MCF7 cells were treated with 100ng/mL leptomycin B or vehicle for 5 hours prior to treatment with 0.4mM H_2O_2 or vehicle for 1 hour. Cytoplasmic fractions were isolated for western analysis as shown in this figure. LDH was used as a cytoplasmic marker, and LAMIN is a nuclear marker to show lack of nuclear contamination. [(Reprinted from (146))]

on a standard SDS-PAGE gel.

We used stably-expressing MCF7 GFP-LC3 cells, kindly provided by Dr Gordon Mills laboratory, as well SKOV3 GFP-LC3 cells to show that ROS induces autophagy. Stable transfection of GFP-LC3 is now broadly appreciated to be necessary for accurate results, since it has been shown that transient transfection alone is problematic because lipid-based transfection reagents such as the commonly used Lipofectamine 2000 induce autophagy both with and without DNA (143). By using stable transfection and making sure experiments were not performed within 2 weeks of thawing cells from cryogenic storage, this transient off-target induction of autophagy is no longer a confounder. Cells were plated in chamber slides and treated with increasing doses of H_2O_2 , and cells were imaged at 1 hour post-treatment using epifluorescence or confocal microscopy. As controls to ensure the system was working we also treated cells with rapamycin or vehicle control (DMSO). To analyze these results, we counted the total number of GFP-positive cells, and determined whether the GFP was diffuse (ie LC3 was not lipidated) or punctate (lipidated LC3, indicating binding to autophagosomal membranes). Figure 37 shows an example of punctate GFP localization in H_2O_2 treated cells, with an inset showing the baseline diffuse pattern, and the accompanying graph quantifies the increase in number of cells with punctate GFP for H_2O_2 and rapamycin normalized separately to their respective controls. We also performed western analysis on SKOV3 ovarian carcinoma cells treated with H_2O_2 and used rapamycin again as a positive control. Figure 38 shows that when mTORC1 is suppressed by rapamycin or H_2O_2 , that LC3 II, the lipidated form of LC3 is increased relative to total proteins shown for signaling pathway members.

Although an increase in LC3 II expression and increased number of punctate GFP-LC3 dots usually signifies an increase in autophagosome formation, it may also indicate a downstream block in the autophagy pathway such as in autophagosome maturation or fusion with the lysosome. In order to rule out these alternative interpretations of the results

Figure 37:

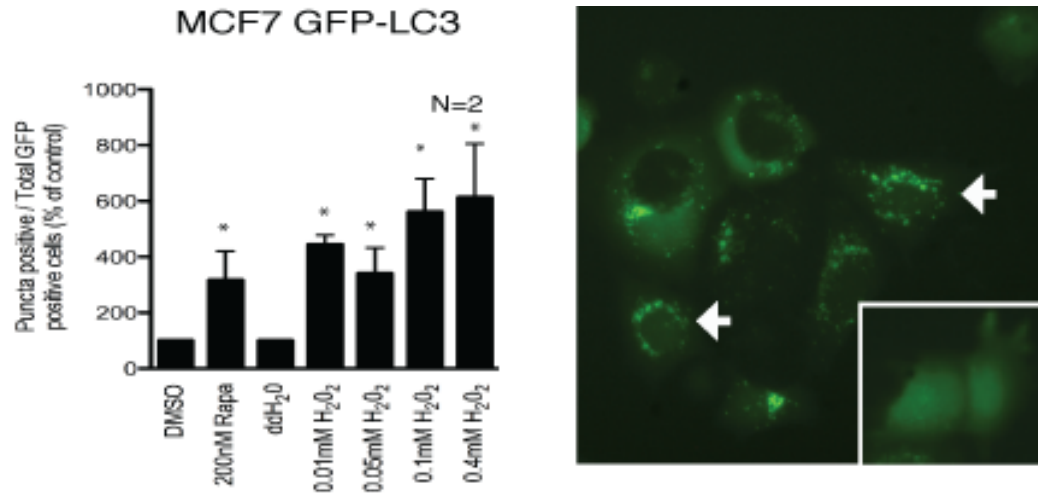


Figure 37: **GFP-LC3 localization in response to ROS.** MCF7 cells stably expressing GFP-LC3 were treated with H₂O₂ or Rapamycin as a positive control for induction of autophagy. Images were taken of fluorescence localization after 1 hour, and cells were scored either as punctate (arrows, represent induction of autophagy) or diffuse (inset image, autophagy not induced). The graph represents the number of punctate cells divided by total GFP positive cells, with each of the vehicles set to 1. Asterisks represent significant increases compared with the matched vehicle ($p < 0.0001$ χ^2 test). [(Reprinted from (146)]

Figure 38:

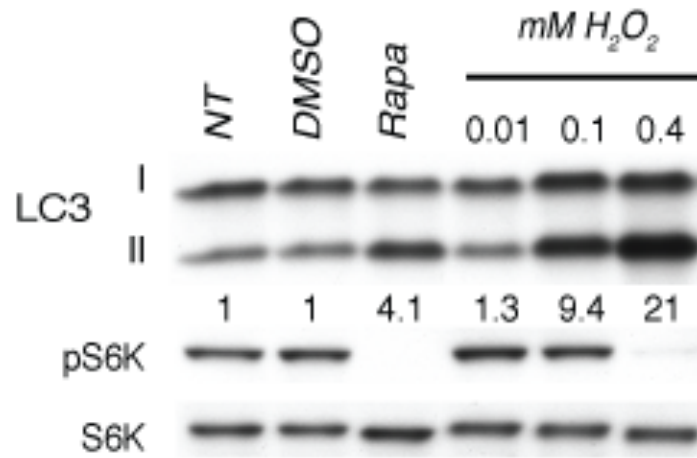


Figure 38: **Increased LC3 lipidation in response to ROS.** SKOV3 cells were treated with the indicated doses of H_2O_2 or DMSO or 400nM rapamycin (Rapa) as a positive control for induction of autophagy. Lysates were analyzed by western blot using the indicated antibodies. The numbers below the LC3 blot represent normalized densitometric ratios of LC3 II / LC I setting the untreated (NT) control to 1. [(Reprinted from (146))]

presented, we used two complementary approaches. Firstly, we blocked lysosomal function using the lysomotropic drug chloroquine, which neutralizes the positive charge in the lysosome, which is necessary for enzymatic degradation of the contents. Figure 39 demonstrates that LC3 II could still be increased in the presence of chloroquine, indicative of increased autophagic flux and not just a downstream block induced by ROS. We obtained more definitive evidence of increased flux by measuring turnover of p62, since p62 is degraded by autophagy – hence if there was a downstream block in degradation, p62 levels would not be decreased over time. Figure 40 shows that p62 is degraded in a time-dependent manner in response to ROS.

Electron microscopy has been the gold standard for observation of autophagosomes at a sub-cellular level for many years now, even though it is rather labor-intensive, not amenable to high-throughput analysis or particularly quantitative without specially written software. Despite these limitations, we did observe an increase autophagosomes filled with cytoplasmic material in cells that were treated with H_2O_2 , as shown in figure 41.

Taken together we have shown by multiple methods that ROS induces autophagosome formation and a subsequent increase in autophagic flux. Future sections will deal with the cellular consequences that this process may play.

Figure 39:

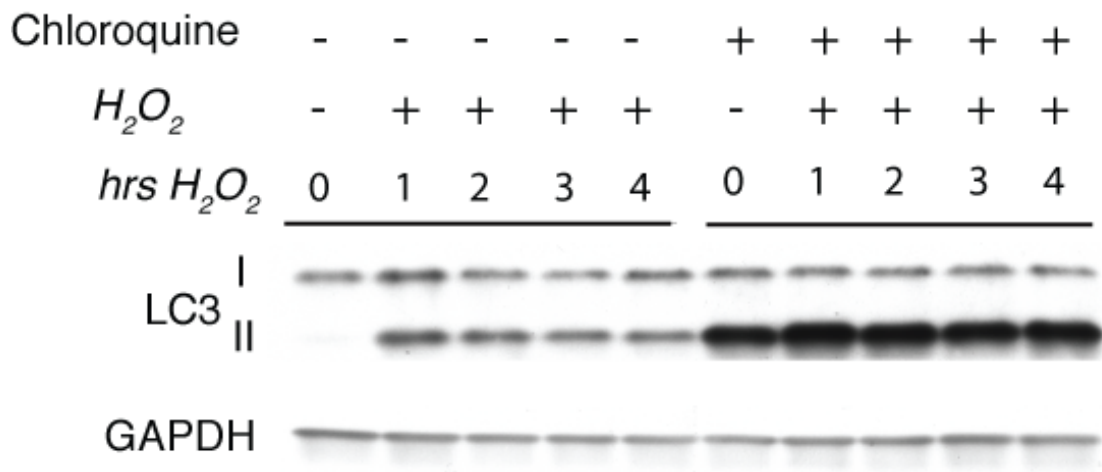


Figure 39: **LC3 II accumulation in the presence of chloroquine indicates increase in autophagic flux.** SKOV3 cells were treated with 100mM chloroquine for 2 hours prior to treatment with 0.4mM H_2O_2 for the indicated times. Lysates were made and analyzed by western blots as shown. [(Reprinted from (146))]

Figure 40:

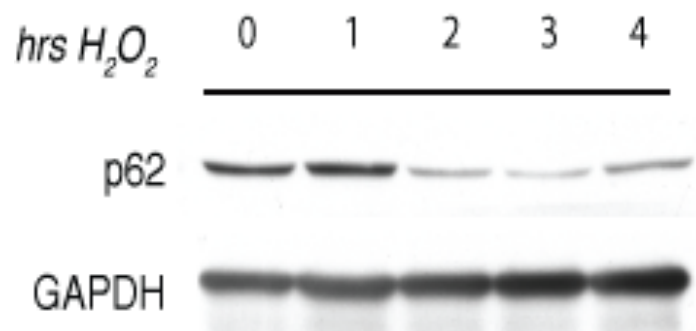


Figure 40: **Degradation of p62 in response to ROS.** SKOV3 cells were treated with 0.4mM H₂O₂ for the indicated periods of time and lysates analyzed by western blot. p62 is an degraded by autophagy, so it represents a measure of autophagic flux. [(Reprinted from (146))]

Figure 41:

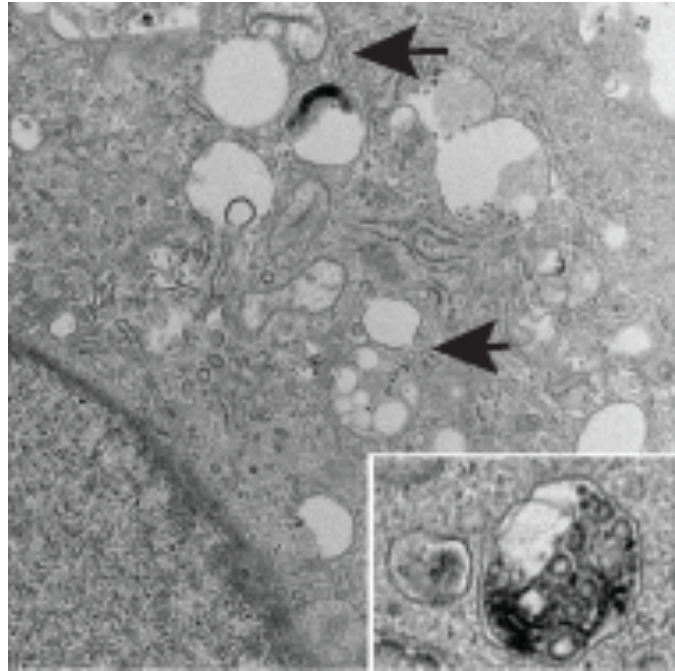


Figure 41: **Electron microscopy images showing autophagosome increase after ROS exposure** The inset is a zoomed in image of an autophagosome filled with cargo. The nucleus is the darker structure on the bottom left side. The arrows point to autophagosomes.
[(Reprinted from (146))]

3.3 Discussion

In this chapter, we have described the discovery of a novel cytoplasmic signaling pathway initiated as a result of ROS activation of ATM, resulting in mTORC1 suppression. This pathway contrasts with another recently identified pathway that is engaged in response to genotoxic stress to repress mTORC1. This alternative pathway involves p53-mediated induction of sestrin 1 and sestrin 2, which were found to lie upstream of AMPK and TSC2 (144). The mechanism we have described is distinct from this due to the requirement for p53 and the fact that it is redox-independent.

In addition to ATM and TSC2, we observed a dependence on LKB1 for mTORC1 suppression by ROS, which contrasts with an earlier report that in HeLa cells, that lack LKB1, AMPK could be activated by etoposide in an ATM-dependent manner to regulate mitochondrial biogenesis (145). In this report, AMPK was phosphorylated at Thr 172 which is the same phosphorylation site as that which is activated by LKB1, indicating that there are multiple routes to the same outcome. On a mechanistic level however, activation of AMPK by etoposide required prolonged treatment, in contrast to the very fast activation of AMPK by ROS, again underscoring that multiple pathways exist to regulate AMPK and mTORC1 that may be differentially engaged based on the type of damage, dose and perhaps in a cell-type dependent manner.

Prior to our report (146), the function of the ATM phosphorylation site on LKB1 (Thr 366) had been somewhat elusive. In G361 melanoma cells which lack endogenous LKB1 expression, reconstitution with a T366A mutant LKB1 was threefold less efficient at suppressing cell growth when compared to wild-type LKB1 (147). Our data support this claim that ATM phosphorylation of LKB1 is important functionally, since AMPK could not be activated in response to ROS in the stable cell lines expressing the T366A mutant LKB1. Although LKB1 activation of AMPK via phosphorylation has been well-documented for many years, its function as an obligate kinase for AMPK is still controversial. In LKB1 deficient cells such as HeLa or *Lkb1*^{-/-} MEFs, AMPK is not activated by classical agonists such as AICAR or

metformin, however AMPK can still be activated and basally phosphorylated at Thr 172 in these cells, suggesting that other AMPK kinases can compensate to regulate the key metabolic processes that are controlled by AMPK (148).

Although we have shown through various approaches that there is an ATM and TSC2-dependent signaling pathway to regulate autophagy in response to ROS, we cannot exclude additional pathways that are independent of ATM and TSC2, especially at higher concentrations of H₂O₂ and/or at later time points. In figure 23, the slight repression of 4E-BP1 phosphorylation at the highest dose (0.4mM) suggests that perhaps a portion of mTORC1 is being inhibited even in the absence of Tsc2. In addition, the TSC2 functional assay suggests that expression of the mutant lacking the AMPK phosphorylation sites was only partially inactive in the ROS response. One potential explanation for the small amount of mTORC1 suppression in Tsc2-deficient cells is based on the fact that AMPK is constitutively active in these cells (149, 150). AMPK was shown a few years ago to phosphorylate raptor, a component of the mTORC1 complex, in response to energy stress to inhibit cell growth, as a survival measure (151). It is plausible therefore that when AMPK is activated by ROS that raptor phosphorylation also increases which induces binding to 14-3-3 and inactivation of the mTORC1 complex kinase activity. This hypothesis could be tested with the newly commercially available phospho-specific antibodies to the raptor phosphorylation sites.

In vivo study of mTOR signaling in Atm-deficient mice

4.1 Background into Atm knockout mouse model

Atm deficient mice have been developed as an in vivo model to understand the etiology of ataxia telangiectasia. However, beyond this rare disease, somatic ATM mutations have been found in other human cancers including breast and ovarian cancers (152), and T-prolymphocytic leukemia, a rare malignancy that occurs in both AT-patients and AT-carriers who lose ATM function due to rearrangements or point mutations (153). These mice therefore have the potential to teach us more general principles about cancer as well as AT-specific concepts.

Atm deficient mice recapitulate most of the phenotypes of the human disease including the significant propensity to develop hematologic malignancies, however the neurodegeneration phenotype is much less pronounced, for reasons that are still not clear. Homozygous knockout mice develop aggressive immature T-cell thymic lymphoblastic lymphomas at an early age, and these tumors are the usual cause of mortality by 3-4 months of age from compression of the heart and lungs or even metastases (or both) (132). The tumors are thought to arise from clonal expansions of CD4/CD8 double positive thymocytes that possess translocations involving chromosomes 12 or 14 near the T-cell receptor loci, similar to the cytogenetic characteristics seen in the lymphoid tumors in humans.

In addition to the cancer predisposition phenotype, the homozygous knockout mice have several other important phenotypes. At the gross level, these mice are growth retarded by 10-25% in comparison to age- and sex-matched littermates, and this persists into adulthood. Development of mouse embryonic fibroblast cell lines from these animals is a challenge since they proliferate very slowly and become senescent within only a few passages to the rapid accumulation of DNA damage which activates p53 and p21 to induce growth arrest. When we attempted to isolate these cells, we found that maintaining the cells in 15% FBS prolonged their survival.

The accumulation of DNA damage in Atm-deficient cells also contributes to infertility. Although the mice possess grossly normal reproductive organs, the gonads are extremely small and completely lack mature gametes. This is because there is an early meiotic arrest due to abnormal chromosomal synapsis causing chromosomes to become broken and induce apoptosis.

Atm appears to be important in normal T-cell development in vivo. Atm-knockout mice have significantly decreased numbers of thymocytes, resulting in an overall hypoplastic thymus (132). Immature B-cells in the bone marrow are also negatively impacted by Atm loss, however mature peripheral B cells are not affected suggesting that other pathways can compensate during later development (132).

As expected, the Atm-deficient mice are also highly radiation sensitive. When the knockout mice were challenged with ionizing radiation at a dose sufficient to kill two-thirds of wild-type and heterozygous mice within 6-18 days of exposure (8 Gy), these mice died in only 3-5 days due to acute gastrointestinal tract toxicity as opposed to a global radiation toxicity involving the immune system (which happens to both the wild-type and mutant mice).

One of the surprises in this model however is the relatively weak neurological defects seen. The mice perform more poorly on tests of motor function, but at first there was little histological evidence of neurodegeneration, leading to the hypothesis that since the development of neurodegeneration in humans occurs later in life, the mice succumb to malignancy too early in life to develop overt degenerative features. Upon further detailed studies by a different group however, a subtle neuronal degeneration was observed by electron microscopy analysis of granule cells, Purkinje neurons and molecular layer neurons in the cortex (154). Several years after being generated, several new interesting aspects of neuronal physiology in these animals were uncovered. In the absence of detectable neuronal degeneration, Carrolee Barlow et al, observed an increased in the number of lysosomes in Purkinje neurons using electron microscopy in Atm knockout mice relative to wild-type controls (155). Also reported in this study was the fact that ATM is exclusively cytoplasmic in Purkinje

neurons and some dorsal root ganglion cells in these mice (similar to what has been reported in adult human cerebellum) suggesting that loss of ATM may impact the autophagic-lysosomal system in multiple ways *in vivo*.

4.2 Rationale for study

Once we uncovered the signaling pathway described in the previous chapter, we wanted to study the *in vivo* relevance of the dysregulation of the oxidative stress-mTORC1-autophagy pathway. We performed studies to investigate:

- (a) whether mTORC1 signaling was dysregulated in Atm-deficient mice and if so,
- (b) whether targeting this abnormality with rapamycin could rescue lymphomagenesis and prolong survival.

4.3 Results

4.3.1 Analysis of mTORC1 signaling and AMPK activation in Atm-mouse model

We began our investigations of mTORC1 pathway activity by studying various normal tissues (including the front and hind brain, liver, kidneys, thymi, cardiac and skeletal muscle) from adult *Atm*^{+/+}, *Atm*^{+/-} and *Atm*^{-/-} mice (2-3 months of age). This approach gave us very mixed results, with the first batch of animals taken showing a trend for elevated mTORC1 activity in the *Atm*^{-/-} mice, however, upon validation with a larger cohort of animals, we did not see this correlation. Also of relevance was that the animals were sacrificed at different times of the day which may have had some impact on signaling due to the time of last feeding. In the literature, evidence for wide-spread significant signaling abnormalities in normal tissues from knockout or transgenic mice is generally lacking, perhaps due to issues similar to this where inter-animal variability due to feeding, physical activity or other factors makes analysis of mTORC1 activity too challenging.

What was consistent from our studies however was that in the older animals, some of which were already developing lymphomas, mTORC1 signaling was elevated in the thymus.

Upon setting up the survival study described below, when we analyzed the tumors from the moribund animals we confirmed that lymphomas possess elevated mTORC1 signaling. Figure 42 shows a representative sample of thymi and lymphomas that were analyzed by western blot. Figure 43 shows quantitation from a larger panel of tissues using both phospho-S6K and phospho-S6 levels as measures of mTORC1 activity.

Next we analyzed AMPK activation based on the hypothesis that loss of Atm would be predicted to cause elevated ROS, but without Atm expression, AMPK would not be activated. Our findings as shown in figures 44 and 45 demonstrate that the lymphomas possessed decreased AMPK activity compared to normal thymi, consistent with elevated mTORC1 activity, and lack of signaling from ATM to LKB1 and AMPK.

4.3.2 Response of lymphomas to rapamycin

The discovery of dysregulated mTORC1 signaling in Atm-deficient lymphomas, raised the question of whether rapamycin or other mTOR-targeted therapeutics would be efficacious in killing these tumors. To study the responses of Atm-deficient lymphomas to rapamycin, we performed two related experiments. In the first study, we administered rapamycin at a dose of 15mg/kg by intraperitoneal injection daily for 7 days to adult mice approximately 3 months of age and sacrificed the animals 2 hours after their last dose. To try to control for food intake, we took some of the animals and starved them overnight (but water was available *ad lib* for all animals). Ultimately however the effects of rapamycin were equally strong in both treatment protocols. Figure 46 demonstrates our findings at the histological level in this short-term study, performed with the assistance of our on-campus veterinary pathologist. While the lymphomas from the vehicle treated mice are large and composed of solid sheets of uniform neoplastic cells, the rapamycin-treated sections show dramatic tumor shrinkage and some suggestion of normal thymic architecture. As expected, rapamycin significantly decreases the number of phospho-S6 positive cells. In addition, these treated tumors express decreased p53, Ki67 (indicative of proliferation) and TUNEL (indicative of apoptosis).

Figure 42:

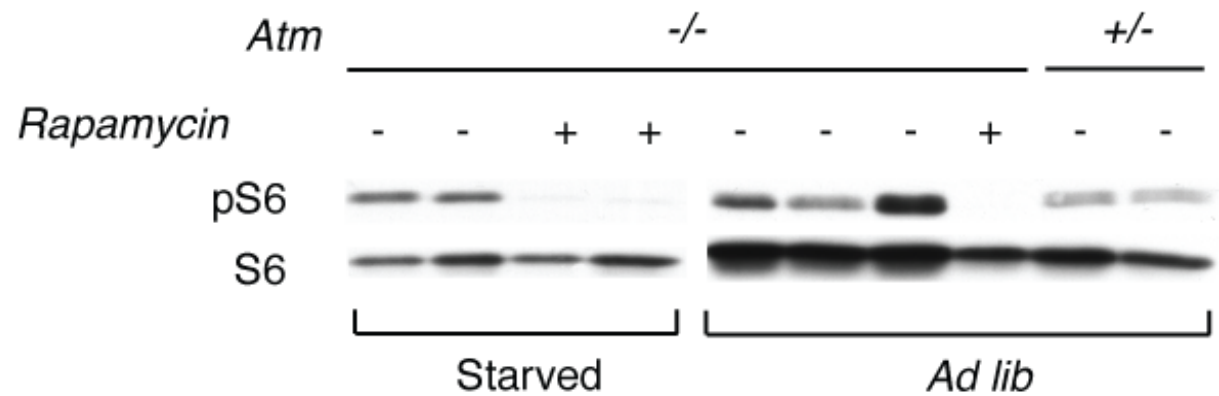


Figure 42: **mTORC1 activity is elevated in lymphomas from *Atm*^{-/-} mice.** Normal thymus from *Atm*^{+/-} mice and lymphomas from *Atm*^{-/-} mice were analyzed by western blotting for mTORC1 activity in both mice that were allowed to feed ad lib, and mice starved from food overnight, and treated with rapamycin or vehicle as indicated.

Figure 43:

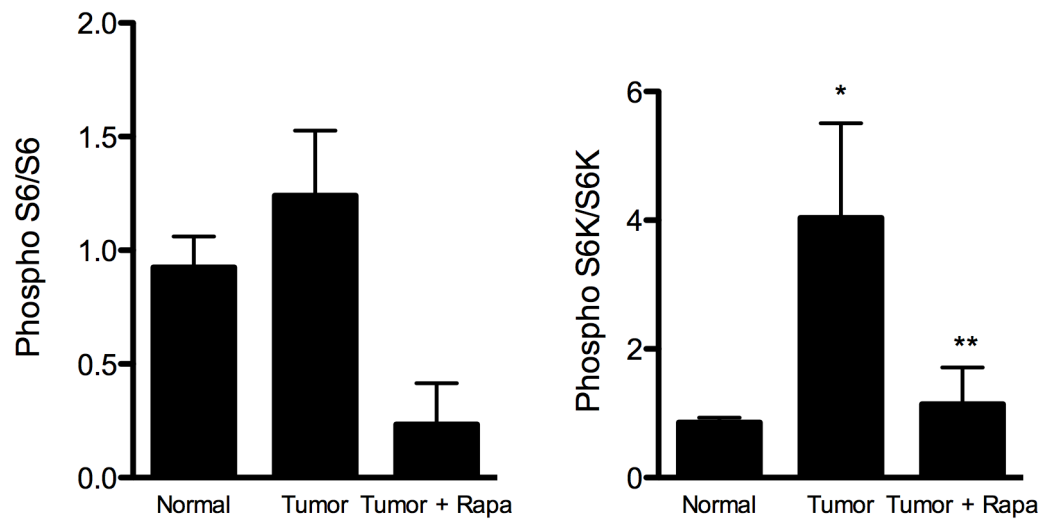


Figure 43: **Quantitation of mTORC1 elevation in lymphomas from *Atm*^{-/-} mice.** Graphs represent densitometric analysis of phosphorylated S6/total S6 or phosphorylated S6K/total S6K in ad lib fed mice. For the S6 graph the sample sizes were: n=7 normal thymus, n=12 tumors and n=6 tumors+rapa. For the S6K graph the sample sizes were n=5 normal thymus, n=9 tumors and n=4 tumors+rapa. The asterisk means p<0.05 (Mann-Whitney test) versus normal thymus and the double asterisks means p<0.05 versus the tumor. [(Reprinted from (146)]

Figure 44:

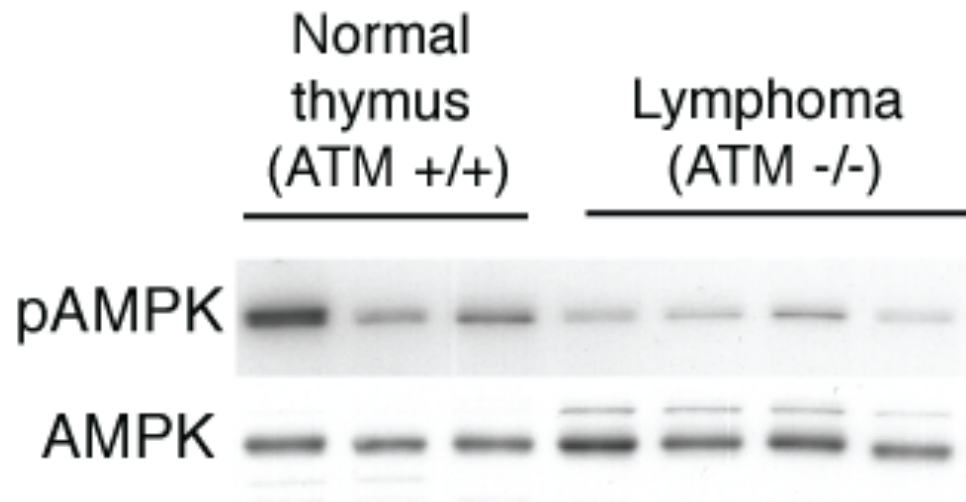


Figure 44: **AMPK is not activated in *Atm*^{-/-} mice.** AMPK phosphorylation was analyzed by western analysis in normal thymus from *Atm*^{+/-} mice and lymphomas from *Atm*^{-/-} mice. Despite elevated ROS in the lymphomas as a result of Atm loss, AMPK is not phosphorylated, consistent with requirement for Atm in this pathway.

Figure 45:

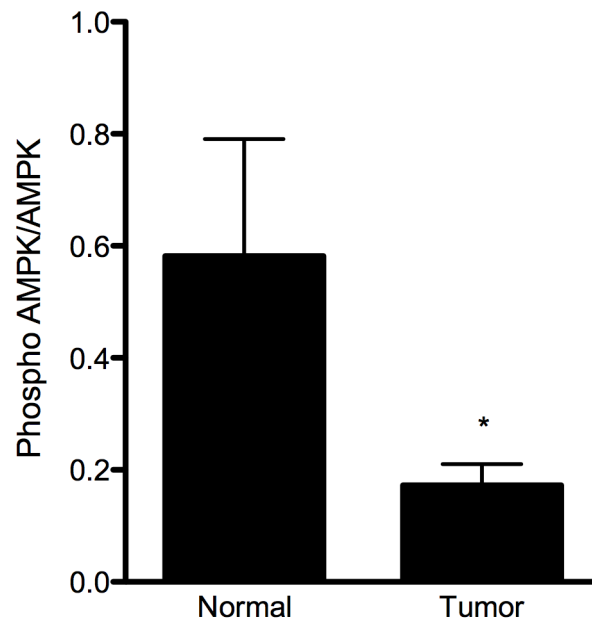


Figure 45: **Quantitation of AMPK activation in *Atm*^{-/-} mice.** Graphs represent densitometric analysis of phosphorylated AMPK/total AMPK in ad lib fed mice. For the S6 graph the sample sizes were: n=3 normal thymus, n=4 tumors. The asterisk means p<0.05 (Mann-Whitney test) versus normal thymus.

Figure 46:

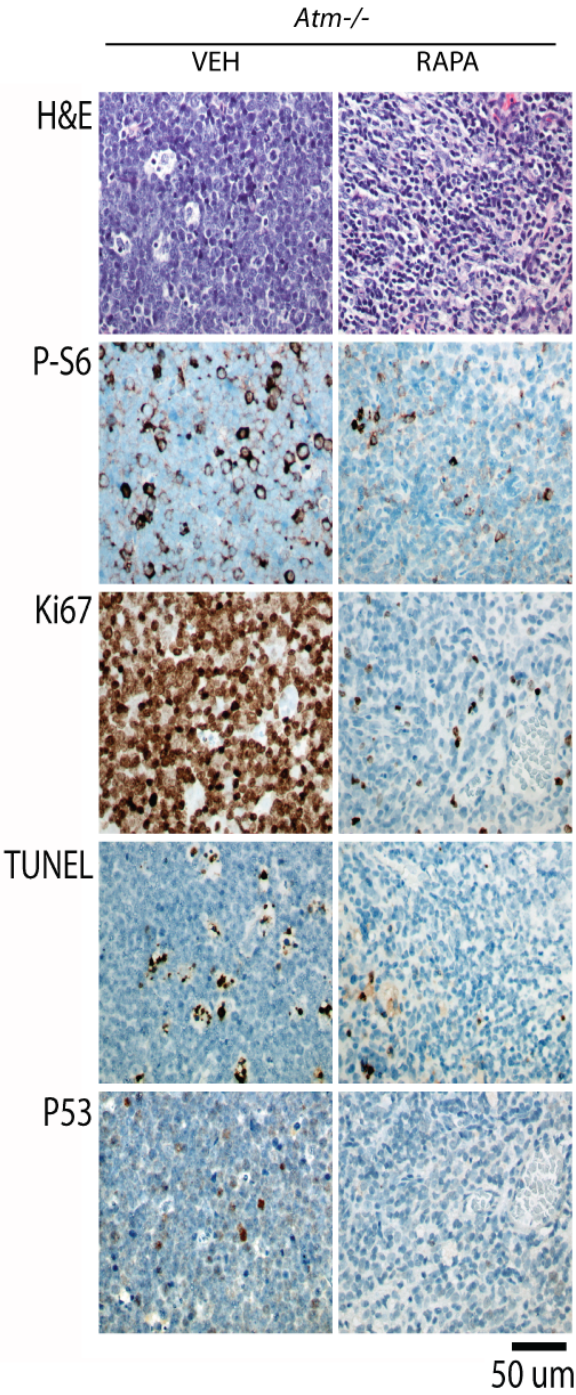


Figure 46: **Histological characterization of response to rapamycin in short-term treated mice** Lymphoma sections from *Atm*^{-/-} mice treated with vehicle or rapamycin for 7 days were stained as indicated. [(Reprinted from (146)]

The second long-term study was similar except we continued dosing the animals daily until the animals became moribund and had to be euthanized in accordance with our institutional animal care and use committee guidelines, in order to measure whether survival was extended due to rescuing lymphomagenesis. Figure 47 shows our Kaplan-Meier survival curve. Our results demonstrated that rapamycin was efficacious in rescuing lymphomagenesis which had an impact on overall survival. All of the vehicle treated mice were dead by 200 days of age, while >50% were still alive beyond 200 days ($p < 0.001$, log-rank test).

4.4 Discussion

The primary focus of this chapter was evaluating mTORC1 signaling in the aggressive lymphomas that arise in Atm-deficient mice. For the first time, we showed that these lymphomas have dysregulated mTORC1 signaling. It is already well-established that ROS plays a key role in the pathogenesis of these tumors, since use of antioxidants such as N-acetyl cysteine act as chemopreventive agents in these animals via modulating levels of oxidative stress (and subsequent DNA damage) (156-159). In the absence of Atm, this state of elevated ROS cannot signal to repress mTORC1 via AMPK, as indicated by the decreased level of AMPK phosphorylation seen in the lymphomas.

Secondly, our exciting finding that rapamycin rescues ATM-dependent lymphomagenesis and extends survival is completely concordant with another large landmark study that showed rapamycin could increase longevity of mice of different genetic backgrounds by 10-15% in aged mice treated with rapamycin late in life, due to rapamycin delaying death from cancer, or diminishing other aging phenotypes (160).

In our system it is not clear whether the therapeutic effect of rapamycin results from rapamycin-induced decrease in ROS levels in thymic cells or rapamycin-induced death of pre-malignant, activated thymic cells as a consequence of the other activities of rapamycin. Some of these other processes that may be influenced by rapamycin include inhibition of protein synthesis, induction of autophagy, inhibition of angiogenesis and modulation of HIF-1 α

Figure 47:

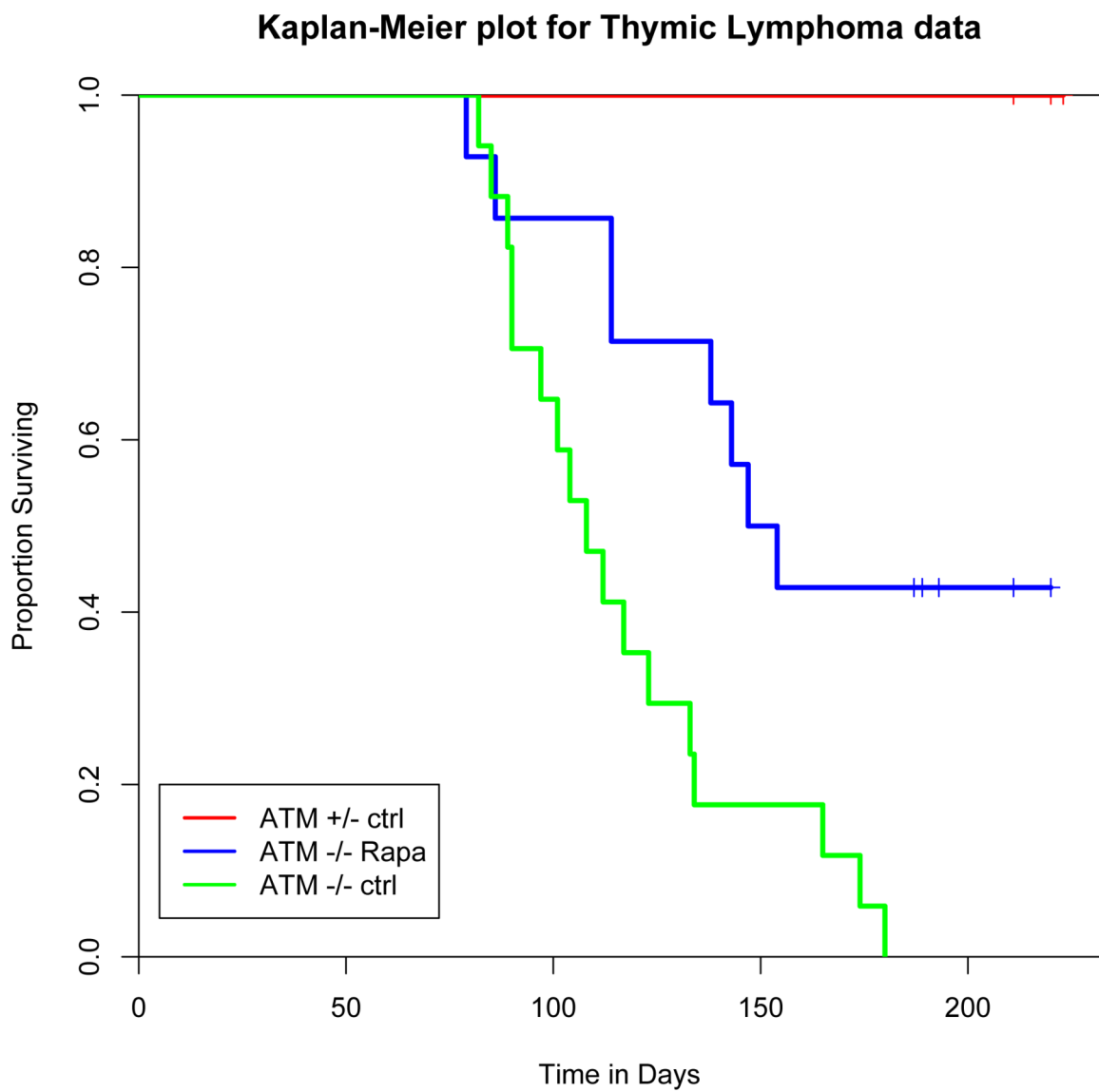


Figure 47: **Kaplan-Meier survival curve for long-term study of rapamycin as a therapeutic for lymphoma** [(Reprinted from (146))]

expression. During preparation of our manuscript for publication, a similar study was published in a mouse model of a chronic liver disease (hereditary tyrosinemia), which is a strong predisposition factor for liver tumorigenesis. Using the rapalog (rapamycin analog) RAD001/everolimus, the authors showed that rapamycin could inhibit the proliferation of hepatocytes during chronic liver injury, via engaging the DNA damage response which induces cell cycle arrest (161). Similar to our results, they observed a decrease in p53 expression (and p53 transcriptional activity, based on p21 expression), and when the mice were treated long-term with RAD001, tumor development was significantly delayed. Taken together these results support a model whereby mTOR inhibition can suppress proliferation of cells that have accumulated DNA damage, which leads to delayed tumorigenesis *in vivo*.

Our data showing lower levels of apoptosis as measured by TUNEL should perhaps be followed up by more detailed studies to determine whether apoptosis is occurring, and the dying cellular matter is being removed before it can be detected at the single time-point we analyzed. However, the TUNEL data seems to suggest that a robust apoptotic response is not the sole factor in the dramatic anti-tumorigenic response of this short-term administration of rapamycin. In addition, autophagy should be examined by electron microscopy and/or LC3 II and p62 western blots to determine whether increased autophagy may be functioning as a cell death mechanism in this model. Based on the findings from this study, perhaps the efficacy of rapamycin could be increased further via novel combinations of drugs (such as chloroquine), especially if autophagy is being utilized by the surviving cells as a survival mechanism. Regardless of mechanism of delaying tumorigenesis however, this observation may have potential therapeutic implications for treatment of AT patients, since mTOR inhibitors are currently in a variety of clinical studies and have been approved for certain indications such as renal cell carcinoma.

Peroxisomal localization of ATM-TSC2 signaling node to regulate pexophagy

5.1 Introduction to problem

In this part of our work, we aimed to understand where in the cytoplasm ATM signals to TSC2 in response to ROS, and what the functional consequences of inducing autophagy are. As mentioned in the introductory chapter, ATM has been found at various organelles including the peroxisome, centrosome and plasma membrane, whereas TSC2 has not previously been definitively localized to a specific endomembrane compartment.

The generally accepted model of TSC2 localization involves association with the outer surface of an organelle membrane, where this protein can be accessible to AKT and other cytoplasmic kinases. In response to signaling pathways such as induction of PI3K by growth factors or mitogens, AKT phosphorylates TSC2 promoting partitioning away from the membrane. This model therefore somewhat limits the possibilities for localization. Previous work from our laboratory has attempted to identify the specific organelle to which TSC2 is localized when active, through a combination of *in silico* approaches and co-immunofluorescence with well-known markers of different organelles. In this section I will describe the discovery of the peroxisome as a major site for TSC2 GAP towards Rheb, and describe ongoing studies that suggest that localization of the ATM:TSC2 signaling node at the peroxisome functions as a redox sensor to induce pexophagy if peroxisome number or function is perturbed.

5.2 Peroxisome biology

Peroxisomes, also known as microbodies, were the last of the major organelles to be discovered, beginning in the early 1950's in Rhodin's doctoral thesis (162) and later biochemically characterized by Christian de Duve in 1966 (163, 164). These discoveries were made by careful observation of electron microscopy images, firstly from mouse proximal tubule cells, and later in rat liver parenchyma, but later discovered to be present in all cells, where

they play a variety of important metabolic roles. One of the major roles is β -oxidation of fatty acids, prostaglandins and leukotrienes which generates significant amount of ROS as a byproduct of these reactions. Other important functions include detoxification of hydrogen peroxide and reactive nitrogen species (RNS) via enzymes such as catalase and superoxide dismutase, biosynthesis of bile and the phospholipid plasmalogen. A complete listing of all these metabolic functions can be found in (165).

Peroxisomal proteins are targeted to this organelle by means of binding to specific import receptor proteins, and imported into the matrix in their finally folded forms. These receptors recognize their cargo based on 3 main types of targeting sequences: PTS1, PTS2 or mPTS. The features of these targeting sequences are summarized in table 3.

Peroxisome number is tightly regulated in cells both via peroxisomal biogenesis as well as degradation via a specific form of autophagy known as pexophagy. Peroxisomes proliferate primarily in response to environmental cues including excess lipids, which in mammals is triggered via transcriptional regulation by the peroxisomal proliferators activator receptor α (PPAR α) protein. Approximately 30 genes have been identified that participate in either macro- or micro-pexophagy, but most of these are core autophagic machinery (166). Signaling pathways that regulate pexophagy have not been well-characterized, particularly in mammalian cells, as most of the pexophagy genes have been discovered through studies in yeast.

Table 3:

Sequence Type	Import receptor	Consensus sequence	Location in protein	Peroxisomal localization information
PTS1	PEX5	S/A/C - K/R/H - L/M	C-terminus	Matrix
PTS2	PEX7	R/K - L/I/V/Q – XX-L/I/V/H/Q- L/G/S/A/K-X - Q/H - L/A/F	N-terminus	Matrix
mPTS	PEX19	Cluster of basic and possibly hydrophobic amino acids	Near transmembrane domain	Membrane

Table 3: Peroxisomal targeting sequence summary

Results

5.31 Predicted peroxisome localization sequences in TSC2, TSC1, mTOR and ATM

To determine whether the critical pathway members may be localized at the peroxisome, we utilized several online *in silico* tools (which were found through www.peroxisomedb.org) to search for any of the peroxisomal targeting sequences as described in previous section (167). Table 4 shows the sequences that we found, with bold highlighting the actual sequence that matches the consensus. Note that for TSC1 the sequences we found both have one mismatch versus the precise consensus sequence, however we felt that this was sufficient rationale to move forward with experimental validation because of what is known about the biology of TSC1 and TSC2 functioning as heterodimers within cells.

5.3.2 Experimental evidence for peroxisomal localization of TSC2, TSC1, mTOR and ATM

To begin studying whether TSC2 and other pathway components were localized to the peroxisome, we overexpressed Flag-tagged TSC2 and Myc-tagged TSC1 (and reverse for TSC1 staining) in HeLa cells and performed standard co-immunofluorescence staining of Flag and PMP70, a peroxisomal membrane protein. As shown in figure 48, we observed a punctate cytoplasmic staining, and significant colocalization between wild-type TSC2 and PMP70, as well as TSC1 and PMP70.

In searching through the tuberous sclerosis complex mutation database (found at http://chromium.liacs.nl/LOVD2/TSC/home.php?select_db=TSC2) we found some 28 patients with mutations that disrupt the putative PTS1 sequence. We performed site-directed mutagenesis to make 3 of these most common mutations (R1743G, R1743W, R1743Q) and when we performed immunofluorescence for these mutants, we found that TSC2 no longer stained in the characteristic punctate pattern, nor co-localized with PMP70 (figure 48).

To confirm these data, we biochemically purified peroxisomes using a differential density gradient method, from cultured cells and performed western blots on isolated

Table 4:

Protein	PTS type	Sequence info
TSC2	PTS1	KWIA RL RHIKR
TSC1	PTS2	KLHSQIRQL or RILELESHL
ATM	PTS1	KNL SRL FPGWK
mTOR	PTS2	RISKQLPQL

Table 4: Peroxisome targeting sequences found in proteins of interest

peroxisomes, and nuclear, membrane and cytosolic fractions. The nuclear, membrane and cytosolic fractionations were performed separately from the peroxisome fractionation to obtain the least contamination of organelles in the respective fractions. We overexpressed both wild-type and mutant TSC2 along with the TSC1, which is necessary for stabilization of TSC2, and performed both sets of fractionations as described. The western blots showing significantly less membrane-associated and peroxisome-localized mutant TSC2 are shown in figure 49. It should be noted that peroxisomes are found in the membrane fraction, since peroxisomes pellet alongside the other endomembranes in the ultra-centrifuge spin. We also used Tsc2-proficient and Tsc2-deficient MEFs to show that endogenous Tsc2 localizes to the peroxisome, and is likewise also found in the membrane fraction. There is also a portion of total TSC2 in the cytoplasm since these cells were cultured in serum-containing media, and therefore AKT signaling would have been activated, causing phosphorylated TSC2 to leave the membrane fraction. Figure 50 shows endogenous Tsc2 localization within these fractions.

The other components of the ROS-induced signaling node also localize to the peroxisome. Fractionation of HEK 293 cells, as shown in figure 51, shows that ATM, AMPK, mTOR and Rheb can localize to the peroxisome and can be also detected in the membrane fraction.

Figure 48:

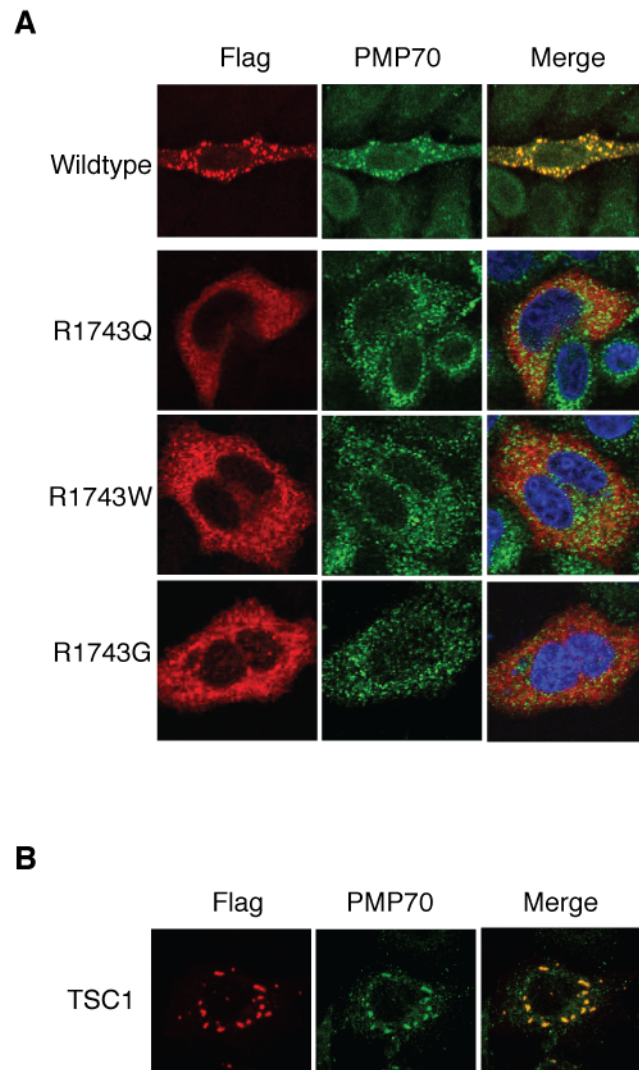


Figure 48: **Immunofluorescence showing TSC2 and TSC1 colocalization with**

peroxisomal marker PMP70 HeLa cells were transfected with (A) Flag-TSC2 and Myc-TSC1 and co-stained for Flag (red) and PMP70 (green) or (B) Flag-TSC1 and Myc-TSC2 and co-stained for Flag (red) and PMP70 (green).

Figure 49:

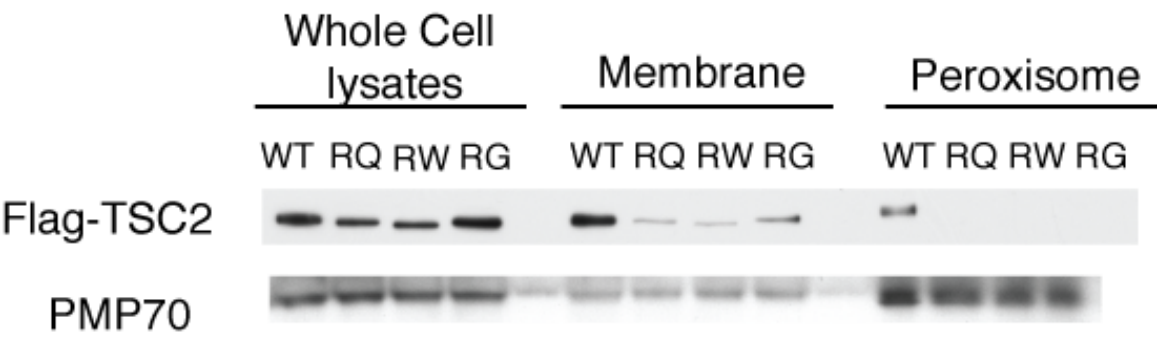


Figure 49: **Fractionation showing PTS1-disrupted mutants fail to localize correctly to membrane and peroxisome fractions.** HEK 203 cells were transfected with Flag-wild-type (WT) TSC2 or mutants, and whole cell lysates, membrane fractions, and purified peroxisomes were obtained for western analysis as shown.

Figure 50:

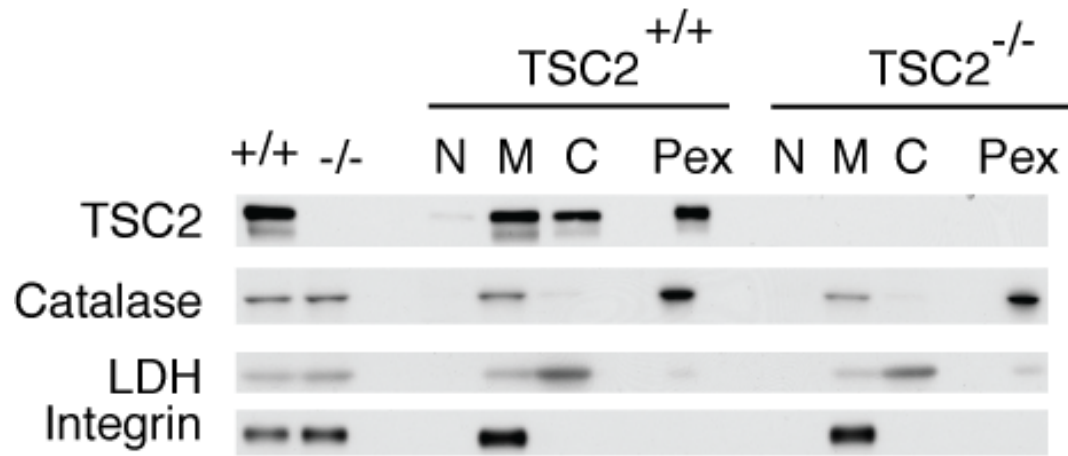


Figure 50: **Fractionation showing endogenous TSC2 localized to the peroxisome and membrane fractions** Whole cell lysates (lanes 1 and 2), nuclear fractions (N), membrane fractions (M), cytosolic fractions (C) and purified peroxisomes (Pex) were isolated from Tsc2-proficient and Tsc2-deficient MEFs and western analysis was performed. Catalase is a peroxisomal marker, LDH is a cytosolic marker, and Integrin (β 1-integrin) is a membrane marker.

Figure 51:

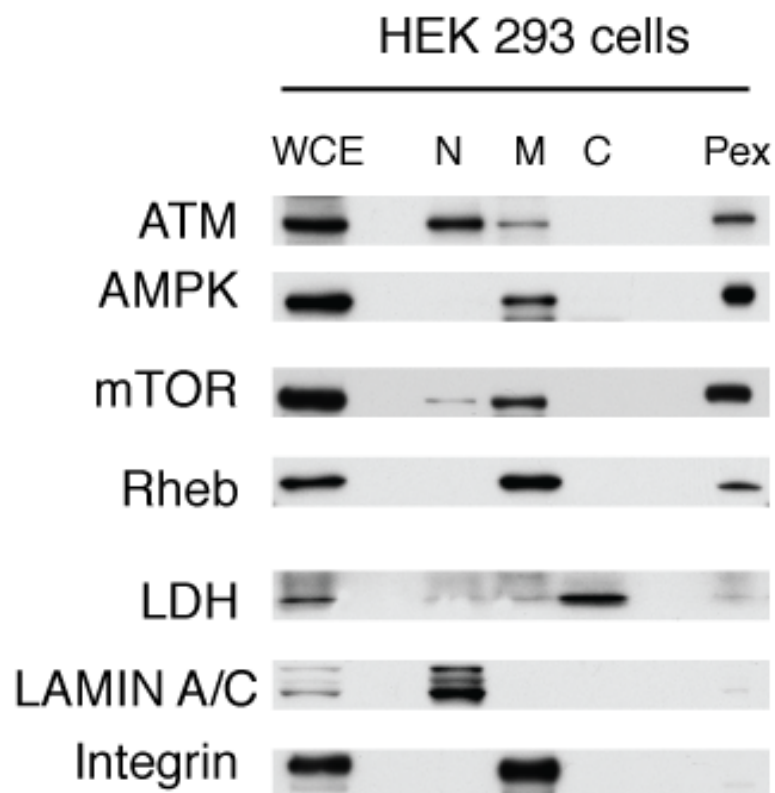


Figure 51: **Fractionation showing ROS-signaling node localized to the peroxisome** Whole cell lysate (lane 1), nuclear fraction (N), membrane fraction (M), cytosolic fraction (C) and purified peroxisomes (Pex) were isolated from HEK 293 cells and western analysis was performed. Catalase is a peroxisomal marker, LDH is a cytosolic marker, and Integrin (β 1-integrin) is a membrane marker.

The finding that the PTS1 sequence in TSC2 targets this protein to the peroxisome outer membrane, must somehow be resolved with the generally accepted view that PTS1 and PTS2 sequences have only been found on peroxisomal matrix proteins such as catalase. A search for potential membrane PTS sequences using the BLOCK algorithm, found only a poorly matched stretch of 5 potential amino acid similarities within a 12 amino acid stretch. Compared to the PTS1 and PTS2 prediction tools however, it has been more difficult to find these potential sites due to the differences in the specificity and sensitivity of the algorithm as noted on the website.

An experimental way of validating whether proteins are localized to the matrix or membrane of the peroxisome has been described previously, and is known as the protease protection assay. Isolated peroxisomes are Proteinase K treated in the presence or absence of Triton X-100 detergent which permeabilizes membranes. Proteins that are found in the membrane would be degraded regardless of the presence of detergent, while matrix proteins would be stable unless Triton-X100 was added. Figure 52 shows the TSC2, TSC1 and ATM are all rapidly degraded by Proteinase K treatment, while catalase is not, providing further evidence that this signaling node is localized to the outside of the peroxisome membrane, allowing TSC2 to be accessible to other cytosolic proteins involved in the many signaling pathways that are known to lie upstream of TSC2..

5.3.3 Loss of peroxisomal targeting sequences perturbs mTORC1 signaling

Given that we identified patient-derived mutations in TSC2 that would disrupt the PTS1 sequence, we asked whether this mutant TSC2 was functional in suppressing mTORC1 signaling. Using a cellular functional assay similar to the one described in chapter 3, we looked at the phosphorylation status of S6K (S6K1) and 4EBP1 in cells transfected with wild-type and all 3 patient-derived mutations (RG, RQ, RW), and found that while wild-type TSC2 could potentially suppress mTORC1 activity, none of the mutants could suppress mTORC1 (see figure 53).

Figure 52:

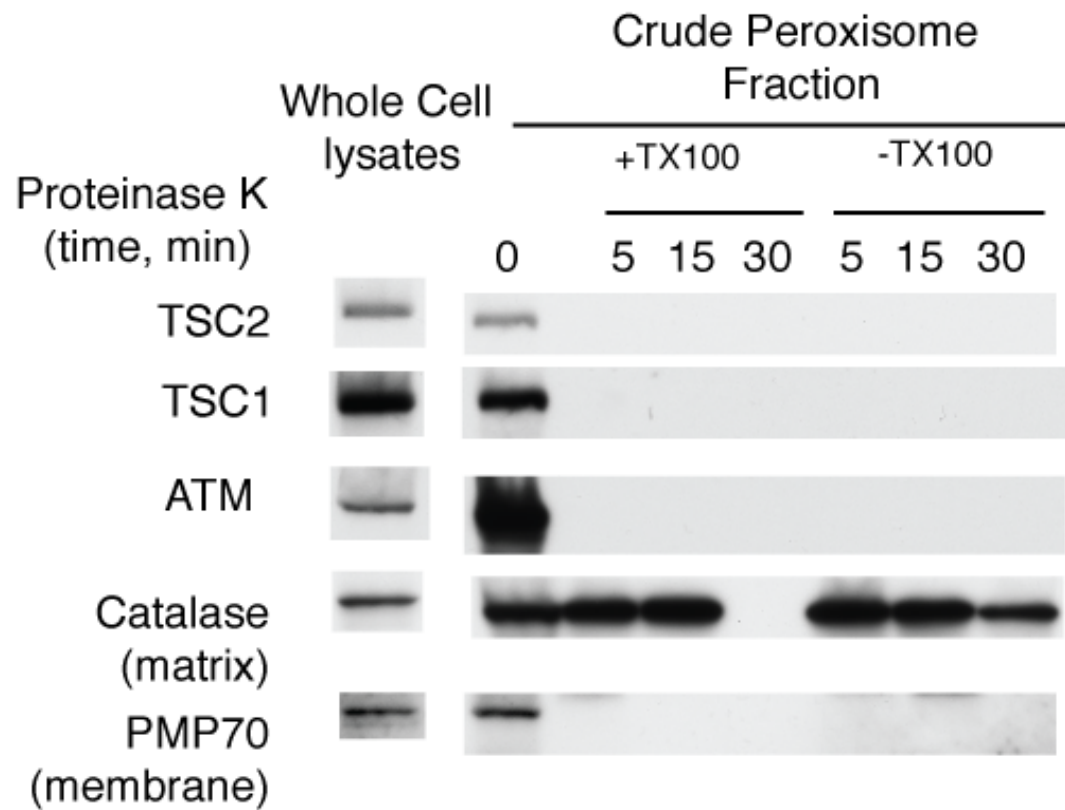


Figure 52: **Protease protection assay showing that TSC2, TSC1 and ATM are localized on the outer surface of the peroxisome** Aliquots of purified peroxisomes were isolated from HEK 293 cells and subjected to the protease protection assay. Once the reactions were completed, the products were loaded onto gels and western blots were performed as indicated. Catalase is used as a peroxisomal matrix marker and PMP70 is a peroxisomal membrane marker.

Figure 53:

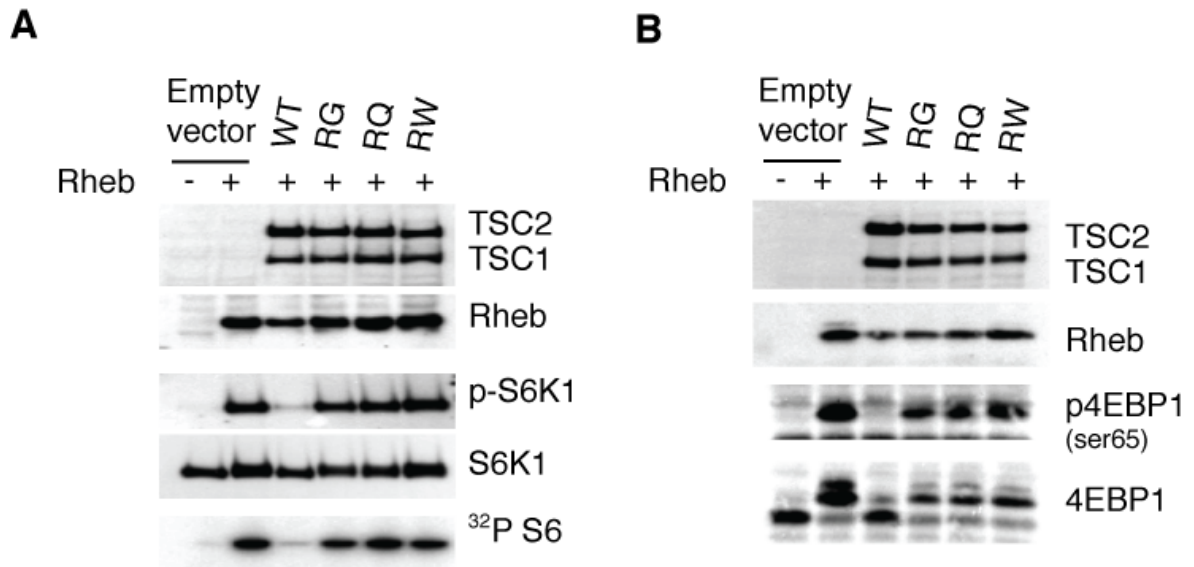


Figure 53: **Functional assay for TSC2 activity towards mTORC1** HEK 293 cells were transfected as described in the methods section, and lysates used for western blots as indicated. All three mutants have no GAP activity based on the high levels of mTORC1 substrate phosphorylation that is equivalent to empty vector + Rheb transfectants.

To conclusively identify the peroxisome as the organelle where TSC2 is functional, as opposed to the alternative hypothesis that the three mutations cause tertiary structure changes that alter TSC2's GAP activity, we reintroduced a PTS1 sequence to the C-terminus of the R1743Q construct. When we performed functional studies on this new construct (RQ-9NT) we found that mTORC1 could now be repressed, consistent with the peroxisome being a major site of TSC2 activity (figure 54).

5.3.4 Cells from Zellweger syndrome patients possess basal elevated oxidative stress and altered mTORC1 regulation

To determine biological significance of the localization of the ATM-TSC2 signaling node at the peroxisome, we looked at cells derived from patients with the Zellweger peroxisome biogenesis disorder. Zellweger's syndrome is one of the most severe peroxisome biogenesis disorders, characterized by a complete absence of peroxisomes, however peroxisome ghost structures presumably made of membrane proteins can be observed in some cells (168). Since the peroxisome plays vital metabolic roles, most patients experience significant problems including neurological abnormalities, hypotonia (poor muscle tone), liver diseases and renal cysts, and typically do not survive much beyond 1 year of age (169).

We proposed that if mTORC1 suppression at the peroxisome by TSC2 is important for maintaining redox homeostasis, that cells lacking peroxisomes such as those from Zellweger would possess elevated ROS levels and that similar to Tsc2-deficient cells as shown previously, rapamycin could decrease ROS levels. Figure 55 shows that the Zellweger fibroblasts had over 4 fold higher ROS levels, and rapamycin could partially rescue this defect. When challenged with a dose-response of H₂O₂, the Zellweger cells were unable to repress mTORC1 until a very high, supra-physiological dose was used (1mM), suggesting that intact functional peroxisomes are important for ROS-induced regulation of mTORC1 activity (figure 56). However, it is intriguing that ATM can still be activated in the absence of peroxisomes quite robustly.

Figure 54:

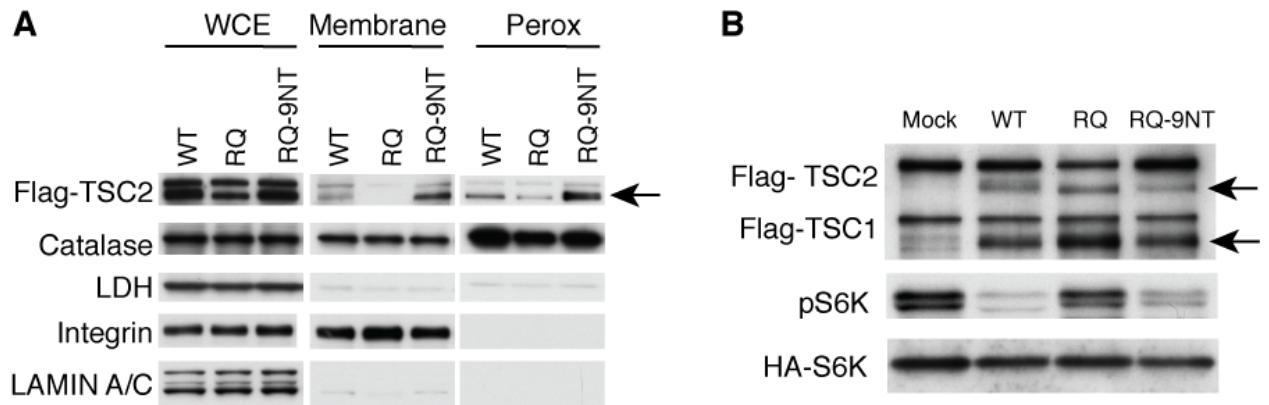


Figure 54: **Reintroducing TSC2 to the peroxisome restores functionality towards**

mTORC1 (A) HEK 293 cells were transfected with Flag-wild-type (WT) TSC2 or mutants and Flag-TSC1, and whole cell lysates, membrane fractions, and purified peroxisomes were obtained for western analysis as shown. (B) *Tsc2*^{-/-} MEF cells were transfected as described in the methods to perform functional assay for TSC2 activity. Unlike the RQ mutant which lacks GAP activity, the RQ-9NT mutant which relocates to the peroxisome regains activity.

Figure 55:

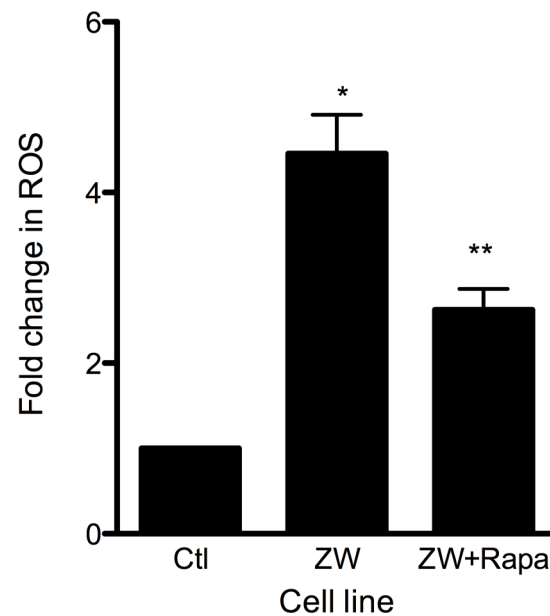


Figure 55: **Elevated ROS in Zellweger cells, and partial rescue by rapamycin** ROS levels were measured using DCFDA in control fibroblasts (Ctl, GM15871) and Zellweger syndrome (ZW, GM13267) fibroblasts treated with vehicle or 200nM rapamycin for 24 hours. The asterisk represents significance between control and Zellweger cells, and the double asterisks represent significance between the vehicle and treated Zellweger cells (both $p < 0.05$, one sided t-tests).

Figure 56:

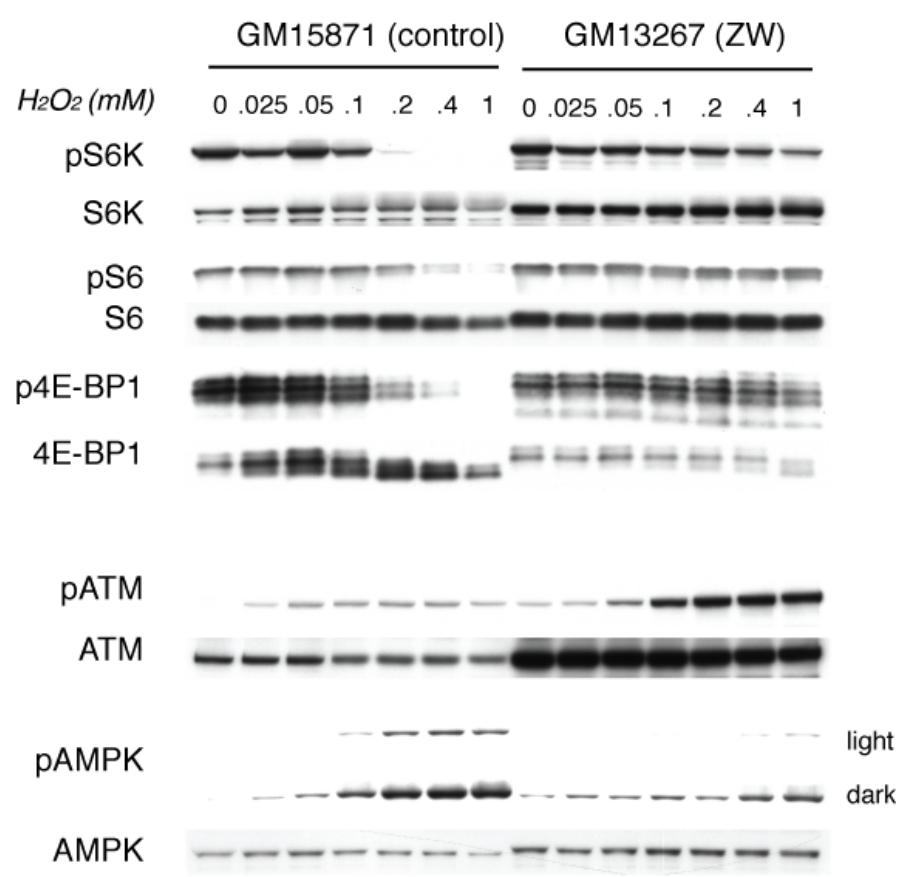


Figure 56: **Dysregulated ROS signaling to mTORC1 in Zellweger cells** Control (GM15871) and Zellweger syndrome (GM13267) fibroblasts were treated with the indicated doses of H₂O₂ for 1 hour prior to harvesting and performing western blots as indicated. Importantly, the Zellweger cells have baseline elevated ATM phosphorylation and this can be induced even further, but mTORC1 cannot be suppressed until the highest dose.

5.3.5 ROS induction of autophagy induces peroxisome turnover

Earlier we (and many others) have established that ROS induces autophagy. With the discovery that the ATM:TSC2 signaling node is localized on the periphery of the peroxisome, we asked whether peroxisomes could be turned over by pexophagy in response to ROS. To test this hypothesis, we utilized MCF7 GFP-LC3 cells which we treated with H₂O₂ and followed protein levels over a 24 hour time course. Figure 49 shows that during this time period, we saw that consistent with mTORC1 suppression and induction of autophagic flux, that catalase expression decreased, suggesting that peroxisomes were being degraded by autophagy. Other peroxisomal proteins including TSC2, TSC1, ATM and mTOR were also decreased consistent with peroxisome turnover by pexophagy.

5.4 Discussion

In this chapter we have described a model whereby peroxisomal ATM and TSC2 signal to mTORC1 to induce pexophagy. This work is novel and exciting for a number of reasons. Firstly, TSC2 has not previously been localized to a specific endomembrane compartment. The recent data on spatial regulation of signaling pathways, such as the amino-acid sensing pathway for activating mTOR via recruitment to the lysosomal membrane, where it associates with both Rheb and the Rag-Ragulator complex and activate downstream signaling, emphasizes the necessity to understand at a sub-cellular level where signaling molecules reside and recognize stimulus-dependent mechanisms of action (170).

We provided evidence that TSC2 can localize to the peroxisome via a class 1 peroxisome targeting sequence (PTS1), and that there are mutations in tuberous sclerosis complex patients that disrupt this sequence, with important consequences for regulation of mTORC1 activity. When we added an ectopic PTS sequence to the C-terminus of TSC2 containing one of these patient-derived mutations, we could restore activity, highlighting the crucial role played by the peroxisome as a site of TSC2 activity.

Figure 57:

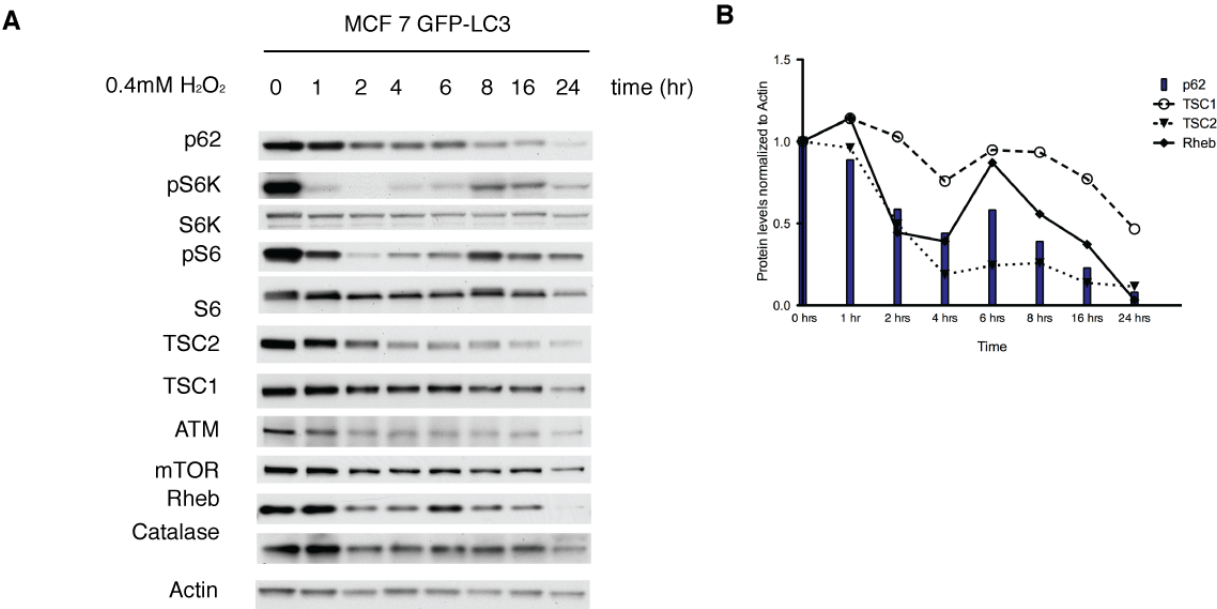


Figure 57: **Degradation of peroxisome proteins in response to ROS** (A) MCF7 cells stably expressing GFP-LC3 were treated with 0.4mM H₂O₂ for the indicated times and western blots performed as indicated. (B) Graph represents densitometric ratios for the time-dependent degradation of several members of the ATM-TSC2 signaling node during autophagy.

The discovery of a PTS1 sequence prior to the C-terminus of TSC2 challenges the current dogma relating to the location of functional PTS1 sequences, and the precise peroxisomal location that peroxin 5 delivers such cargo to. Our finding that TSC2 contains a functional PTS1 sequence, and is delivered to the peroxisomal membrane (based on our results from the protease protection experiment) therefore may be surprising.

While we showed that Rheb can be detected in the peroxisomal fraction, we could not find any classical peroxisome targeting sequences. However, it is already known that Rheb contains a CaaX motif which allows farnesylation, which serves as the membrane-targeting mechanism, and is necessary for mTORC1 activation (171).

Peroxisomes are significant ROS-generating organelles due to the activities of enzymes involved in β -oxidation, and possess a variety of enzymes responsible for scavenging this ROS so that the cell does not become damaged by excessive ROS. Our data support a model whereby peroxisomal ROS signals locally to activate TSC2 via ATM and AMPK to repress mTORC1 and induce autophagy which can regulate peroxisome number. In the literature, there is not very much known about the mechanisms of peroxisome turnover. Most of these studies focus on the role of the PPAR α transcription factor which transcriptionally activates many genes important in peroxisome biogenesis (172). PPARs are activated by drugs such as hypolipidemic fibrates and thiazolidinediones, and in animals, withdrawal of these drugs induces autophagy-dependent removal of the excess proliferated peroxisomes. PPAR activation has been shown to result in elevated oxidative stress, due to an imbalance in upregulation of ROS-generating enzymes versus ROS-scavenging enzymes, which is thought to be a contributing factor to the hepatocarcinogenicity in rodents (173, 174).

One of the remaining unresolved mechanistic questions is how ATM signals to LKB1 since we did not find any PTS sequences in LKB1, nor found it localized in peroxisome fractions. One potential explanation for this once activated by ROS, ATM can transiently leave the peroxisome membrane to interact with LKB1 in the cytoplasm, and then return to the peroxisome to activate AMPK and downstream signaling. It is also possible that LKB1 could

activate AMPK in the cytoplasm, and phosphorylated AMPK could traffic back to the peroxisome to activate TSC2 to suppress mTOR. Studies are now underway in the laboratory to determine which of these possibilities is correct. It would also be interesting to determine whether other mechanisms of AMPK activation such as starvation also activate a peroxisomal pool of AMPK, or whether this ATM-regulated pathway is specific for ROS.

Identification of ATM and TSC2-dependent, but AMPK-independent DNA damage signaling pathway to regulate mTOR

6.1 Introduction

In the first section of this dissertation we described an ATM and TSC2-dependent pathway that is engaged in response to ROS to signal to mTORC1. We next asked whether nuclear DNA damage, such as that generated by etoposide or ionizing radiation, could also signal via this same pathway. ATM is known to be activated by DNA damage, and as described in the opening chapter, can translocate out of the nucleus in response to DNA damage, making this a plausible scenario. In addition, it is already known that DNA damage can activate p53, which was reported to be a mechanism of suppressing mTORC1, via AMPK activation, but it was not shown whether TSC2 was required for this pathway (134). In this chapter however, we present evidence that in a cell-type dependent manner, DNA damage can induce mTORC1 suppression without activating AMPK and can do so in p53-deficient cells.

There is some literature on the role of LKB1 and AMPK in the DNA damage response, which we have published a review on recently, but much of this research did not extend the findings downstream of AMPK (175). For example, when the ATM phosphorylation site on LKB1 was first discovered, downstream signaling to AMPK and mTORC1 was not analyzed, raising the question about whether LKB1 phosphorylation by ATM plays a role in signaling to mTORC1 (147). ATM was also shown to directly phosphorylate AMPK on the LKB1 phosphorylation site to induce mitochondrial biogenesis (145). Finally a third potential mechanism that has been identified for activating AMPK involves the p53 transcriptional targets sestrin 1 and sestrin 2 (144). More recently, AMPK has been shown to directly phosphorylate histone H2B in the nucleus after DNA damage or other stresses, resulting in transcription of stress-responsive genes (176). Based on these results, we expected to find that in response to DNA damage, ATM could translocate out of the nucleus and into the cytoplasm to engage the same pathway as previously identified, or alternatively signal to

AMPK in the nucleus, and then phosphorylated AMPK could translocate out to the peroxisome where TSC2 is active. However, our results that indicate AMPK is not necessary for mTORC1 suppression in a small panel of cell lines tested, indicating that there are other mechanisms that exist for DNA damage-induced signaling to mTORC1.

6.2 Results

6.2.1 Characterization of mTORC1 regulation by DNA damage

In order to begin studying the mechanisms by which DNA damage regulates mTORC1 we began testing several different methods of generating DNA damage in a panel of cell lines to characterize the kinetics and magnitude of responses. Our primary model continued to be MCF7 breast carcinoma cells. Figure 58 shows that etoposide treatment induces mTORC1 suppression, but only after a 24 hour treatment, while ATM is rapidly activated. However, unlike some of the previous reports, AMPK is not activated, or at least does not remain activated until the earliest time point taken (6 hours). Despite suppression of mTORC1, autophagy is not induced by etoposide in MCF7 cells, as seen in figure 59, where no significant increase in LC3 II or decrease in p62 is seen.

We next looked at the response to ionizing radiation (IR) over a similar time period, and we observed a similar profile of signaling, whereby mTORC1 suppression took an extended period of time, and did not involve AMPK activation (figure 60). Due to equipment challenges during these studies we also utilized a radiomimetic drug called neocarzinostatin (NCS) which is frequently used to activate ATM. In MCF7 cells, treatment with NCS for 4 hours induced ATM activation and mTORC1 suppression, but also did not activate AMPK (figure 61). In spite of mTORC1 suppression, autophagy does not appear to be increased – even though LC3 II levels increase slightly, p62 levels increase (figure 62). Further definitive studies were not performed based on this negative preliminary result relating to DNA damage inducing autophagy via mTORC1 repression.

Figure 58:



Figure 58: **mTORC1 signaling in response to etoposide in MCF7 cells** MCF7 cells were treated with 50 μ M etoposide for the time periods indicated and western blots performed to analyze ATM-AMPK-mTORC1 signaling.

Figure 59:

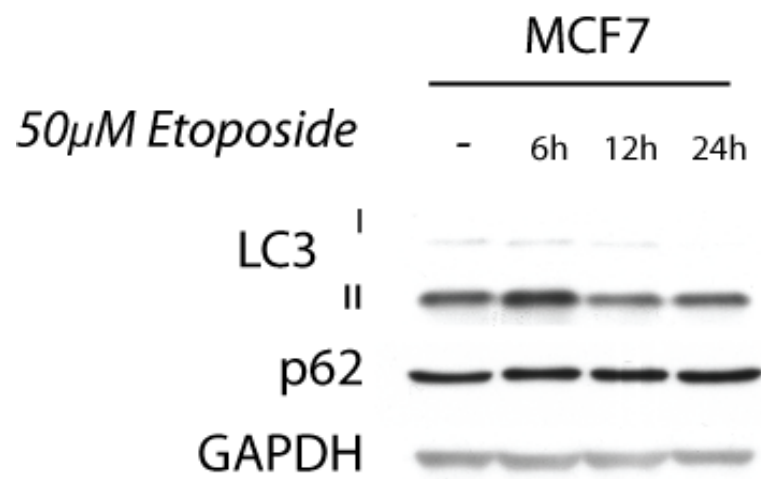


Figure 59: **Etoposide does not induce autophagy in MCF7 cells** MCF7 cells were treated with 50 μ M etoposide for the time periods indicated and western blots performed to analyze autophagy induction. The lysates used in this figure were from the same experiment as figure 58.

Figure 60:

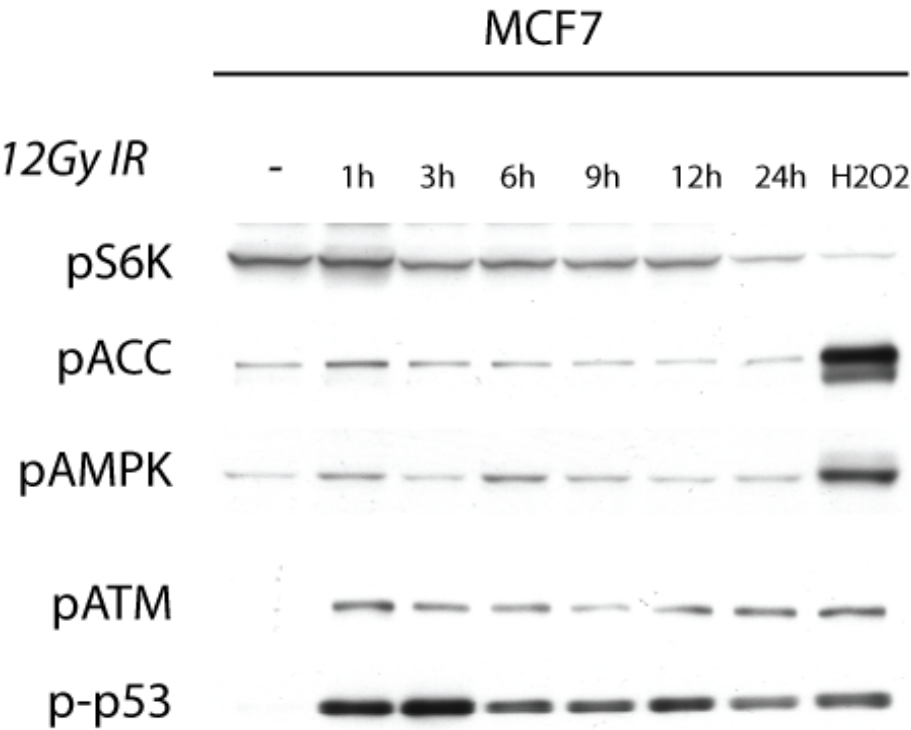


Figure 60: **mTORC1 signaling in response to ionizing radiation in MCF7 cells** MCF7 cells were irradiated with 12 Gy IR and incubated for the time periods indicated and western blots performed to analyze ATM-AMPK-mTORC1 signaling.

Figure 61:

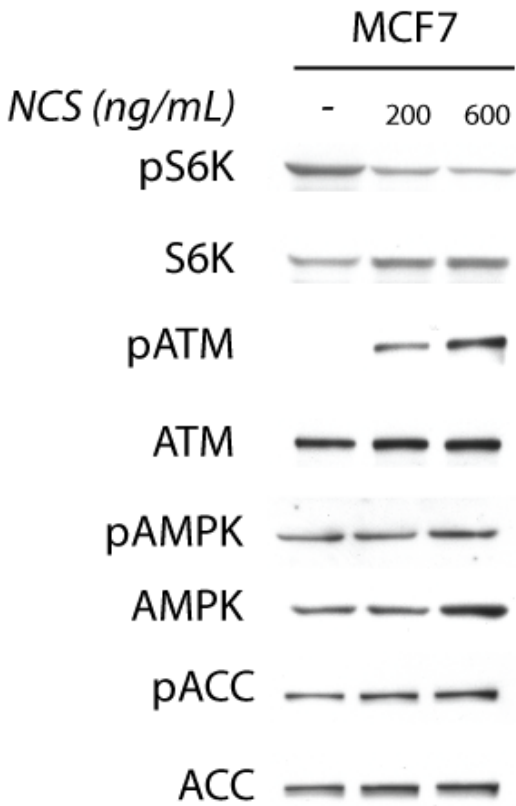


Figure 61: **mTORC1 signaling in response to neocarzinostatin in MCF7 cells** MCF7 cells were treated with 200ng/mL neocarzinostatin or 600ng/mL neocarzinostatin for the time periods indicated and western blots performed to analyze ATM-AMPK-mTORC1 signaling.

Figure 62:

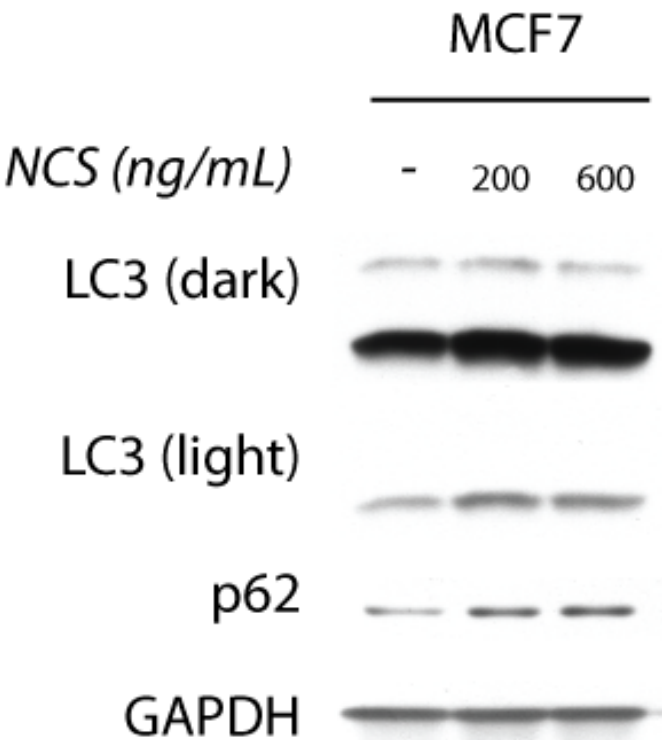


Figure 62: **Neocarzinostatin does not induce autophagy in MCF7 cells** MCF7 cells were treated with 200ng/mL neocarzinostatin or 600ng/mL neocarzinostatin for the time periods indicated and western blots performed to analyze ATM-AMPK-mTORC1 signaling. The lysates used in this figure were from the same experiment as figure 61.

We characterized signaling pathway regulation in a number of other cell lines to determine how generalizable the findings from the MCF7 experiments were. These results are summarized table 5, which shows the significant amount of heterogeneity among cell lines in their responsiveness to the various methods we used to generate DNA damage.

To begin to dissect out the mechanism, we asked whether TSC2 is required for mTORC1 suppression using Tsc2-proficient and Tsc2-deficient MEFs, which as previously mentioned are p53-deficient as well, allowing us to rule out p53-dependent pathways. Figures 63 and 64 demonstrate that in the absense of Tsc2, there is attenuated mTORC1 suppression by etoposide and NCS, suggesting at least 1 Tsc2-dependent pathway exists.

To confirm the dependence on TSC2 and determine whether ATM plays a role in the DNA damage signaling pathway, we used siRNAs targeted against both proteins. Figure 65 shows that when TSC2 or ATM are depleted, there is a significant decrease in mTORC1 suppression by IR. Intriguingly when we performed a similar experiment looking at the response to etoposide, we saw a striking lack of ATM activation in the TSC2-knockdown cells, as seen in figure 66. Once we had observed this, we attempted to look at whether in Tsc2^{-/-} MEFs or kidney tumor cells from the Eker rat (which arise as a result of losing both Tsc2 alleles) this is also the case; however the phospho-ATM antibody that we used to use for mouse and rat cell lines does not work any more, and the replacement antibody only works in human samples.

6.2.2 Determination of the mechanism of ATM signaling to mTORC1 in response to DNA damage

Once we had determined that ATM and TSC2 participate in a signaling pathway to regulate mTORC1, we focused on determining the mechanism of this signaling. One ATM and TSC2 independent mechanism we ruled out was mTOR sequestration in the nucleus due to a report of a DNA damage inducible gene, promyelocytic leukemia (PML) that is also activated by

Table 5:

Cell Line	Drug	mTORC1 suppressed?	AMPK activated?	Autophagy induced?
MCF7	Etoposide	Yes - 24 hrs	No	No
	IR	Yes - 12-24 hrs	No	No
	NCS	Yes - 4 hrs	No	No
HEK 293	Etoposide	No	ND	ND
	IR	Yes - 1 hr	No	No
	NCS	Yes - 24 hrs	No	No
Tsc2 ^{+/+} MEFs	Etoposide	Yes - 24 hrs	No	Yes *
	IR	ND	ND	ND
	NCS	Yes - 2-4 hrs	No	ND
Tsc2 ^{-/-} MEFs	Etoposide	A little (less than +/+)	No	Yes *
	IR	ND	ND	ND
	NCS	No	No	ND
<ul style="list-style-type: none"> • Autophagy induced is not mTORC1-dependent • ND = not determined 				

Table 5: **Summary of cell-type differences in response to DNA damage**

Figure 63:

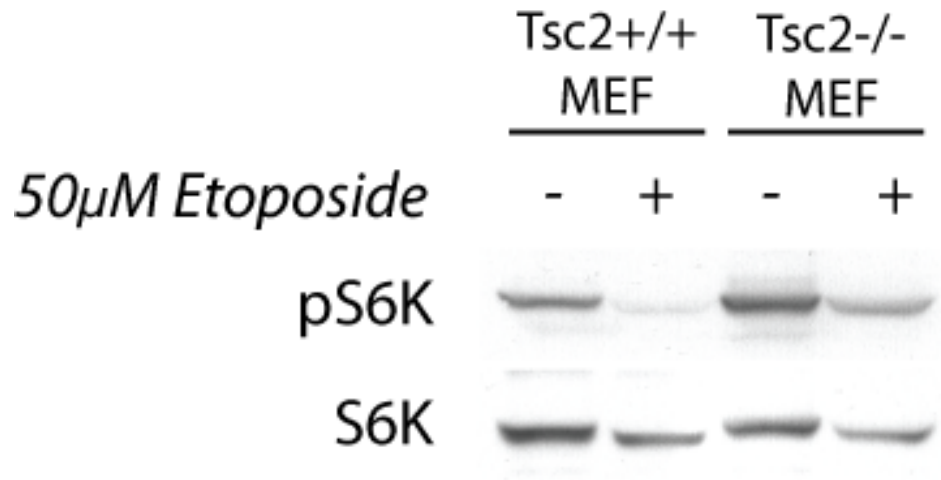


Figure 63: **mTORC1 response to etoposide in MEFs** Tsc2-proficient and Tsc2-deficient MEFs were treated with 50 μ M etoposide 24 hours and western blots performed to analyze mTORC1 signaling. mTORC1 repression is at least partially dependent on Tsc2 expression.

hypoxia, and as a result binds and sequesters mTOR in the nucleus away from its targets in the cytoplasm (177). We fractionated MCF7 cells into cytoplasmic and nuclear fractions, after treatment with all the damaging agents, we could observe no significant difference in mTOR localization between vehicle and drug/IR, suggesting that this PML-mTOR pathway was not being engaged, at least in this cell line (figure 67). We could also rule out the previously reported p53-sestrin-AMPK-mTORC1 pathway since AMPK is not activated, and mTORC1 could be suppressed in p53-deficient MEFs.

We next considered the possibility that TSC2 could be a direct ATM phosphorylation target, despite the fact that TSC2 was not identified in the unbiased screen for ATM regulated proteins recently published (178). When we performed a scansite search (<http://scansite.mit.edu>) to look for potential novel phosphorylation sites in TSC2, we found 2 sites that match the ATM consensus sequence (SQ/TQ). The schematic of human TSC2 protein shown in figure 68 shows that these putative phosphorylation sites, Ser 403 and Ser 1379 are in the middle of the protein not within any currently defined functional domain (such as the GAP domain). We have constructed a 2A (both serines mutated to alanines) mutant and studies are underway to characterize whether TSC2 activity is altered as a consequence of losing the ability to be phosphorylated by ATM.

6.3 Discussion

In this chapter we demonstrate the complexity of damage responses even within a single cell line. In contrast to the previously described pathway for ROS-induced activation of a cytoplasmic ATM-LKB1-AMPK-TSC2-mTORC1 pathway, we find that DNA damage induces ATM activation leading to TSC2 activation and mTORC1 suppression independent of AMPK activation. This suggests a dual model for damage-induced ATM signaling to mTORC1, as illustrated in figure 69. These results differ from a few isolated reports that claim that AMPK mediates a DNA damage induced pathway, but due to the differences in cell lines, damaging

Figure 64:

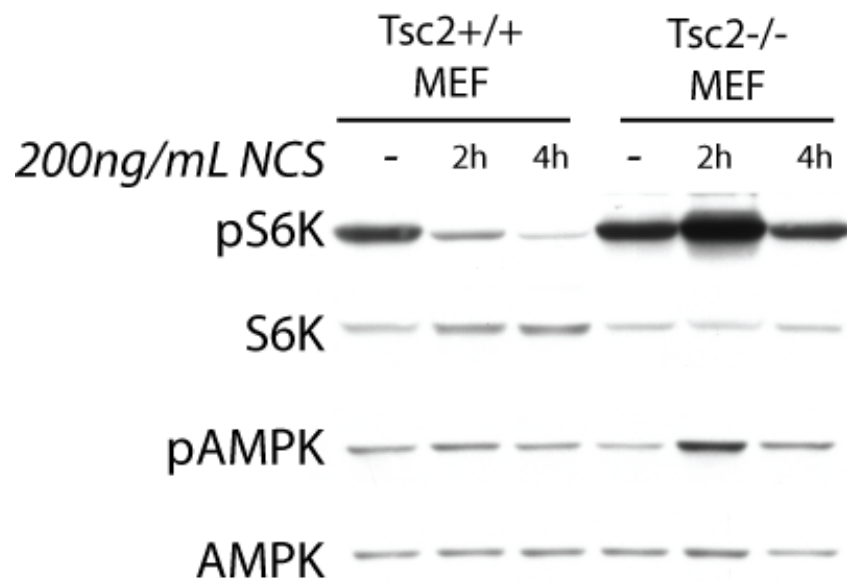


Figure 64: **mTORC1 response to neocarzinostatin in MEFs** Tsc2-proficient and Tsc2-deficient MEFs were treated with 200ng/mL neocarzinostatin for 2 or 4 hours and western blots performed to analyze mTORC1 signaling.

Figure 65:

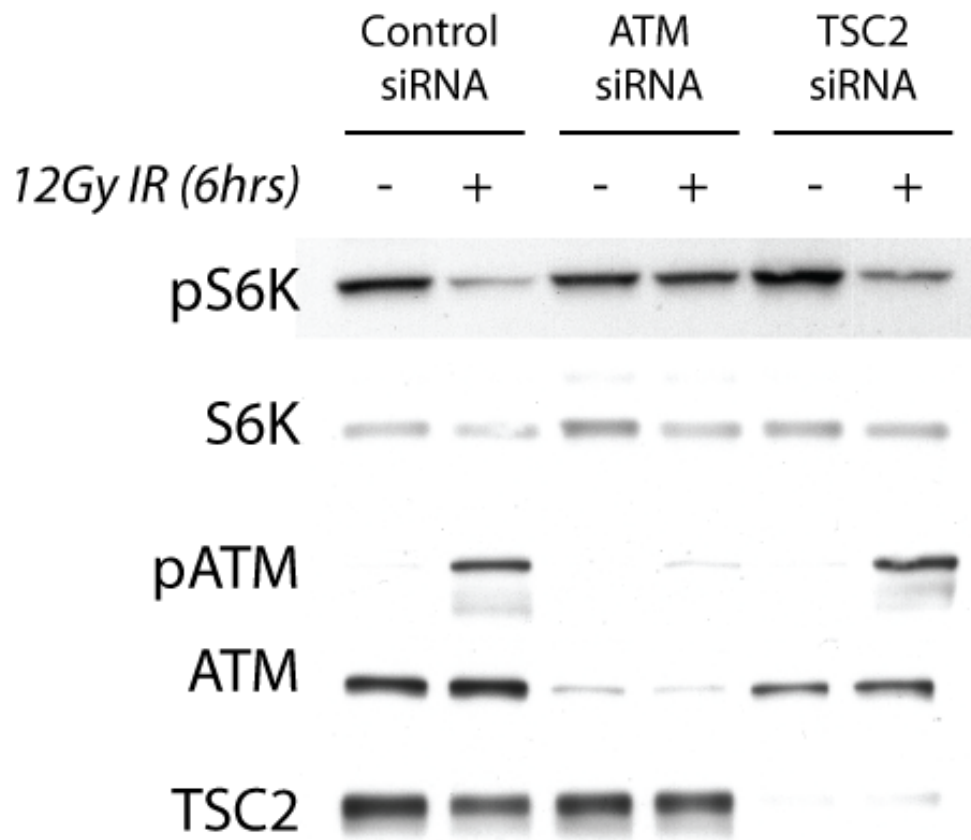


Figure 65: **siRNA validation of role of TSC2 and ATM in mTORC1 suppression by IR**

MCF7 cells were transfected with the indicated siRNAs 48 hours prior to irradiation with 12 Gy. After 6 hours of incubation after IR, lysates were made and western blots performed. mTORC1 repression by IR is dependent on ATM and at least partially dependent on TSC2.

Figure 66:

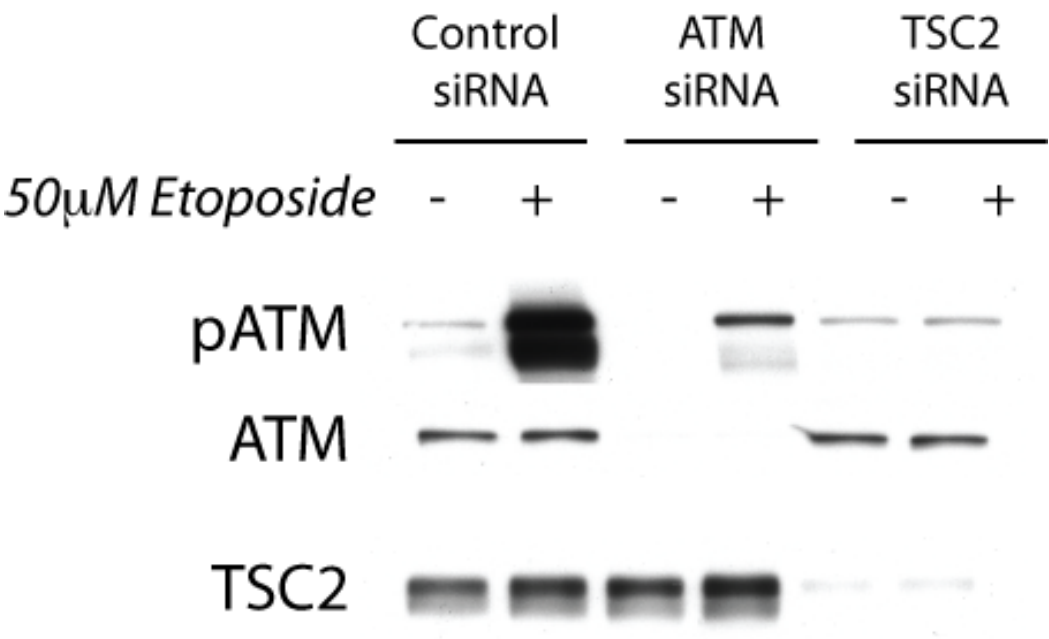


Figure 66: **siRNA showing a role for TSC2 in ATM activation** MCF7 cells were transfected with the indicated siRNAs 48 hours prior to addition of etoposide. After 24 hours of incubation, lysates were made and western blots performed.

Figure 67:

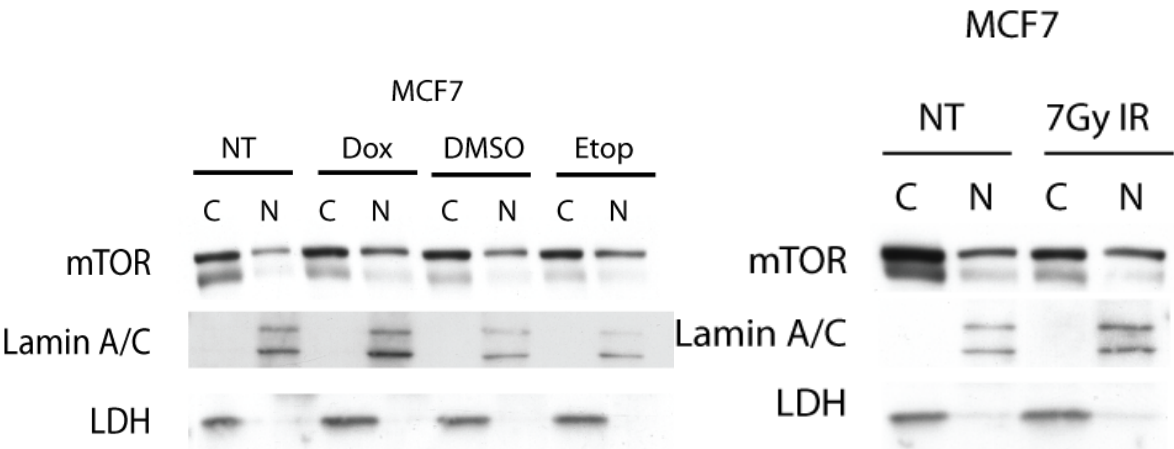


Figure 67: **mTOR localization does not change in response to DNA damaging agents**

MCF7 cells treated with the damaging agents (1 μ M doxorubicin, 50 μ M etoposide, 7Gy IR) for 24 hours were fractionated into cytoplasmic (C) and nuclear (N) fractions. These lysates were used for western analysis.

agent concentration and time of exposure, our results cannot be directly compared. Even within these reports the role of AMPK in cellular responses is far from clear or even necessarily internally consistent – for example, in Sanli et al's recent paper, where they claim in lung, prostate and MCF7 cells that IR activates AMPK independently of LKB1 but in an ATM dependent manner, AMPK activation is proposed to be a mechanism of inducing apoptosis however compound C treatment (and siRNA knockdown of AMPK α) also sensitizes the cells to IR (179). Zhang et al also identified that the methylating agent, temozolomide, which is frequently used in the treatment of gliomas can activate AMPK leading to p53-dependent apoptosis (180). Ultraviolet radiation has also been studied in keratinocytes and there are contradictory reports about whether AMPK is activated or inhibited as a result of damage (181, 182).

Our results suggesting that autophagy is not induced directly as a consequence of DNA damage signaling to mTORC1 in human cancer cells are also a bit surprising, even though there are indeed other potential autophagy regulatory pathways that could be engaged by DNA damage that are independent of ATM and TSC2. For example, it is known that p53 can both positively regulate autophagy (via transcriptional activation of autophagy genes) as well as negatively regulate autophagy (via a newly discovered cytoplasmic role in inhibiting AMPK activation) (109, 183). It is possible that in MCF7 cells which express wild-type p53, that the cytoplasmic function of p53 may be dominant, and therefore in spite of activating ATM and p53, p53 may prevent AMPK activation, which maintains autophagy at a low basal level. Experiments to tease out this possibility will be a challenge since it is known that genetic deletion or potent pharmacological inhibition of p53 also increase autophagy (109), so it may be difficult to detect additional stress-induced autophagy without careful optimization/testing of different strategies to modulate p53 availability.

The mechanism of ATM signaling to TSC2 is still unknown. The predicted ATM phosphorylation sites in TSC2 may provide the missing link in this pathway. If these sites are found to be phosphorylated by ATM, our study would have uncovered another cytoplasmic

substrate for ATM (figure 68).

Figure 68:

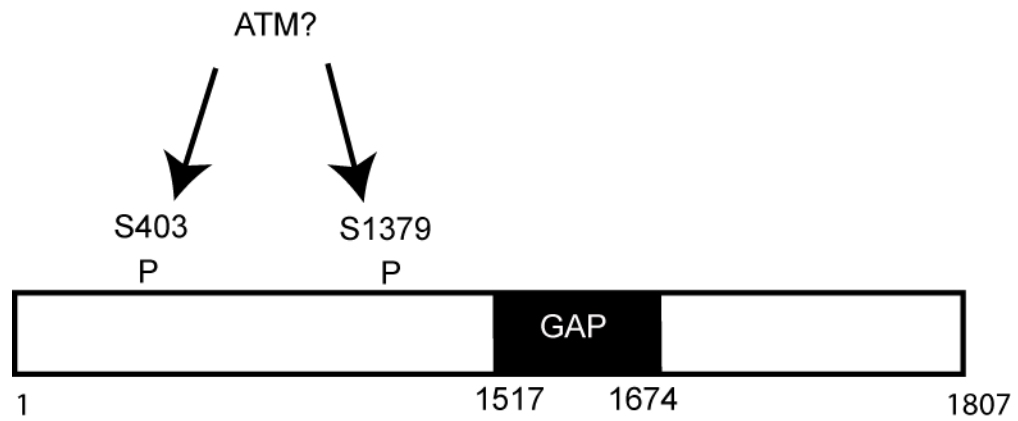


Figure 68: **Schematic of TSC2 showing putative ATM phosphorylation sites in relation to selected other known features**

Figure 69:

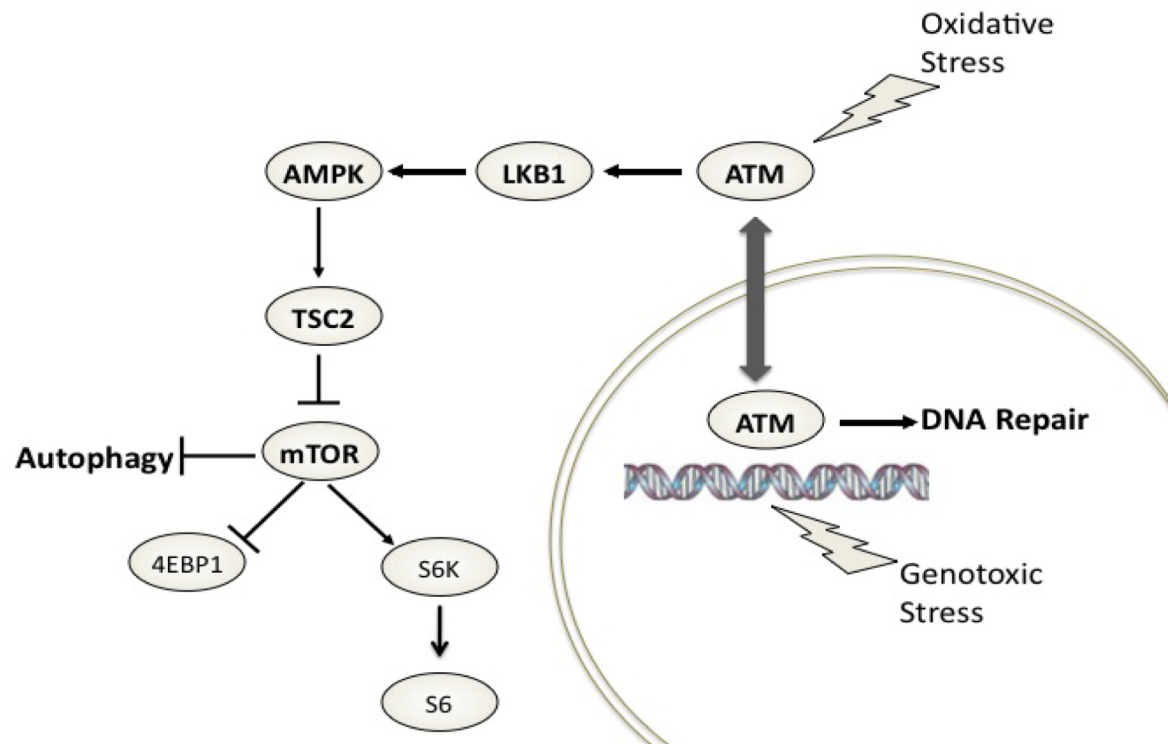


Figure 69: **Model for dual mechanisms for signaling from ATM to TSC2**

Is mTOR suppression and autophagy induction relevant with regard to response to therapy in ovarian cancer?

7.1 Introduction

In the final section of my thesis I will discuss some preliminary studies aimed at understanding the clinical relevance of mTORC1 suppression and autophagy induction in cancer therapy. While there have been many studies looking at autophagy regulation in some tumor types such as breast cancer and prostate cancer, there were relatively few studies in ovarian cancer when we began this work. The main questions we focused on were to identify whether cisplatin induced autophagy in ovarian cell lines, and if so is this mTORC1 dependent and does autophagy lead to cell death or promote survival.

7.1.1 Ovarian cancer and therapeutics

Ovarian cancer is a relatively rare but serious cancer type. According to the American Cancer Society, in 2010, there were an estimated 21,880 new cases of ovarian cancer (9th most frequent in women) in the US, leading to approximately 14,000 deaths (5th most common in women, and most lethal gynecological malignancy) (184). There are several reasons for the disproportionate number of deaths – including the natural history of the disease being aggressive, relatively late diagnosis and a lack of effective curative treatment options. At present only about 20% of ovarian cancers are diagnosed while they are still restricted to the ovary, when they have an almost 90% chance of being cured by current therapy. However once the disease has spread to the pelvic organs or beyond, the cure rate decreases significantly.

Currently, virtually all patients diagnosed with ovarian cancer initially undergo surgery to remove the bulk of the tumor which also allows accurate staging of the disease, even if complete resection is no longer possible. After recovery from surgery, the most common chemotherapeutic protocols that patients receive a combination of a platinum and taxane-

based treatment, although other agents such as doxorubicin, etoposide and gemcitabine are sometimes used.

The platinum containing drugs cisplatin and carboplatin (and more recently oxaliplatin) have been the mainstay of treatment for more than 30 years for not only ovarian cancer but other tumors such as bladder, testicular, HNSCC and NSCLC (185, 186). These platinum containing alkylating agents primarily function as intrastrand crosslinking agents that form adducts on the DNA that must be removed in order for replication or transcription to occur. Despite cisplatin being approved as a first-line therapy based on impressive results in progression-free survival, there are significant toxicities involved with exposure including nephrotoxicity and neutropenia, and responses are typically not durable due to acquired resistance mechanisms which will be discussed below. Carboplatin is more commonly being used nowadays since it has been shown to be equally effective with less side effects than cisplatin.

Taxanes which are usually used in combination with cisplatin/carboplatin include paclitaxel or less commonly docetaxel. Unlike the DNA damaging agents, these drugs block mitosis by disrupting microtubule function. Paclitaxel binds to β -tubulin which stabilizes the GDP-bound form, microtubules are hyper-stabilized due to enhanced polymerization in the absence of GTP as well as blocking de-polymerization. The net result is a mitotic arrest and induction of apoptosis independently of p53 (187).

As mentioned previously, the major clinical problem preventing long-term treatment efficacy is the development of resistance to these drugs. Ovarian cancer cells have been shown to devise strategies for platinum as well as taxane-resistance, and unsurprisingly since these work by different mechanisms, their resistance mechanisms differ. It is interesting that often resistance to one class of agent, is correlated with sensitivity to the other (188). Cisplatin resistance is characterized by a number of alterations including:

- Decreased drug accumulation in cells due to decreased uptake (by both passive and active methods such as copper transporters) (189) as well as increased efflux.

- Increased glutathione which inactivates cisplatin, by binding and preventing its reaction with DNA, also possibly decreasing the level of oxidative stress and increasing DNA repair mechanisms (186).
- Increased DNA repair pathways including nucleotide excision repair, the major pathway for platinum adduct removal.
- Activation of anti-apoptotic pathways (such as Bcl2 overexpression, and activation of the PI3K-AKT pathway) and downregulation of pro-apoptotic pathways (such as Bax/Bak and p53).

In contrast, taxane resistance, which is less well characterized at the molecular level, appears to be mediated more by alterations in the composition of microtubules. This can be due to changes in the expression of different isoforms of tubulin, mutations in tubulin decreasing affinity for taxanes or other post-translational modifications of microtubules. Expression of drug transporter pumps such as P-glycoprotein/other ABC transporters are also thought to play a role in taxane-resistance (187).

7.1.2 Role of autophagy in ovarian cancer

There have been a few reports regarding the role of autophagy induction in ovarian cancer by both genetic alternations as well as in response to drugs, and like many other tumor types the outcome of autophagy induction is complex and context dependent. One of the most completely characterized responses is the autophagy upregulation due to re-expression of a gene called ARHI, which is genetically or epigenetically silenced in approximately 60% of all ovarian cancers (190). Dr Bast's laboratory found that re-expression of ARHI at physiological levels, blocked cell growth and induced autophagy by inhibiting PI3K resulting in mTORC1 suppression, as well as by directly regulating autophagosome formation by upregulating ATG 4, which is one of the enzymes involved in cleaving LC3 prior to lipidation (191). Autophagy in this scenario led to autophagic cell death *in vitro* within a few days, however, *in vivo*, ARHI induction led to tumor dormancy and rapid regrowth later once ARHI is downregulated. This

suggests that autophagy can be used as a survival mechanism in vivo, and therefore blocking autophagy may be beneficial. Chloroquine, a drug which inhibits the completion of autophagy via increasing the pH in the lysosome was found to delay the regrowth of these dormant cells that were depending on autophagy to survive. This finding has potential implications in human therapy since chloroquine or its metabolite hydroxychloroquine has been used as an anti-malarial drug for many years, and despite its low therapeutic index, is thought to be a potential radiosensitizing or chemosensitizing agent.

In a different cellular context autophagy induction has been linked to improved clinical outcome. During studies on E1A-mediated gene therapy in ovarian cancer, another pathway for regulating autophagy was discovered (192). The PEA-15 protein was found to inhibit the ERK pathway (due to cytoplasmic sequestration of phosphorylated ERK) which led to autophagic cell death. While these studies did not examine dormancy using a xenograft system like in the ARHI studies mentioned previously, the authors did examine PEA-15 expression in an clinically-annotated tissue microarray and observed that high expression of PEA-15 correlated with better overall survival, suggesting that the pro-autophagic nature of these tumors was not being utilized as a cancer cell survival mechanism.

Targeting cancer cells by increasing their levels of oxidative stress beyond a permissible threshold has been proposed as a way of inducing cell death (193, 194). Ovarian cancer cells, even highly chemo-resistant lines such as SKOV3 have been shown to die when exposed to ROS-generating drugs such as PEITC or arsenic trioxide (193, 195). Given the numerous links between ROS and autophagy, it seems likely that autophagy in this context would participate in cell death, however no studies have been performed directly testing this hypothesis.

A final study that should be mentioned regarding the role of autophagy in ovarian cancer is a recent study published last year regarding the src inhibitor, dasatinib (196). Treatment of ovarian cancer cells with dasatinib was shown to induce autophagic cell death in a beclin 1 and ATG12 dependent manner involving inhibition of AKT. In xenograft tumors

treated with dasatinib, signs of both apoptosis and autophagy were observed by electron microscopy, suggesting that in this setting, autophagy can promote death.

7.2 Results

Firstly we aimed to characterize whether cisplatin and paclitaxel induce repress mTORC1 repression. We started these studies off using SKOV3 cells, which we treated with various doses of cisplatin for 6 or 24 hours. Figure 70 shows that similar to the other DNA damaging agents discussed in chapter 6, mTORC1 could be suppressed after 24 hours of treatment without activating AMPK (using phospho-ACC as a readout of AMPK activity). One of the proposed DNA-damage independent mechanisms of cisplatin cytotoxicity is an early generation of ROS (specifically superoxide) (197-199). ROS has been observed in vitro culture of an ovarian cell line (A2780), however the role and magnitude of this response is questionable since scavenging the ROS with superoxide dismutase did not increase cell survival as would be expected if cellular damage and cell death was occurring due to ROS. Based on the lack of activation of AMPK in SKOV3 cells, we next measured whether ROS was being generated in response to cisplatin, and found that consistent with no AMPK activation, ROS levels were not increased over control (figure 71). In colon cancer, it has been reported that cisplatin-induced ROS requires p53 activity (200); these data would suggest that in ovarian cancer this is also the case since SKOV3 are p53-deficient.

Since autophagy could occur by ROS-dependent or independent mechanisms, we looked at whether autophagy was induced upon cisplatin exposure. Figure 72 shows that upon treatment with cisplatin, LC3 II levels increased, suggesting increased autophagosome formation. We also looked at p62 levels to measure autophagic flux, and only saw a decrease at the highest dose tested, while levels increased slightly in the other samples. Although p62 is sometimes a good indicator of autophagic activity, other factors (such as transcriptional

Figure 70:

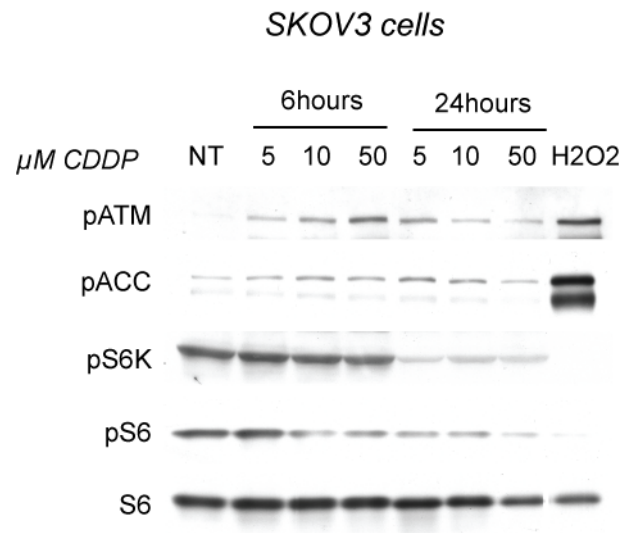


Figure 70: **Cisplatin induces mTORC1 suppression without AMPK activation in SKOV3 cells** SKOV3 cells were treated with the indicated doses of cisplatin (CDDP) for 6 or 24 hours (with the NT control being harvested with the 6 hour group), or with 0.4mM H₂O₂ for 1 hour as a positive control. Western analysis shows that at late time points mTORC1 can be suppressed but AMPK is not activated.

Figure 71:

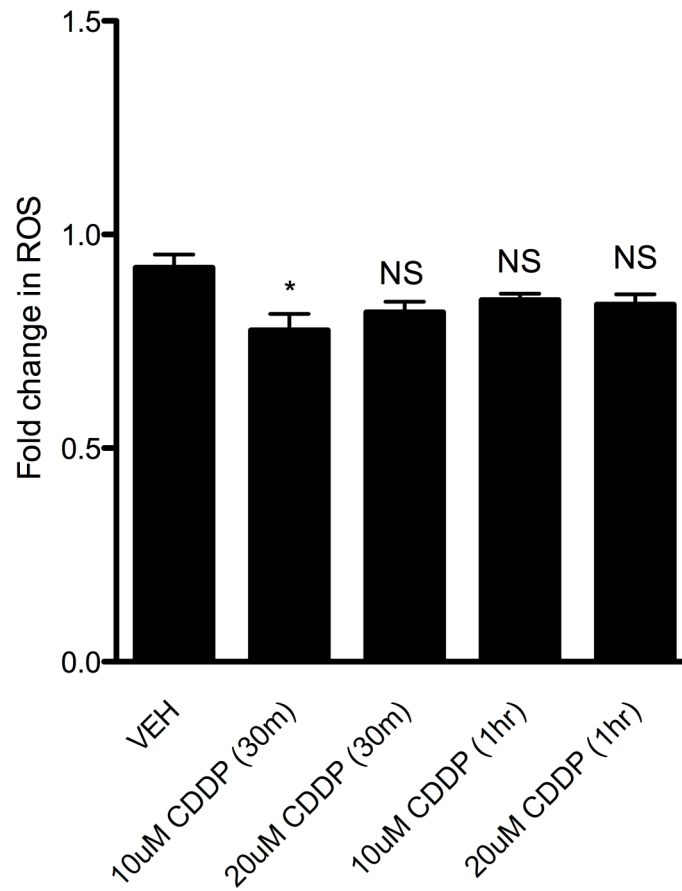


Figure 71: **ROS is not generated by cisplatin in SKOV3 cells** SKOV3 cells were treated with cisplatin (CDDP) or vehicle for the time periods noted, and ROS levels were measured using DCFDA. Bar represents a mean of 5 wells. The asterisk represents significance between cisplatin and vehicle (ANOVA with Tukey's Multiple Comparisons test), and NS represents a non-significant difference versus the control.

Figure 72:

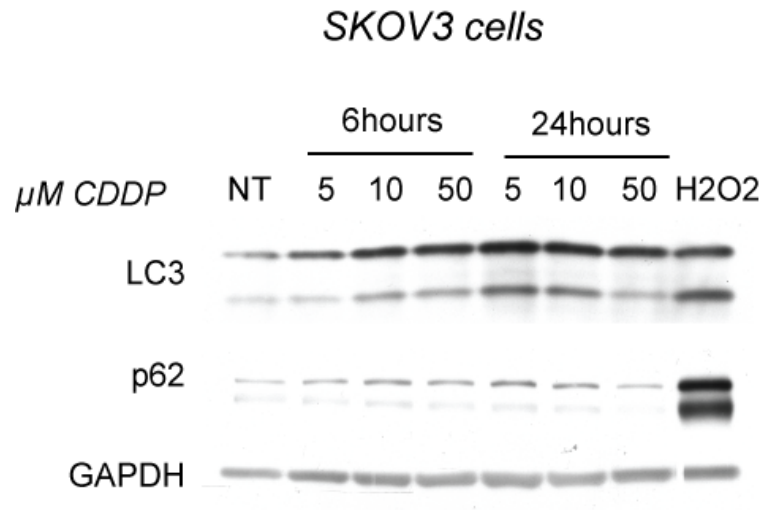


Figure 72: **Autophagy induction by cisplatin in SKOV3 cells** SKOV3 cells were treated with the indicated doses of cisplatin (CDDP) for 6 or 24 hours (with the NT control being harvested with the 6 hour group), or with 0.4mM H₂O₂ for 1 hour as a positive control. Western analysis shows that although LC3 lipidation is increasing there is no impact on autophagic flux.

These lysates were from the same experiment as in figure 70..

upregulation by Nrf2) may regulate its abundance, making interpretation of this result challenging.

To determine whether autophagy induced by cisplatin contributes to cell death or is induced as a survival mechanism we took two approaches: firstly we compared an isogenic pair of sensitive and resistant cell lines to see if the magnitude of autophagy induction varied among them, and secondly, we generated sublines of SKOV3 cells with decreased ATG5 expression to inhibit the induction of autophagy, and compared the sensitivity of these cells with vector transfected controls.

The isogenic cell line pair we selected was the Ov2008 and Ov2008/C13 pair generated by Dr Steven Howell's laboratory. The resistant subline (Ov2008/C13) was generated via long term in vitro culture in the presence of cisplatin, which selects for cells that can tolerate the damage. Both cell lines were treated with increasing doses of cisplatin for 24 hours, and autophagy induction measured by LC3 II and p62 western analysis. Figure 73 shows that autophagy was induced in the Ov2008 cell line, which is sensitive to cisplatin, but not in the resistant subline.

The second approach we took for determining the role of autophagy in cell death responses was generation of autophagy-deficient cells. We used a commercially available shRNA construct to knockdown ATG5 expression and isolated multiple clones of these. Expression of ATG5 was screened by western blot, as shown in Figure 74, and the clones with the best knockdown efficiency were utilized for a cell survival study. In total 8 ATG5 knockdown clones were compared to 6 vector-control clones, and cell number was counted after 48 hours of exposure to cisplatin, which was left in the media for the duration of the experiment. Figure 75 shows that there was no significant difference in the magnitude of cell growth inhibition between vector and ATG5 shRNA clones.

Figure 73:

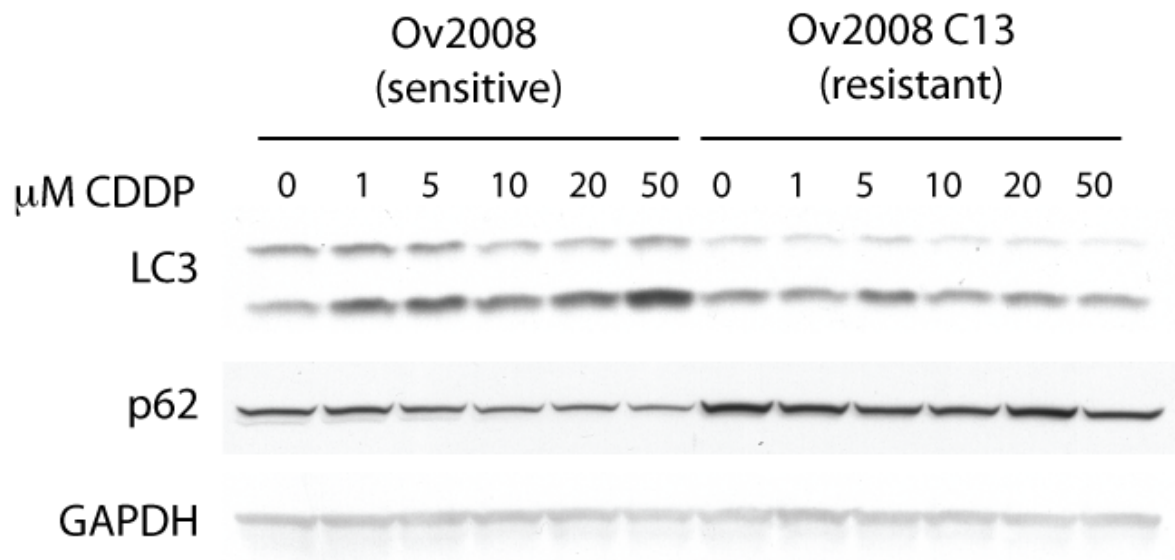


Figure 73: **Comparison of autophagy induction in isogenic cisplatin-sensitive and cisplatin-resistant cells** Ov2008 and Ov2008 C13 cells were treated with the indicated doses of cisplatin (CDDP) for 24 hours, and lysates were analyzed by western blots shown above. There is a trend for increased autophagic flux in the cisplatin sensitive parental cell line.

Figure 74:

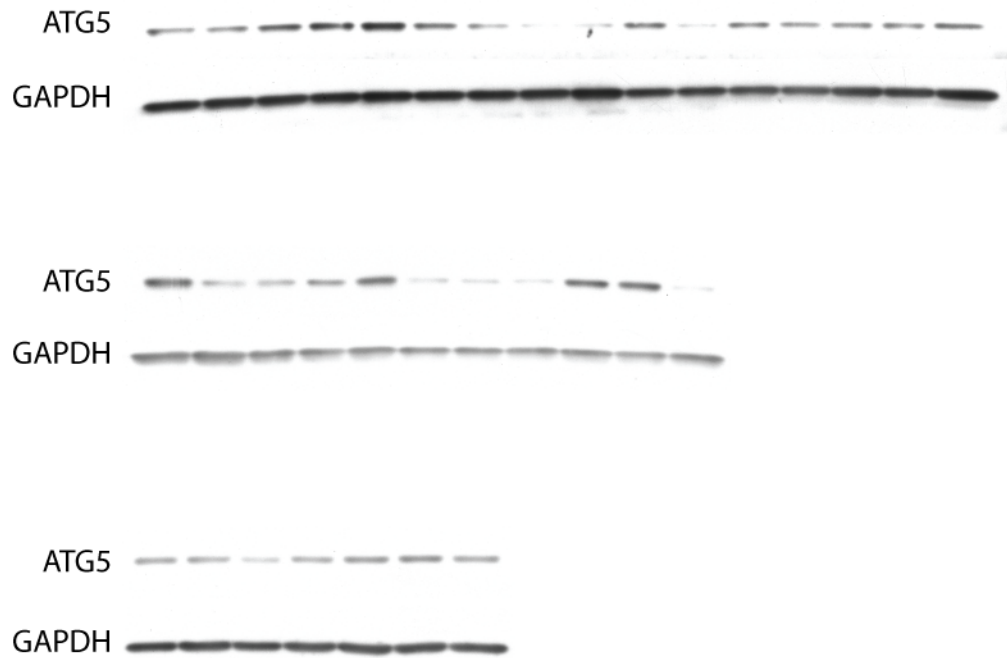


Figure 74: **ATG5 expression in isolated clones** SKOV3 cells stably transfected with ATG5 shRNA were screened for knockdown of ATG5 by western analysis. The best clones were chosen for cell growth experiment.

Figure 75:

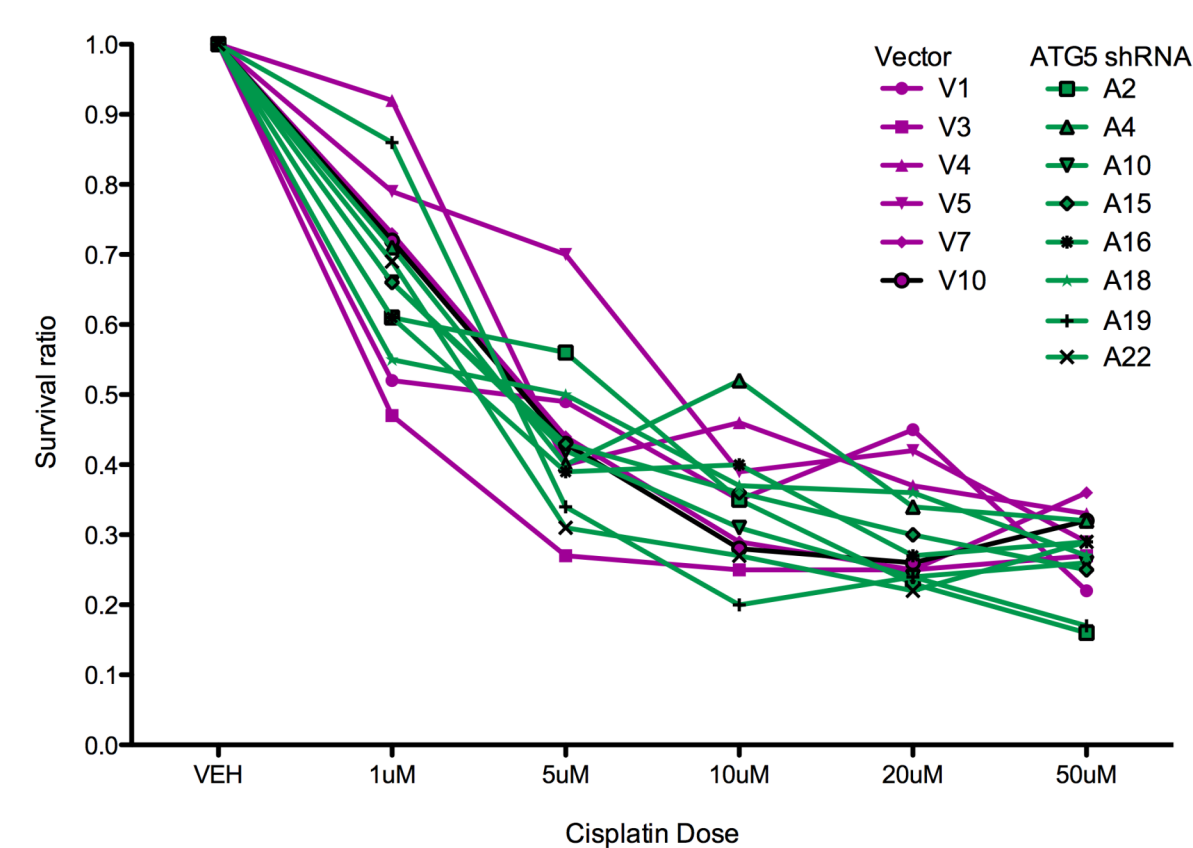


Figure 75: **Cell death in response to cisplatin does not depend on ATG5 expression in SKOV3 cells** Cell counts to measure viability after 48 hours of treatment with the indicated doses of cisplatin in vector transfected clones (purple) and ATG5 knockdown clones (green).

7.3 Discussion

In this section, we made a number of surprising discoveries regarding the induction of autophagy by cisplatin ovarian cancer cells. For the majority of the experiments we utilized the SKOV3 cell line, which is a highly aggressive, multi-drug resistant, p53-deficient serous adenocarcinoma-derived cell line with numerous oncogenic drivers including overexpression of HER2 and constitutively active AKT (201, 202), which might be predicted to keep basal autophagy levels low due to elevated mTOR levels dampening autophagy induction. We showed that LC3 II expression increased moderately from a low baseline level after 24 hours of treatment with cisplatin, but p62 levels only decreased at the highest dose of cisplatin tested.

Cisplatin has been shown to induce cytoprotective autophagy in other cancer cell lines including human and rat glioma cells and fibrosarcoma cells via activating AMPK, while in NIH 3T3 fibroblasts, cisplatin induces a form of autophagic cell death (203, 204). In contrast to this report regarding cancer cells, cisplatin did not activate AMPK in the relatively resistant SKOV3 cells, indicating significant cell type specificity in response to chemotherapeutic agents. There is some evidence that activating AMPK in ovarian cancer could be a viable therapeutic strategy, from several reports that metformin induces cell death *in vitro* (205, 206) and that the chemopreventive drug curcumin can induce apoptosis via activating AMPK and p38 in ovarian cancer cells (207). Based on these promising results further studies are warranted to investigate whether these results translate into tumor shrinkage *in vivo*, and whether autophagy plays a role in this mechanism. Alternatively, it may be possible to target upstream signaling to activate AMPK via ROS-induction of ATM for example.

The observation that knockdown of ATG5 played no role in cisplatin-induced cell death is somewhat surprising. One potential explanation is that the degree of knockdown even though noticeable by western blot was not enough to block autophagy induction in these clones. Alternatively, cisplatin could be inducing ATG5-independent forms of autophagy such as the ATG5/ATG7-independent forms of macroautophagy identified 2 years ago (208). This

alternative autophagy pathway is ULK1 and beclin 1-dependent and involves Rab9-dependent fusion of autophagosomes with vesicles from the golgi and endoplasmic reticulum. It would be worthwhile to make knockdown cells for ULK1, beclin1 and Rab9 before ruling out a role for autophagy in the cytotoxicity of cisplatin.

The other novel discovery we made was that autophagy was induced more robustly in cisplatin-sensitive cells versus an isogenic subline. Unlike the SKOV3 cells, both the parental and resistant subline express wild-type p53, which may or may not participate in the regulation of autophagy. Detailed analysis of the underlying signaling mechanisms remains to be completed, but there are some clues in the literature about some of the pathways that might be differentially regulated. These include the JNK and p38 MAPK pathways which can induce apoptosis via upregulating FasL if activation of these pathways is prolonged (209). On the other hand, in drug resistant cells, constitutive activation of AKT provides a strong survival signal and inhibits apoptosis by blocking the cisplatin-induced mitochondrial accumulation of p53 and subsequent early events in apoptosis such as Smac release (210). IGF-1R, mTORC1 and ERK signaling have also been shown to be specifically upregulated in cisplatin resistant cells, which would be predicted to again dampen autophagy levels (211, 212). Taken together, these results suggest that perhaps combining inhibitors of growth factor receptors or downstream signaling pathways with cisplatin may improve the efficacy of therapy once resistance has set in.

Summary and future directions

8.1 Summary

In this thesis, I unravel a number of novel aspects about damage signaling to the mTORC1 pathway that may have important implications for cancer therapy and understanding basic cell biological mechanisms. Many cancer chemotherapeutics work by either directly damaging DNA or generating oxidative stress, and understanding mechanistically what occurs in response to these agents can help us tailor more effective treatment strategies.

I started out describing the discovery of an oxidative-stress induced signaling pathway that involves activation of a cytoplasmic pool of ATM, which signals to LKB1, AMPK and TSC2 to repress mTORC1 and induce autophagy. I then went on to show that this signaling node is localized at the peroxisome, likely to serve as a ROS homeostasis mechanism to detect when peroxisome number or ROS output is too high, and induce pexophagy to remove these organelles. This process may serve to protect the cell from further damage to proteins and organelles. Next I uncovered another non-overlapping pathway that is activated in response to DNA damage that is ATM and TSC2-dependent but does not involve activating AMPK. The precise mechanism for this is unclear though a potential ATM:TSC2 interaction was proposed based on *in silico* analysis and identification of putative phosphorylation sites. Finally I investigated whether in ovarian cancer cells cisplatin affected mTORC1 and autophagy based on knowing that ATM would be activated either by the DNA damage or potentially by oxidative stress. I showed that in the SKOV3 model at least, that cisplatin does not induce ROS, nor the ROS-signaling pathway, but that mTORC1 could be repressed with slow kinetics similar to the DNA damaging agents in MCF7 cells. However the functional consequence of mTORC1 suppression by cisplatin is still unclear based on our results with the ATG5-knockdown clones showing no difference in cell death after cisplatin exposure when compared with the vector-transfected clones.

8.2 Future Directions

The future areas of research I foresee fall into a few separate areas:

- Mechanism of ROS-induced ATM activation
- The role and regulation of pexophagy
- Determining the DNA damage-regulated pathway(s)
- Revisiting targeting ATM in cancer integrating the newly discovered ATM-autophagy knowledge.

Each of these areas will now be described more thoroughly.

8.2.1 Mechanism of ROS-induced ATM activation

One of the critical questions still remaining in the field is how ATM is differentially regulated by ROS versus DNA damage. As mentioned in the first chapter, the classical model for ATM activation posits that an inactive dimer is activated upon DNA double-strand breaks to become active monomers. In contrast, Tanya's Paull's group identified a cysteine in ATM that is directly oxidized by ROS, and as a result ATM molecules form disulfide bonds, to create an active dimer. Based on our fractionation data that ATM can be phosphorylated in the cytoplasm and nucleus rapidly in response to ROS, the obvious question is whether these 2 species are equivalent, or whether the cytoplasmic pool is really the disulfide-linked active dimer, and the nuclear pool is a monomer or some combination of both forms. To answer this question, some of the mutant ATM constructs and reconstitution cell lines that Tanya Paull's laboratory generated could be useful tools for more detailed cellular localization analysis when combined with the ability to detect monomers versus dimers using native gel conditions that they have optimized. Secondly to build on this topic, it would be interesting to know whether peroxisomal ATM that is activated by ROS is a monomer or dimer, how it is modified and the mechanisms of how it travels to the peroxisome (ie whether the putative PTS1 sequence identified previously in ATM actually mediates binding to PEX5, or whether another membrane PTS sequence exists that allows binding to PEX19).

At a conference I recently attended, some interesting research was presented regarding a small pool of mitochondrial localized ATM, which may explain some of the mitochondrial dysfunction phenotypes seen in ATM-deficient cells. Given that we have linked ATM to autophagy, it would be interesting to know whether ATM participates in the regulation of mitophagy in response to ROS in an analogous manner to our model for regulation of pexophagy.

Finally, our results in the fibroblasts from Zellweger syndrome patients present an interesting question regarding a peroxisome-independent mechanism of ATM activation by ROS. The cellular localization of phosphorylated ATM needs to be analyzed in these cells to begin to understand this mechanism. The baseline moderate level of phosphorylated ATM in these cells relative to the control cells suggest that the intracellular milieu is tipped towards a damaged state even in the absence of exogenous damaging agents, which might be correlated with some of the disease phenotypes, and therefore perhaps treatment with rapamycin or other agents to decrease ROS might be a logical therapeutic option.

8.2.2 The role and regulation of pexophagy

The study of pexophagy in mammalian systems is still at a very elemental level, and there are few if any links to disease. Given the wide spectrum of diseases associated with aberrant redox homeostasis and autophagy, it would be surprising if pexophagy dysregulation failed to lead to disease. Peroxisome number has not been analyzed in cancer, perhaps due to a paucity of accurate methods to do so in archival samples and likely the overall lack of awareness of the importance of this organelle in basic metabolism. Cancer cells are known to possess aberrantly wired metabolic networks, so a whole area of research into peroxisome biology with regard to metabolic networks may be a future direction to explore.

A more immediate area of investigation will need to focus on providing in vivo evidence of ROS-induced pexophagy, whether that is via the ATM-LKB1-AMPK-TSC2-mTORC1 pathway or otherwise.

8.2.3 Determination of p53-independent DNA-damage-induced mTORC1 suppression mechanisms

In the DNA damage chapter of this thesis I presented evidence for multiple mechanisms of mTORC1 suppression by DNA damage, beyond the previously identified p53-dependent pathways. These mechanisms need to be explored further. To follow up on the putative direct ATM phosphorylation sites that have been proposed, we have generated a TSC2 mutant construct that lacks these sites. Some type of functional assay will need to be performed to compare the DNA damage-regulated activity of this mutant with the wild-type, and if these studies provide preliminary evidence of some role, then more detailed studies will need to be performed to determine whether ATM and TSC2 interact in cells (e.g. by immunoprecipitation). In addition, the pan-ATM substrate antibody might be used on Tsc2^{+/+} and Tsc2^{-/-} cells to determine whether TSC2 is a potential substrate, which could be validated by generating a phospho-specific antibody to these sites and showing that the signal increases in response to DNA damage.

8.2.4 ATM as a therapeutic target in cancer

ATM has been proposed as a target for chemo- or radiosensitization in cancer, based on the observation that AT-cells are hypersensitive to radiation. Further rationale for targeting ATM has been proposed based on the cytoplasmic functions of ATM in regulating AKT signaling, since although AKT would be an ideal target in a large variety in cancer cells, direct AKT inhibitors have been too non-specific. Last year it was shown that an ATM chemical inhibitor could also inhibit AKT signaling, resulting in tumor growth inhibition via inducing cell cycle arrest and mTORC1 inhibition, making this a more worthwhile potential approach to try out in preclinical and clinical models (213). Since ATM not only regulates apoptosis but autophagy, future studies with ATM inhibitors should focus on identifying the role of both processes in the cellular responses/lack of response, so that if autophagy induction limits the efficacy combinations with autophagy inhibitors can be tested.

References

1. Hoeijmakers, J. H. 2009. DNA damage, aging, and cancer. *N Engl J Med* 361:1475-1485.
2. Hoeijmakers, J. H. 2001. Genome maintenance mechanisms for preventing cancer. *Nature* 411:366-374.
3. Ciccica, A., and S. J. Elledge. 2010. The DNA damage response: making it safe to play with knives. *Mol Cell* 40:179-204.
4. Shiloh, Y. 2003. ATM and related protein kinases: safeguarding genome integrity. *Nat Rev Cancer* 3:155-168.
5. Bartkova, J., Z. Horejsí, K. Koed, A. Krämer, F. Tort, K. Zieger, P. Guldberg, M. Sehested, J. M. Nesland, C. Lukas, T. Ørntoft, J. Lukas, and J. Bartek. 2005. DNA damage response as a candidate anti-cancer barrier in early human tumorigenesis. *Nature* 434:864-870.
6. Vafa, O., M. Wade, S. Kern, M. Beeche, T. K. Pandita, G. M. Hampton, and G. M. Wahl. 2002. c-Myc can induce DNA damage, increase reactive oxygen species, and mitigate p53 function: a mechanism for oncogene-induced genetic instability. *Mol Cell* 9:1031-1044.
7. Ray, S., K. R. Atkuri, D. Deb-Basu, A. S. Adler, H. Y. Chang, L. A. Herzenberg, and D. W. Felsher. 2006. MYC can induce DNA breaks in vivo and in vitro independent of reactive oxygen species. *Cancer Res* 66:6598-6605.
8. DiTullio, R. A., T. A. Mochan, M. Venere, J. Bartkova, M. Sehested, J. Bartek, and T. D. Halazonetis. 2002. 53BP1 functions in an ATM-dependent checkpoint pathway that is constitutively activated in human cancer. *Nat Cell Biol* 4:998-1002.
9. Kamata, H., and H. Hirata. 1999. Redox regulation of cellular signalling. *Cell Signal* 11:1-14.

10. Benhar, M., D. Engelberg, and A. Levitzki. 2002. ROS, stress-activated kinases and stress signaling in cancer. *EMBO Rep* 3:420-425.
11. Yamaguchi, Y., N. Yoshikawa, S. Kagota, K. Nakamura, J. Haginaka, and M. Kunitomo. 2006. Elevated circulating levels of markers of oxidative-nitrative stress and inflammation in a genetic rat model of metabolic syndrome. *Nitric Oxide* 15:380-386.
12. Fruehauf, J. P., and F. L. Meyskens. 2007. Reactive oxygen species: a breath of life or death? *Clin Cancer Res* 13:789-794.
13. Valko, M., C. J. Rhodes, J. Moncol, M. Izakovic, and M. Mazur. 2006. Free radicals, metals and antioxidants in oxidative stress-induced cancer. *Chem Biol Interact* 160:1-40.
14. Wu, W. S. 2006. The signaling mechanism of ROS in tumor progression. *Cancer Metastasis Rev* 25:695-705.
15. Hansel, B., P. Giral, E. Nobecourt, S. Chantepie, E. Bruckert, M. J. Chapman, and A. Kontush. 2004. Metabolic syndrome is associated with elevated oxidative stress and dysfunctional dense high-density lipoprotein particles displaying impaired antioxidative activity. *J Clin Endocrinol Metab* 89:4963-4971.
16. Furukawa, S., T. Fujita, M. Shimabukuro, M. Iwaki, Y. Yamada, Y. Nakajima, O. Nakayama, M. Makishima, M. Matsuda, and I. Shimomura. 2004. Increased oxidative stress in obesity and its impact on metabolic syndrome. *J Clin Invest* 114:1752-1761.
17. Ambrosone, C. B. 2000. Oxidants and antioxidants in breast cancer. *Antioxid Redox Signal* 2:903-917.
18. Klaunig, J. E., Y. Xu, J. S. Isenberg, S. Bachowski, K. L. Kolaja, J. Jiang, D. E. Stevenson, and E. F. Walborg. 1998. The role of oxidative stress in chemical carcinogenesis. *Environ Health Perspect* 106 Suppl 1:289-295.
19. van Waveren, C., Y. Sun, H. S. Cheung, and C. T. Moraes. 2006. Oxidative phosphorylation dysfunction modulates expression of extracellular matrix--remodeling genes and invasion. *Carcinogenesis* 27:409-418.

20. Czarnecka, A. M., P. Golik, and E. Bartnik. 2006. Mitochondrial DNA mutations in human neoplasia. *J Appl Genet* 47:67-78.
21. Szatrowski, T. P., and C. F. Nathan. 1991. Production of large amounts of hydrogen peroxide by human tumor cells. *Cancer Res* 51:794-798.
22. Benhar, M., I. Dalyot, D. Engelberg, and A. Levitzki. 2001. Enhanced ROS production in oncogenically transformed cells potentiates c-Jun N-terminal kinase and p38 mitogen-activated protein kinase activation and sensitization to genotoxic stress. *Mol Cell Biol* 21:6913-6926.
23. Wang, X., J. L. Martindale, Y. Liu, and N. J. Holbrook. 1998. The cellular response to oxidative stress: influences of mitogen-activated protein kinase signalling pathways on cell survival. *Biochem J* 333 (Pt 2):291-300.
24. Leslie, N. R., D. Bennett, Y. E. Lindsay, H. Stewart, A. Gray, and C. P. Downes. 2003. Redox regulation of PI 3-kinase signalling via inactivation of PTEN. *EMBO J* 22:5501-5510.
25. Adler, V., Z. Yin, K. D. Tew, and Z. Ronai. 1999. Role of redox potential and reactive oxygen species in stress signaling. *Oncogene* 18:6104-6111.
26. Le Belle, J. E., N. M. Orozco, A. A. Paucar, J. P. Saxe, J. Mottahedeh, A. D. Pyle, H. Wu, and H. I. Kornblum. 2011. Proliferative neural stem cells have high endogenous ROS levels that regulate self-renewal and neurogenesis in a PI3K/Akt-dependant manner. *Cell Stem Cell* 8:59-71.
27. Tran, H., A. Brunet, J. M. Grenier, S. R. Datta, A. J. Fornace, P. S. DiStefano, L. W. Chiang, and M. E. Greenberg. 2002. DNA repair pathway stimulated by the forkhead transcription factor FOXO3a through the Gadd45 protein. *Science* 296:530-534.
28. Yang, Z., L. Song, and C. Huang. 2009. Gadd45 proteins as critical signal transducers linking NF-kappaB to MAPK cascades. *Curr Cancer Drug Targets* 9:915-930.
29. Savitsky, K., A. Bar-Shira, S. Gilad, G. Rotman, Y. Ziv, L. Vanagaite, D. A. Tagle, S. Smith, T. Uziel, S. Sfez, M. Ashkenazi, I. Pecker, M. Frydman, R. Harnik, S. R.

- Patanjali, A. Simmons, G. A. Clines, A. Sartiell, R. A. Gatti, L. Chessa, O. Sanal, M. F. Lavin, N. G. Jaspers, A. M. Taylor, C. F. Arlett, T. Miki, S. M. Weissman, M. Lovett, F. S. Collins, and Y. Shiloh. 1995. A single ataxia telangiectasia gene with a product similar to PI-3 kinase. *Science* 268:1749-1753.
30. Gatti, R. A., I. Berkel, E. Boder, G. Braedt, P. Charmley, P. Concannon, F. Ersoy, T. Foroud, N. G. Jaspers, and K. Lange. 1988. Localization of an ataxia-telangiectasia gene to chromosome 11q22-23. *Nature* 336:577-580.
 31. Lavin, M. F. 2008. Ataxia-telangiectasia: from a rare disorder to a paradigm for cell signalling and cancer. *Nat Rev Mol Cell Biol* 9:759-769.
 32. Rotman, G., and Y. Shiloh. 1998. ATM: from gene to function. *Hum Mol Genet* 7:1555-1563.
 33. **Julianne, S., S. Kathleen, and M. Christine.** 2001. Tying up Loose Ends: Generation and Repair of DNA Double-Strand Breaks. In *Atlas Genet Cytogenet Oncol Haematol*.
 34. Pellegrini, M., A. Celeste, S. Difilippantonio, R. Guo, W. Wang, L. Feigenbaum, and A. Nussenzweig. 2006. Autophosphorylation at serine 1987 is dispensable for murine Atm activation in vivo. *Nature* 443:222-225.
 35. Kozlov, S. V., M. E. Graham, C. Peng, P. Chen, P. J. Robinson, and M. F. Lavin. 2006. Involvement of novel autophosphorylation sites in ATM activation. *EMBO J* 25:3504-3514.
 36. Kozlov, S. V., M. E. Graham, B. Jakob, F. Tobias, A. W. Kijas, M. Tanuji, P. Chen, P. J. Robinson, G. Taucher-Scholz, K. Suzuki, S. So, D. Chen, and M. F. Lavin. 2011. Autophosphorylation and ATM Activation: ADDITIONAL SITES ADD TO THE COMPLEXITY. *J Biol Chem* 286:9107-9119.
 37. Sun, Y., X. Jiang, S. Chen, N. Fernandes, and B. D. Price. 2005. A role for the Tip60 histone acetyltransferase in the acetylation and activation of ATM. *Proc Natl Acad Sci U S A* 102:13182-13187.

38. Sun, Y., Y. Xu, K. Roy, and B. D. Price. 2007. DNA damage-induced acetylation of lysine 3016 of ATM activates ATM kinase activity. *Mol Cell Biol* 27:8502-8509.
39. Gupta, A., G. G. Sharma, C. S. Young, M. Agarwal, E. R. Smith, T. T. Paull, J. C. Lucchesi, K. K. Khanna, T. Ludwig, and T. K. Pandita. 2005. Involvement of human MOF in ATM function. *Mol Cell Biol* 25:5292-5305.
40. Goodarzi, A. A., J. C. Jonnalagadda, P. Douglas, D. Young, R. Ye, G. B. Moorhead, S. P. Lees-Miller, and K. K. Khanna. 2004. Autophosphorylation of ataxia-telangiectasia mutated is regulated by protein phosphatase 2A. *EMBO J* 23:4451-4461.
41. Ali, A., J. Zhang, S. Bao, I. Liu, D. Otterness, N. M. Dean, R. T. Abraham, and X. F. Wang. 2004. Requirement of protein phosphatase 5 in DNA-damage-induced ATM activation. *Genes Dev* 18:249-254.
42. Bakkenist, C. J., and M. B. Kastan. 2003. DNA damage activates ATM through intermolecular autophosphorylation and dimer dissociation. *Nature* 421:499-506.
43. Kobayashi, M., H. Ono, K. Mihara, H. Tauchi, K. Komatsu, T. Shibata, H. Shimizu, K. Uchida, and K. Yamamoto. 2006. ATM activation by a sulfhydryl-reactive inflammatory cyclopentenone prostaglandin. *Genes Cells* 11:779-789.
44. Zhang, Y., W. Y. Ma, A. Kaji, A. M. Bode, and Z. Dong. 2002. Requirement of ATM in UVA-induced signaling and apoptosis. *J Biol Chem* 277:3124-3131.
45. Giuliano, P., T. De Cristofaro, A. Affaitati, G. M. Pizzulo, A. Feliciello, C. Criscuolo, G. De Michele, A. Filla, E. V. Avvedimento, and S. Varrone. 2003. DNA damage induced by polyglutamine-expanded proteins. *Hum Mol Genet* 12:2301-2309.
46. Lavin, M. F., and S. Kozlov. 2007. ATM activation and DNA damage response. *Cell Cycle* 6:931-942.
47. Watters, D., P. Kedar, K. Spring, J. Bjorkman, P. Chen, M. Gatei, G. Birrell, B. Garrone, P. Srinivasa, D. I. Crane, and M. F. Lavin. 1999. Localization of a portion of extranuclear ATM to peroxisomes. *J Biol Chem* 274:34277-34282.

48. Lim, D. S., D. G. Kirsch, C. E. Canman, J. H. Ahn, Y. Ziv, L. S. Newman, R. B. Darnell, Y. Shiloh, and M. B. Kastan. 1998. ATM binds to beta-adaptin in cytoplasmic vesicles. *Proc Natl Acad Sci U S A* 95:10146-10151.
49. Zhang, L., Y. Tie, C. Tian, G. Xing, Y. Song, Y. Zhu, Z. Sun, and F. He. 2006. CKIP-1 recruits nuclear ATM partially to the plasma membrane through interaction with ATM. *Cell Signal* 18:1386-1395.
50. Kastan, M. B., and D. S. Lim. 2000. The many substrates and functions of ATM. *Nat Rev Mol Cell Biol* 1:179-186.
51. Shen, K., Y. Wang, S. C. Brooks, A. Raz, and Y. A. Wang. 2006. ATM is activated by mitotic stress and suppresses centrosome amplification in primary but not in tumor cells. *J Cell Biochem* 99:1267-1274.
52. Jang, Y. J., J. H. Ji, Y. C. Choi, C. J. Ryu, and S. Y. Ko. 2007. Regulation of Polo-like kinase 1 by DNA damage in mitosis. Inhibition of mitotic PLK-1 by protein phosphatase 2A. *J Biol Chem* 282:2473-2482.
53. Wu, Z. H., Y. Shi, R. S. Tibbetts, and S. Miyamoto. 2006. Molecular linkage between the kinase ATM and NF-kappaB signaling in response to genotoxic stimuli. *Science* 311:1141-1146.
54. Gomez, M. R. 1991. Phenotypes of the tuberous sclerosis complex with a revision of diagnostic criteria. *Ann N Y Acad Sci* 615:1-7.
55. Tee, A. R., D. C. Fingar, B. D. Manning, D. J. Kwiatkowski, L. C. Cantley, and J. Blenis. 2002. Tuberous sclerosis complex-1 and -2 gene products function together to inhibit mammalian target of rapamycin (mTOR)-mediated downstream signaling. *Proc Natl Acad Sci U S A* 99:13571-13576.
56. Murakami, M., T. Ichisaka, M. Maeda, N. Oshiro, K. Hara, F. Edenhofer, H. Kiyama, K. Yonezawa, and S. Yamanaka. 2004. mTOR is essential for growth and proliferation in early mouse embryos and embryonic stem cells. *Mol Cell Biol* 24:6710-6718.

57. Long, X., C. Spycher, Z. S. Han, A. M. Rose, F. Müller, and J. Avruch. 2002. TOR deficiency in *C. elegans* causes developmental arrest and intestinal atrophy by inhibition of mRNA translation. *Curr Biol* 12:1448-1461.
58. Oldham, S., J. Montagne, T. Radimerski, G. Thomas, and E. Hafen. 2000. Genetic and biochemical characterization of dTOR, the *Drosophila* homolog of the target of rapamycin. *Genes Dev* 14:2689-2694.
59. Zhang, H., J. P. Stallock, J. C. Ng, C. Reinhard, and T. P. Neufeld. 2000. Regulation of cellular growth by the *Drosophila* target of rapamycin dTOR. *Genes Dev* 14:2712-2724.
60. Guertin, D. A., and D. M. Sabatini. 2007. Defining the role of mTOR in cancer. *Cancer Cell* 12:9-22.
61. Sarbassov, D. D., S. M. Ali, S. Sengupta, J. H. Sheen, P. P. Hsu, A. F. Bagley, A. L. Markhard, and D. M. Sabatini. 2006. Prolonged rapamycin treatment inhibits mTORC2 assembly and Akt/PKB. *Mol Cell* 22:159-168.
62. Huang, J., and B. D. Manning. 2008. The TSC1-TSC2 complex: a molecular switchboard controlling cell growth. *Biochem J* 412:179-190.
63. Lawrence, J. C., and R. T. Abraham. 1997. PHAS/4E-BPs as regulators of mRNA translation and cell proliferation. *Trends Biochem Sci* 22:345-349.
64. Rousseau, D., A. C. Gingras, A. Pause, and N. Sonenberg. 1996. The eIF4E-binding proteins 1 and 2 are negative regulators of cell growth. *Oncogene* 13:2415-2420.
65. Sengupta, S., T. R. Peterson, and D. M. Sabatini. 2010. Regulation of the mTOR complex 1 pathway by nutrients, growth factors, and stress. *Mol Cell* 40:310-322.
66. Inoki, K., T. Zhu, and K. L. Guan. 2003. TSC2 mediates cellular energy response to control cell growth and survival. *Cell* 115:577-590.
67. Inoki, K., H. Ouyang, T. Zhu, C. Lindvall, Y. Wang, X. Zhang, Q. Yang, C. Bennett, Y. Harada, K. Stankunas, C. Y. Wang, X. He, O. A. MacDougald, M. You, B. O. Williams, and K. L. Guan. 2006. TSC2 integrates Wnt and energy signals via a coordinated phosphorylation by AMPK and GSK3 to regulate cell growth. *Cell* 126:955-968.

68. Inoki, K., Y. Li, T. Zhu, J. Wu, and K. L. Guan. 2002. TSC2 is phosphorylated and inhibited by Akt and suppresses mTOR signalling. *Nat Cell Biol* 4:648-657.
69. Dan, H. C., M. Sun, L. Yang, R. I. Feldman, X. M. Sui, C. C. Ou, M. Nellist, R. S. Yeung, D. J. Halley, S. V. Nicosia, W. J. Pledger, and J. Q. Cheng. 2002. Phosphatidylinositol 3-kinase/Akt pathway regulates tuberous sclerosis tumor suppressor complex by phosphorylation of tuberin. *J Biol Chem* 277:35364-35370.
70. Manning, B. D., A. R. Tee, M. N. Logsdon, J. Blenis, and L. C. Cantley. 2002. Identification of the tuberous sclerosis complex-2 tumor suppressor gene product tuberin as a target of the phosphoinositide 3-kinase/akt pathway. *Mol Cell* 10:151-162.
71. Li, Y., K. Inoki, R. Yeung, and K. L. Guan. 2002. Regulation of TSC2 by 14-3-3 binding. *J Biol Chem* 277:44593-44596.
72. Cai, S. L., A. R. Tee, J. D. Short, J. M. Bergeron, J. Kim, J. Shen, R. Guo, C. L. Johnson, K. Kiguchi, and C. L. Walker. 2006. Activity of TSC2 is inhibited by AKT-mediated phosphorylation and membrane partitioning. *J Cell Biol* 173:279-289.
73. Ma, L., Z. Chen, H. Erdjument-Bromage, P. Tempst, and P. P. Pandolfi. 2005. Phosphorylation and functional inactivation of TSC2 by Erk implications for tuberous sclerosis and cancer pathogenesis. *Cell* 121:179-193.
74. Ballif, B. A., P. P. Roux, S. A. Gerber, J. P. MacKeigan, J. Blenis, and S. P. Gygi. 2005. Quantitative phosphorylation profiling of the ERK/p90 ribosomal S6 kinase-signaling cassette and its targets, the tuberous sclerosis tumor suppressors. *Proc Natl Acad Sci U S A* 102:667-672.
75. Mizushima, N., B. Levine, A. M. Cuervo, and D. J. Klionsky. 2008. Autophagy fights disease through cellular self-digestion. *Nature* 451:1069-1075.
76. Santambrogio, L., and A. M. Cuervo. 2011. Chasing the elusive mammalian microautophagy. *Autophagy* 7.
77. Li, W., Q. Yang, and Z. Mao. 2011. Chaperone-mediated autophagy: machinery, regulation and biological consequences. *Cell Mol Life Sci* 68:749-763.

78. Hamasaki, M., and T. Yoshimori. 2010. Where do they come from? Insights into autophagosome formation. *FEBS Lett* 584:1296-1301.
79. Ravikumar, B., K. Moreau, L. Jahreiss, C. Puri, and D. C. Rubinsztein. 2010. Plasma membrane contributes to the formation of pre-autophagosomal structures. *Nat Cell Biol* 12:747-757.
80. Hailey, D. W., A. S. Rambold, P. Satpute-Krishnan, K. Mitra, R. Sougrat, P. K. Kim, and J. Lippincott-Schwartz. 2010. Mitochondria supply membranes for autophagosome biogenesis during starvation. *Cell* 141:656-667.
81. Geng, J., U. Nair, K. Yasumura-Yorimitsu, and D. J. Klionsky. 2010. Post-Golgi Sec proteins are required for autophagy in *Saccharomyces cerevisiae*. *Mol Biol Cell* 21:2257-2269.
82. Geng, J., and D. J. Klionsky. 2010. The Golgi as a potential membrane source for autophagy. *Autophagy* 6:950-951.
83. Meléndez, A., and B. Levine. 2009. Autophagy in *C. elegans*. *WormBook*:1-26.
84. Kroemer, G., G. Mariño, and B. Levine. 2010. Autophagy and the integrated stress response. *Mol Cell* 40:280-293.
85. Yang, Z., and D. J. Klionsky. 2010. Mammalian autophagy: core molecular machinery and signaling regulation. *Curr Opin Cell Biol* 22:124-131.
86. Cuervo, A. M. 2004. Autophagy: in sickness and in health. *Trends Cell Biol* 14:70-77.
87. Levine, B., and G. Kroemer. 2008. Autophagy in the pathogenesis of disease. *Cell* 132:27-42.
88. Mathew, R., V. Karantza-Wadsworth, and E. White. 2007. Role of autophagy in cancer. *Nat Rev Cancer* 7:961-967.
89. Liang, X. H., S. Jackson, M. Seaman, K. Brown, B. Kempkes, H. Hibshoosh, and B. Levine. 1999. Induction of autophagy and inhibition of tumorigenesis by beclin 1. *Nature* 402:672-676.

90. Qu, X., J. Yu, G. Bhagat, N. Furuya, H. Hibshoosh, A. Troxel, J. Rosen, E. L. Eskelinen, N. Mizushima, Y. Ohsumi, G. Cattoretti, and B. Levine. 2003. Promotion of tumorigenesis by heterozygous disruption of the beclin 1 autophagy gene. *J Clin Invest* 112:1809-1820.
91. Yang, S., X. Wang, G. Contino, M. Liesa, E. Sahin, H. Ying, A. Bause, Y. Li, J. M. Stommel, G. Dell'antonio, J. Mautner, G. Tonon, M. Haigis, O. S. Shirihai, C. Doglioni, N. Bardeesy, and A. C. Kimmelman. 2011. Pancreatic cancers require autophagy for tumor growth. *Genes Dev* 25:717-729.
92. Guo, J. Y., H. Y. Chen, R. Mathew, J. Fan, A. M. Strohecker, G. Karsli-Uzunbas, J. J. Kamphorst, G. Chen, J. M. Lemons, V. Karantza, H. A. Coller, R. S. Dipaola, C. Gelinas, J. D. Rabinowitz, and E. White. 2011. Activated Ras requires autophagy to maintain oxidative metabolism and tumorigenesis. *Genes Dev* 25:460-470.
93. Abedin, M. J., D. Wang, M. A. McDonnell, U. Lehmann, and A. Kelekar. 2007. Autophagy delays apoptotic death in breast cancer cells following DNA damage. *Cell Death Differ* 14:500-510.
94. Fujita, N., and T. Yoshimori. 2011. Ubiquitination-mediated autophagy against invading bacteria. *Curr Opin Cell Biol*.
95. Espert, L., P. Codogno, and M. Biard-Piechaczyk. 2007. Involvement of autophagy in viral infections: antiviral function and subversion by viruses. *J Mol Med* 85:811-823.
96. Sumpter, R., and B. Levine. 2011. Selective autophagy and viruses. *Autophagy* 7.
97. Mariño, G., F. Madeo, and G. Kroemer. 2011. Autophagy for tissue homeostasis and neuroprotection. *Curr Opin Cell Biol* 23:198-206.
98. Ravikumar, B., S. Sarkar, J. E. Davies, M. Futter, M. Garcia-Arencibia, Z. W. Green-Thompson, M. Jimenez-Sanchez, V. I. Korolchuk, M. Lichtenberg, S. Luo, D. C. Massey, F. M. Menzies, K. Moreau, U. Narayanan, M. Renna, F. H. Siddiqi, B. R. Underwood, A. R. Winslow, and D. C. Rubinsztein. 2010. Regulation of mammalian autophagy in physiology and pathophysiology. *Physiol Rev* 90:1383-1435.

99. Narendra, D., A. Tanaka, D. F. Suen, and R. J. Youle. 2009. Parkin-induced mitophagy in the pathogenesis of Parkinson disease. *Autophagy* 5:706-708.
100. Ganley, I. G., d. H. Lam, J. Wang, X. Ding, S. Chen, and X. Jiang. 2009. ULK1.ATG13.FIP200 complex mediates mTOR signaling and is essential for autophagy. *J Biol Chem* 284:12297-12305.
101. Jung, C. H., C. B. Jun, S. H. Ro, Y. M. Kim, N. M. Otto, J. Cao, M. Kundu, and D. H. Kim. 2009. ULK-Atg13-FIP200 complexes mediate mTOR signaling to the autophagy machinery. *Mol Biol Cell* 20:1992-2003.
102. Hosokawa, N., T. Hara, T. Kaizuka, C. Kishi, A. Takamura, Y. Miura, S. Iemura, T. Natsume, K. Takehana, N. Yamada, J. L. Guan, N. Oshiro, and N. Mizushima. 2009. Nutrient-dependent mTORC1 association with the ULK1-Atg13-FIP200 complex required for autophagy. *Mol Biol Cell* 20:1981-1991.
103. Kim, J., M. Kundu, B. Viollet, and K. L. Guan. 2011. AMPK and mTOR regulate autophagy through direct phosphorylation of Ulk1. *Nat Cell Biol* 13:132-141.
104. Meek, D. W. 2009. Tumour suppression by p53: a role for the DNA damage response? *Nat Rev Cancer* 9:714-723.
105. Vousden, K. H., and D. P. Lane. 2007. p53 in health and disease. *Nat Rev Mol Cell Biol* 8:275-283.
106. Maiuri, M. C., S. A. Malik, E. Morselli, O. Kepp, A. Criollo, P. L. Mouchel, R. Carnuccio, and G. Kroemer. 2009. Stimulation of autophagy by the p53 target gene Sestrin2. *Cell Cycle* 8:1571-1576.
107. Eby, K. G., J. M. Rosenbluth, D. J. Mays, C. B. Marshall, C. E. Barton, S. Sinha, K. N. Johnson, L. Tang, and J. A. Pietsenpol. 2010. ISG20L1 is a p53 family target gene that modulates genotoxic stress-induced autophagy. *Mol Cancer* 9:95.
108. Crighton, D., S. Wilkinson, J. O'Prey, N. Syed, P. Smith, P. R. Harrison, M. Gasco, O. Garrone, T. Crook, and K. M. Ryan. 2006. DRAM, a p53-induced modulator of autophagy, is critical for apoptosis. *Cell* 126:121-134.

109. Tasdemir, E., M. C. Maiuri, L. Galluzzi, I. Vitale, M. Djavaheiri-Mergny, M. D'Amelio, A. Criollo, E. Morselli, C. Zhu, F. Harper, U. Nannmark, C. Samara, P. Pinton, J. M. Vicencio, R. Carnuccio, U. M. Moll, F. Madeo, P. Paterlini-Brechot, R. Rizzuto, G. Szabadkai, G. Pierron, K. Blomgren, N. Tavernarakis, P. Codogno, F. Cecconi, and G. Kroemer. 2008. Regulation of autophagy by cytoplasmic p53. *Nat Cell Biol* 10:676-687.
110. Ogier-Denis, E., S. Pattingre, J. El Benna, and P. Codogno. 2000. Erk1/2-dependent phosphorylation of Galpha-interacting protein stimulates its GTPase accelerating activity and autophagy in human colon cancer cells. *J Biol Chem* 275:39090-39095.
111. Pattingre, S., C. Bauvy, and P. Codogno. 2003. Amino acids interfere with the ERK1/2-dependent control of macroautophagy by controlling the activation of Raf-1 in human colon cancer HT-29 cells. *J Biol Chem* 278:16667-16674.
112. Dagda, R. K., J. Zhu, S. M. Kulich, and C. T. Chu. 2008. Mitochondrially localized ERK2 regulates mitophagy and autophagic cell stress: implications for Parkinson's disease. *Autophagy* 4:770-782.
113. Wang, S. H., Y. L. Shih, W. C. Ko, Y. H. Wei, and C. M. Shih. 2008. Cadmium-induced autophagy and apoptosis are mediated by a calcium signaling pathway. *Cell Mol Life Sci* 65:3640-3652.
114. Yang, L. Y., K. H. Wu, W. T. Chiu, S. H. Wang, and C. M. Shih. 2009. The cadmium-induced death of mesangial cells results in nephrotoxicity. *Autophagy* 5:571-572.
115. Sivaprasad, U., and A. Basu. 2008. Inhibition of ERK attenuates autophagy and potentiates tumour necrosis factor-alpha-induced cell death in MCF-7 cells. *J Cell Mol Med* 12:1265-1271.
116. Chu, C. T., D. J. Levinthal, S. M. Kulich, E. M. Chalovich, and D. B. DeFranco. 2004. Oxidative neuronal injury. The dark side of ERK1/2. *Eur J Biochem* 271:2060-2066.
117. Subramaniam, S., and K. Unsicker. 2006. Extracellular signal-regulated kinase as an inducer of non-apoptotic neuronal death. *Neuroscience* 138:1055-1065.

118. Ogata, M., S. Hino, A. Saito, K. Morikawa, S. Kondo, S. Kanemoto, T. Murakami, M. Taniguchi, I. Tanii, K. Yoshinaga, S. Shiosaka, J. A. Hammarback, F. Urano, and K. Imaizumi. 2006. Autophagy is activated for cell survival after endoplasmic reticulum stress. *Mol Cell Biol* 26:9220-9231.
119. Li, D. D., L. L. Wang, R. Deng, J. Tang, Y. Shen, J. F. Guo, Y. Wang, L. P. Xia, G. K. Feng, Q. Q. Liu, W. L. Huang, Y. X. Zeng, and X. F. Zhu. 2009. The pivotal role of c-Jun NH2-terminal kinase-mediated Beclin 1 expression during anticancer agents-induced autophagy in cancer cells. *Oncogene* 28:886-898.
120. Shimizu, S., A. Konishi, Y. Nishida, T. Mizuta, H. Nishina, A. Yamamoto, and Y. Tsujimoto. 2010. Involvement of JNK in the regulation of autophagic cell death. *Oncogene* 29:2070-2082.
121. Wong, C. H., K. B. Iskandar, S. K. Yadav, J. L. Hirpara, T. Loh, and S. Pervaiz. 2010. Simultaneous induction of non-canonical autophagy and apoptosis in cancer cells by ROS-dependent ERK and JNK activation. *PLoS One* 5:e9996.
122. Webber, J. L., and S. A. Tooze. 2010. Coordinated regulation of autophagy by p38alpha MAPK through mAtg9 and p38IP. *EMBO J* 29:27-40.
123. Häussinger, D., F. Schliess, F. Dombrowski, and S. Vom Dahl. 1999. Involvement of p38MAPK in the regulation of proteolysis by liver cell hydration. *Gastroenterology* 116:921-935.
124. Comes, F., A. Matrone, P. Lastella, B. Nico, F. C. Susca, R. Bagnulo, G. Ingravallo, S. Modica, G. Lo Sasso, A. Moschetta, G. Guanti, and C. Simone. 2007. A novel cell type-specific role of p38alpha in the control of autophagy and cell death in colorectal cancer cells. *Cell Death Differ* 14:693-702.
125. Kiyono, K., H. I. Suzuki, H. Matsuyama, Y. Morishita, A. Komuro, M. R. Kano, K. Sugimoto, and K. Miyazono. 2009. Autophagy is activated by TGF-beta and potentiates TGF-beta-mediated growth inhibition in human hepatocellular carcinoma cells. *Cancer Res* 69:8844-8852.

126. Polager, S., M. Ofir, and D. Ginsberg. 2008. E2F1 regulates autophagy and the transcription of autophagy genes. *Oncogene* 27:4860-4864.
127. Jiang, H., V. Martin, M. Alonso, C. Gomez-Manzano, and J. Fueyo. 2010. RB-E2F1: molecular rheostat for autophagy and apoptosis. *Autophagy* 6:1216-1217.
128. Jiang, H., V. Martin, C. Gomez-Manzano, D. G. Johnson, M. Alonso, E. White, J. Xu, T. J. McDonnell, N. Shinojima, and J. Fueyo. 2010. The RB-E2F1 pathway regulates autophagy. *Cancer Res* 70:7882-7893.
129. Lin, W. C., F. T. Lin, and J. R. Nevins. 2001. Selective induction of E2F1 in response to DNA damage, mediated by ATM-dependent phosphorylation. *Genes Dev* 15:1833-1844.
130. Rhee, S. G., T. S. Chang, W. Jeong, and D. Kang. 2010. Methods for detection and measurement of hydrogen peroxide inside and outside of cells. *Mol Cells* 29:539-549.
131. Kim, J., E. Jonasch, A. Alexander, J. D. Short, S. Cai, S. Wen, D. Tsavachidou, P. Tamboli, B. A. Czerniak, K. A. Do, K. J. Wu, L. A. Marlow, C. G. Wood, J. A. Copland, and C. L. Walker. 2009. Cytoplasmic sequestration of p27 via AKT phosphorylation in renal cell carcinoma. *Clin Cancer Res* 15:81-90.
132. Barlow, C., S. Hirotsune, R. Paylor, M. Liyanage, M. Eckhaus, F. Collins, Y. Shiloh, J. N. Crawley, T. Ried, D. Tagle, and A. Wynshaw-Boris. 1996. Atm-deficient mice: a paradigm of ataxia telangiectasia. *Cell* 86:159-171.
133. Gouveia, A. M., C. Reguenga, M. E. Oliveira, C. Sa-Miranda, and J. E. Azevedo. 2000. Characterization of peroxisomal Pex5p from rat liver. Pex5p in the Pex5p-Pex14p membrane complex is a transmembrane protein. *J Biol Chem* 275:32444-32451.
134. Feng, Z., H. Zhang, A. J. Levine, and S. Jin. 2005. The coordinate regulation of the p53 and mTOR pathways in cells. *Proc Natl Acad Sci U S A* 102:8204-8209.
135. Zhang, H., G. Cicchetti, H. Onda, H. B. Koon, K. Asrican, N. Bajraszewski, F. Vazquez, C. L. Carpenter, and D. J. Kwiatkowski. 2003. Loss of Tsc1/Tsc2 activates mTOR and

- disrupts PI3K-Akt signaling through downregulation of PDGFR. *J Clin Invest* 112:1223-1233.
136. Mukhopadhyay, P., M. Rajesh, S. Bátkai, Y. Kashiwaya, G. Haskó, L. Liaudet, C. Szabó, and P. Pacher. 2009. Role of superoxide, nitric oxide, and peroxynitrite in doxorubicin-induced cell death in vivo and in vitro. *Am J Physiol Heart Circ Physiol* 296:H1466-1483.
 137. Sapkota, G. P., M. Deak, A. Kieloch, N. Morrice, A. A. Goodarzi, C. Smythe, Y. Shiloh, S. P. Lees-Miller, and D. R. Alessi. 2002. Ionizing radiation induces ataxia telangiectasia mutated kinase (ATM)-mediated phosphorylation of LKB1/STK11 at Thr-366. *Biochem J* 368:507-516.
 138. Lou, D., N. Griffith, and D. J. Noonan. 2001. The tuberous sclerosis 2 gene product can localize to nuclei in a phosphorylation-dependent manner. *Mol Cell Biol Res Commun* 4:374-380.
 139. Rosner, M., A. Freilinger, and M. Hengstschläger. 2007. Akt regulates nuclear/cytoplasmic localization of tuberin. *Oncogene* 26:521-531.
 140. Matsui, Y., H. Takagi, X. Qu, M. Abdellatif, H. Sakoda, T. Asano, B. Levine, and J. Sadoshima. 2007. Distinct roles of autophagy in the heart during ischemia and reperfusion: roles of AMP-activated protein kinase and Beclin 1 in mediating autophagy. *Circ Res* 100:914-922.
 141. Scherz-Shouval, R., E. Shvets, E. Fass, H. Shorer, L. Gil, and Z. Elazar. 2007. Reactive oxygen species are essential for autophagy and specifically regulate the activity of Atg4. *EMBO J* 26:1749-1760.
 142. Tanida, I., T. Ueno, and E. Kominami. 2004. LC3 conjugation system in mammalian autophagy. *Int J Biochem Cell Biol* 36:2503-2518.
 143. Man, N., Y. Chen, F. Zheng, W. Zhou, and L. P. Wen. 2010. Induction of genuine autophagy by cationic lipids in mammalian cells. *Autophagy* 6.

144. Budanov, A. V., and M. Karin. 2008. p53 target genes sestrin1 and sestrin2 connect genotoxic stress and mTOR signaling. *Cell* 134:451-460.
145. Fu, X., S. Wan, Y. L. Lyu, L. F. Liu, and H. Qi. 2008. Etoposide induces ATM-dependent mitochondrial biogenesis through AMPK activation. *PLoS One* 3:e2009.
146. Alexander, A., S. L. Cai, J. Kim, A. Nanez, M. Sahin, K. H. MacLean, K. Inoki, K. L. Guan, J. Shen, M. D. Person, D. Kusewitt, G. B. Mills, M. B. Kastan, and C. L. Walker. 2010. ATM signals to TSC2 in the cytoplasm to regulate mTORC1 in response to ROS. *Proc Natl Acad Sci U S A* 107:4153-4158.
147. Sapkota, G. P., J. Boudeau, M. Deak, A. Kieloch, N. Morrice, and D. R. Alessi. 2002. Identification and characterization of four novel phosphorylation sites (Ser31, Ser325, Thr336 and Thr366) on LKB1/STK11, the protein kinase mutated in Peutz-Jeghers cancer syndrome. *Biochem J* 362:481-490.
148. Alessi, D. R., K. Sakamoto, and J. R. Bayascas. 2006. LKB1-dependent signaling pathways. *Annu Rev Biochem* 75:137-163.
149. Short, J. D., K. D. Houston, R. Dere, S. L. Cai, J. Kim, C. L. Johnson, R. R. Broaddus, J. Shen, S. Miyamoto, F. Tamanoi, D. Kwiatkowski, G. B. Mills, and C. L. Walker. 2008. AMP-activated protein kinase signaling results in cytoplasmic sequestration of p27. *Cancer Res* 68:6496-6506.
150. Hahn-Windgassen, A., V. Nogueira, C. C. Chen, J. E. Skeen, N. Sonenberg, and N. Hay. 2005. Akt activates the mammalian target of rapamycin by regulating cellular ATP level and AMPK activity. *J Biol Chem* 280:32081-32089.
151. Gwinn, D. M., D. B. Shackelford, D. F. Egan, M. M. Mihaylova, A. Mery, D. S. Vasquez, B. E. Turk, and R. J. Shaw. 2008. AMPK phosphorylation of raptor mediates a metabolic checkpoint. *Mol Cell* 30:214-226.
152. Thorstenson, Y. R., A. Roxas, R. Kroiss, M. A. Jenkins, K. M. Yu, T. Bachrich, D. Muhr, T. L. Wayne, G. Chu, R. W. Davis, T. M. Wagner, and P. J. Oefner. 2003.

- Contributions of ATM mutations to familial breast and ovarian cancer. *Cancer Res* 63:3325-3333.
153. Stoppa-Lyonnet, D., J. Soulier, A. Laugé, H. Dastot, R. Garand, F. Sigaux, and M. H. Stern. 1998. Inactivation of the ATM gene in T-cell prolymphocytic leukemias. *Blood* 91:3920-3926.
154. Kuljis, R. O., Y. Xu, M. C. Aguila, and D. Baltimore. 1997. Degeneration of neurons, synapses, and neuropil and glial activation in a murine *Atm* knockout model of ataxia-telangiectasia. *Proc Natl Acad Sci U S A* 94:12688-12693.
155. Barlow, C., C. Ribaut-Barassin, T. A. Zwingman, A. J. Pope, K. D. Brown, J. W. Owens, D. Larson, E. A. Harrington, A. M. Haeberle, J. Mariani, M. Eckhaus, K. Herrup, Y. Bailly, and A. Wynshaw-Boris. 2000. ATM is a cytoplasmic protein in mouse brain required to prevent lysosomal accumulation. *Proc Natl Acad Sci U S A* 97:871-876.
156. Barzilai, A., G. Rotman, and Y. Shiloh. 2002. ATM deficiency and oxidative stress: a new dimension of defective response to DNA damage. *DNA Repair (Amst)* 1:3-25.
157. Reliene, R., E. Fischer, and R. H. Schiestl. 2004. Effect of N-acetyl cysteine on oxidative DNA damage and the frequency of DNA deletions in *atm*-deficient mice. *Cancer Res* 64:5148-5153.
158. Reliene, R., and R. H. Schiestl. 2006. Antioxidant N-acetyl cysteine reduces incidence and multiplicity of lymphoma in *Atm* deficient mice. *DNA Repair (Amst)* 5:852-859.
159. Reliene, R., and R. H. Schiestl. 2007. Antioxidants suppress lymphoma and increase longevity in *Atm*-deficient mice. *J Nutr* 137:229S-232S.
160. Harrison, D. E., R. Strong, Z. D. Sharp, J. F. Nelson, C. M. Astle, K. Flurkey, N. L. Nadon, J. E. Wilkinson, K. Frenkel, C. S. Carter, M. Pahor, M. A. Javors, E. Fernandez, and R. A. Miller. 2009. Rapamycin fed late in life extends lifespan in genetically heterogeneous mice. *Nature* 460:392-395.

161. Buitrago-Molina, L. E., D. Pothiraju, J. Lamlé, S. Marhenke, U. Kossatz, K. Breuhahn, M. P. Manns, N. Malek, and A. Vogel. 2009. Rapamycin delays tumor development in murine livers by inhibiting proliferation of hepatocytes with DNA damage. *Hepatology* 50:500-509.
162. Rhodin, J. 1954. Correlation of ultrastructural organization and function in normal and experimentally changed proximal convoluted tubule cells of the mouse kidney: An electron microscopic study including an experimental analysis of the conditions for fixation of the renal tissue for high resolution electron microscopy.
163. De Duve, C., and P. Baudhuin. 1966. Peroxisomes (microbodies and related particles). *Physiol Rev* 46:323-357.
164. de Duve, C. 1969. The peroxisome: a new cytoplasmic organelle. *Proc R Soc Lond B Biol Sci* 173:71-83.
165. Schrader, M., and H. D. Fahimi. 2008. The peroxisome: still a mysterious organelle. *Histochem Cell Biol* 129:421-440.
166. Sakai, Y., M. Oku, I. J. van der Klei, and J. A. Kiel. 2006. Pexophagy: autophagic degradation of peroxisomes. *Biochim Biophys Acta* 1763:1767-1775.
167. Schlüter, A., A. Real-Chicharro, T. Gabaldón, F. Sánchez-Jiménez, and A. Pujol. 2010. PeroxisomeDB 2.0: an integrative view of the global peroxisomal metabolome. *Nucleic Acids Res* 38:D800-805.
168. Santos, M. J., S. C. Henderson, A. B. Moser, H. W. Moser, and P. B. Lazarow. 2000. Peroxisomal ghosts are intracellular structures distinct from lysosomal compartments in Zellweger syndrome: a confocal laser scanning microscopy study. *Biol Cell* 92:85-94.
169. Brosius, U., and J. Gärtner. 2002. Cellular and molecular aspects of Zellweger syndrome and other peroxisome biogenesis disorders. *Cell Mol Life Sci* 59:1058-1069.
170. Sancak, Y., L. Bar-Peled, R. Zoncu, A. L. Markhard, S. Nada, and D. M. Sabatini. 2010. Ragulator-Rag complex targets mTORC1 to the lysosomal surface and is necessary for its activation by amino acids. *Cell* 141:290-303.

171. Aspuria, P. J., and F. Tamanoi. 2004. The Rheb family of GTP-binding proteins. *Cell Signal* 16:1105-1112.
172. Rout, M. P. 2008. The peroxisome: a production in four acts. *J Cell Biol* 181:185-187.
173. Yoshida, H. 2009. ER stress response, peroxisome proliferation, mitochondrial unfolded protein response and Golgi stress response. *IUBMB Life* 61:871-879.
174. Gonzalez, F. J., and Y. M. Shah. 2008. PPARalpha: mechanism of species differences and hepatocarcinogenesis of peroxisome proliferators. *Toxicology* 246:2-8.
175. Alexander, A., and C. L. Walker. 2011. The role of LKB1 and AMPK in cellular responses to stress and damage. *FEBS Lett* 585:952-957.
176. Bungard, D., B. J. Fuerth, P. Y. Zeng, B. Faubert, N. L. Maas, B. Viollet, D. Carling, C. B. Thompson, R. G. Jones, and S. L. Berger. 2010. Signaling kinase AMPK activates stress-promoted transcription via histone H2B phosphorylation. *Science* 329:1201-1205.
177. Bernardi, R., I. Guernah, D. Jin, S. Grisendi, A. Alimonti, J. Teruya-Feldstein, C. Cordon-Cardo, M. C. Simon, S. Rafii, and P. P. Pandolfi. 2006. PML inhibits HIF-1alpha translation and neoangiogenesis through repression of mTOR. *Nature* 442:779-785.
178. Matsuoka, S., B. A. Ballif, A. Smogorzewska, E. R. McDonald, K. E. Hurov, J. Luo, C. E. Bakalarski, Z. Zhao, N. Solimini, Y. Lerenthal, Y. Shiloh, S. P. Gygi, and S. J. Elledge. 2007. ATM and ATR substrate analysis reveals extensive protein networks responsive to DNA damage. *Science* 316:1160-1166.
179. Sanli, T., A. Rashid, C. Liu, S. Harding, R. G. Bristow, J. C. Cutz, G. Singh, J. Wright, and T. Tsakiridis. 2010. Ionizing radiation activates AMP-activated kinase (AMPK): a target for radiosensitization of human cancer cells. *Int J Radiat Oncol Biol Phys* 78:221-229.
180. Zhang, W. B., Z. Wang, F. Shu, Y. H. Jin, H. Y. Liu, Q. J. Wang, and Y. Yang. 2010. Activation of AMP-activated protein kinase by temozolomide contributes to apoptosis in

- glioblastoma cells via p53 activation and mTORC1 inhibition. *J Biol Chem* 285:40461-40471.
181. Zhang, J., and G. T. Bowden. 2008. UVB irradiation regulates Cox-2 mRNA stability through AMPK and HuR in human keratinocytes. *Mol Carcinog* 47:974-983.
 182. Cao, C., S. Lu, R. Kivlin, B. Wallin, E. Card, A. Bagdasarian, T. Tamakloe, W. M. Chu, K. L. Guan, and Y. Wan. 2008. AMP-activated protein kinase contributes to UV- and H₂O₂-induced apoptosis in human skin keratinocytes. *J Biol Chem* 283:28897-28908.
 183. Tasdemir, E., M. Chiara Maiuri, E. Morselli, A. Criollo, M. D'Amelio, M. Djavaheri-Mergny, F. Cecconi, N. Tavernarakis, and G. Kroemer. 2008. A dual role of p53 in the control of autophagy. *Autophagy* 4:810-814.
 184. Jemal, A., R. Siegel, J. Xu, and E. Ward. 2010. Cancer statistics, 2010. *CA Cancer J Clin* 60:277-300.
 185. Muggia, F. 2009. Platinum compounds 30 years after the introduction of cisplatin: implications for the treatment of ovarian cancer. *Gynecol Oncol* 112:275-281.
 186. Siddik, Z. H. 2003. Cisplatin: mode of cytotoxic action and molecular basis of resistance. *Oncogene* 22:7265-7279.
 187. Chien, A. J., and M. M. Moasser. 2008. Cellular mechanisms of resistance to anthracyclines and taxanes in cancer: intrinsic and acquired. *Semin Oncol* 35:S1-S14; quiz S39.
 188. Stordal, B., N. Pavlakakis, and R. Davey. 2007. A systematic review of platinum and taxane resistance from bench to clinic: an inverse relationship. *Cancer Treat Rev* 33:688-703.
 189. Kuo, M. T., H. H. Chen, I. S. Song, N. Savaraj, and T. Ishikawa. 2007. The roles of copper transporters in cisplatin resistance. *Cancer Metastasis Rev* 26:71-83.
 190. Yu, Y., S. Fujii, J. Yuan, R. Z. Luo, L. Wang, J. Bao, M. Kadota, M. Oshimura, S. R. Dent, J. P. Issa, and R. C. Bast. 2003. Epigenetic regulation of ARHI in breast and ovarian cancer cells. *Ann N Y Acad Sci* 983:268-277.

191. Lu, Z., R. Z. Luo, Y. Lu, X. Zhang, Q. Yu, S. Khare, S. Kondo, Y. Kondo, Y. Yu, G. B. Mills, W. S. Liao, and R. C. Bast. 2008. The tumor suppressor gene ARHI regulates autophagy and tumor dormancy in human ovarian cancer cells. *J Clin Invest* 118:3917-3929.
192. Bartholomeusz, C., D. Rosen, C. Wei, A. Kazansky, F. Yamasaki, T. Takahashi, H. Itamochi, S. Kondo, J. Liu, and N. T. Ueno. 2008. PEA-15 induces autophagy in human ovarian cancer cells and is associated with prolonged overall survival. *Cancer Res* 68:9302-9310.
193. Trachootham, D., Y. Zhou, H. Zhang, Y. Demizu, Z. Chen, H. Pelicano, P. J. Chiao, G. Achanta, R. B. Arlinghaus, J. Liu, and P. Huang. 2006. Selective killing of oncogenically transformed cells through a ROS-mediated mechanism by beta-phenylethyl isothiocyanate. *Cancer Cell* 10:241-252.
194. Trachootham, D., J. Alexandre, and P. Huang. 2009. Targeting cancer cells by ROS-mediated mechanisms: a radical therapeutic approach? *Nat Rev Drug Discov* 8:579-591.
195. Bornstein, J., S. Sagi, A. Haj, J. Harroch, and F. Fares. 2005. Arsenic Trioxide inhibits the growth of human ovarian carcinoma cell line. *Gynecol Oncol* 99:726-729.
196. Le, X. F., W. Mao, Z. Lu, B. Z. Carter, and R. C. Bast. 2010. Dasatinib induces autophagic cell death in human ovarian cancer. *Cancer* 116:4980-4990.
197. Matsushima, H., K. Yonemura, K. Ohishi, and A. Hishida. 1998. The role of oxygen free radicals in cisplatin-induced acute renal failure in rats. *J Lab Clin Med* 131:518-526.
198. Miyajima, A., J. Nakashima, K. Yoshioka, M. Tachibana, H. Tazaki, and M. Murai. 1997. Role of reactive oxygen species in cis-dichlorodiammineplatinum-induced cytotoxicity on bladder cancer cells. *Br J Cancer* 76:206-210.

199. Uslu, R., and B. Bonavida. 1996. Involvement of the mitochondrion respiratory chain in the synergy achieved by treatment of human ovarian carcinoma cell lines with both tumor necrosis factor-alpha and cis-diamminedichloroplatinum. *Cancer* 77:725-732.
200. Masuda, H., T. Tanaka, M. Tateishi, M. Naito, and H. Tamai. 2001. Detection and cytotoxicity of cisplatin-induced superoxide anion in monolayer cultures of a human ovarian cancer cell line. *Cancer Chemother Pharmacol* 47:155-160.
201. Wang, H. Q., D. A. Altomare, K. L. Skele, P. I. Poulikakos, F. P. Kuhajda, A. Di Cristofano, and J. R. Testa. 2005. Positive feedback regulation between AKT activation and fatty acid synthase expression in ovarian carcinoma cells. *Oncogene* 24:3574-3582.
202. Yu, D., J. K. Wolf, M. Scanlon, J. E. Price, and M. C. Hung. 1993. Enhanced c-erbB-2/neu expression in human ovarian cancer cells correlates with more severe malignancy that can be suppressed by E1A. *Cancer Res* 53:891-898.
203. Harhaji-Trajkovic, L., U. Vilimanovich, T. Kravic-Stevovic, V. Bumbasirevic, and V. Trajkovic. 2009. AMPK-mediated autophagy inhibits apoptosis in cisplatin-treated tumour cells. *J Cell Mol Med* 13:3644-3654.
204. Spano, A., G. Monaco, S. Barni, and L. Sciola. 2008. Cisplatin treatment of NIH/3T3 cultures induces a form of autophagic death in polyploid cells. *Histol Histopathol* 23:717-730.
205. Gotlieb, W. H., J. Saumet, M. C. Beauchamp, J. Gu, S. Lau, M. N. Pollak, and I. Bruchim. 2008. In vitro metformin anti-neoplastic activity in epithelial ovarian cancer. *Gynecol Oncol* 110:246-250.
206. Rattan, R., S. Giri, L. C. Hartmann, and V. Shridhar. 2011. Metformin attenuates ovarian cancer cell growth in an AMP-kinase dispensable manner. *J Cell Mol Med* 15:166-178.

207. Pan, W., H. Yang, C. Cao, X. Song, B. Wallin, R. Kivlin, S. Lu, G. Hu, W. Di, and Y. Wan. 2008. AMPK mediates curcumin-induced cell death in CaOV3 ovarian cancer cells. *Oncol Rep* 20:1553-1559.
208. Nishida, Y., S. Arakawa, K. Fujitani, H. Yamaguchi, T. Mizuta, T. Kanaseki, M. Komatsu, K. Otsu, Y. Tsujimoto, and S. Shimizu. 2009. Discovery of Atg5/Atg7-independent alternative macroautophagy. *Nature* 461:654-658.
209. Brozovic, A., G. Fritz, M. Christmann, J. Zisowsky, U. Jaehde, M. Osmak, and B. Kaina. 2004. Long-term activation of SAPK/JNK, p38 kinase and fas-L expression by cisplatin is attenuated in human carcinoma cells that acquired drug resistance. *Int J Cancer* 112:974-985.
210. Yang, X., M. Fraser, U. M. Moll, A. Basak, and B. K. Tsang. 2006. Akt-mediated cisplatin resistance in ovarian cancer: modulation of p53 action on caspase-dependent mitochondrial death pathway. *Cancer Res* 66:3126-3136.
211. Eckstein, N., K. Servan, B. Hildebrandt, A. Pölit, G. von Jonquières, S. Wolf-Kümmeth, I. Napierski, A. Hamacher, M. U. Kassack, J. Budczies, M. Beier, M. Dietel, B. Royer-Pokora, C. Denkert, and H. D. Royer. 2009. Hyperactivation of the insulin-like growth factor receptor I signaling pathway is an essential event for cisplatin resistance of ovarian cancer cells. *Cancer Res* 69:2996-3003.
212. Foster, H., H. M. Coley, A. Goumenou, G. Pados, A. Harvey, and E. Karteris. 2010. Differential expression of mTOR signalling components in drug resistance in ovarian cancer. *Anticancer Res* 30:3529-3534.
213. Li, Y., and D. Q. Yang. 2010. The ATM inhibitor KU-55933 suppresses cell proliferation and induces apoptosis by blocking Akt in cancer cells with overactivated Akt. *Mol Cancer Ther* 9:113-125.

Vita

Angela Alexander was born on March 27, 1983 in London, United Kingdom to Joseph and Behdjat Alexander. She was raised as a citizen of the world, moving around several times throughout her childhood. She only stayed in the UK for her first 5 years of life, before her family moved to Riyadh, Saudi Arabia in October 1988 where she attended the Saudi Arabian International School-British Section until it was again time to move on in May 1996, when she and her family moved to Cumbernauld, Scotland, where she attended Abronhill High School until May 1999. After completing high school, Angela worked for a few months in the internal revenue service before crossing the Atlantic ocean to start another chapter of her life in Delaware, USA. During her year off between high school and college while moving to the US, Angela applied to the University of Delaware Lerner School of Business, where she matriculated in September 2000, and pursued a BS in Finance, and later became a Dean's Scholar which allowed her to design an individual major to merge both business course work and science.

In August of 2004 she entered graduate school at the University of Texas M.D Anderson Cancer Center-Science Park-Research Division, and she will graduate in May 2011 with a Ph.D. in Molecular Carcinogenesis from the University of Texas Health Science Center at Houston and the University of Texas M.D. Anderson Cancer Center. She has accepted a position in the TRIUMPH (Translational Research in Multi-Disciplinary Program) postdoctoral fellowship in translational cancer research at the University of Texas MD Anderson Cancer Center in Houston, which she will be starting this summer.

Permanent address:
529 Diamond Drive
Middletown, DE 19709